

CHAPTER VII

APPLICATION OF PROPAGATION PREDICTIONS TO EARTH/SPACE TELECOMMUNICATIONS SYSTEM DESIGN

7.1 INTRODUCTION

A function of the satellite communication system designer, or system engineer, is to interface between the source of system requirements (*i.e.*, the user) and the sources of performance data. Stated in terms of the present problem, the system engineer uses propagation and other technical data to achieve a system design that will meet the requirements specified by the user. These requirements are specified in terms of a gross quantitative need (e.g., number of channels), a quantitative expression of performance (e.g., percent of time available), and, sometimes, more qualitative expressions (e.g., "highly reliable"). Even though both the propagation data and the requirements are often expressed in terms of cumulative probability distributions, it is not always straightforward to relate one distribution to the other. The correspondence between a given propagation phenomenon and system performance may be complex. The purpose of this chapter is to relate propagation data to system performance parameters. It should allow the system engineer to perform the analyses telling how well requirements are met by a given system design, thereupon enabling the system engineer to modify that design if necessary. First (in Section 7.2), the various ways of specifying performance criteria for different kinds of systems are discussed. In addition, examples of specific satellite communication systems are discussed. Procedures for designing such systems are then described in section 7.3.

There are engineering disciplines for which true synthesis procedures exist, but the design of complex systems with interactive elements is usually not a true synthesis. Instead, iterative

analyses are **performed**, starting with a preliminary design **choice**, until the refined design can be shown by analysis to meet the requirements. The application of this philosophy of system design or synthesis to satellite communications is summarized here and detailed in Section 7.3.

The system design procedure is based on criteria that take the form of discrete cumulative probability distribution functions of performance. The steps necessary to go from this set of performance requirements and propagation statistics to a system design are (see Figure 7.1-1):

INITIAL PHASE

- 1) Establish system performance requirements (discrete distribution of baseband/digital performance).
- 2) Apply modulation equations to convert system performance requirements to discrete distribution of the received composite CNR (carrier-to-noise ratio) .
- 3) Prepare initial design with parameters sized according to free space propagation conditions (apply power budget equations).

DESIGN SYNTHESIS AND TRADE OFF PHASE

- 4) Employ
 - a) Composite CNR distribution from step 2
 - b) System architecture
 - c) Multiple Access equations
 - d) Availability sub-allocation philosophy

to develop distribution functions for CNR on each Path.

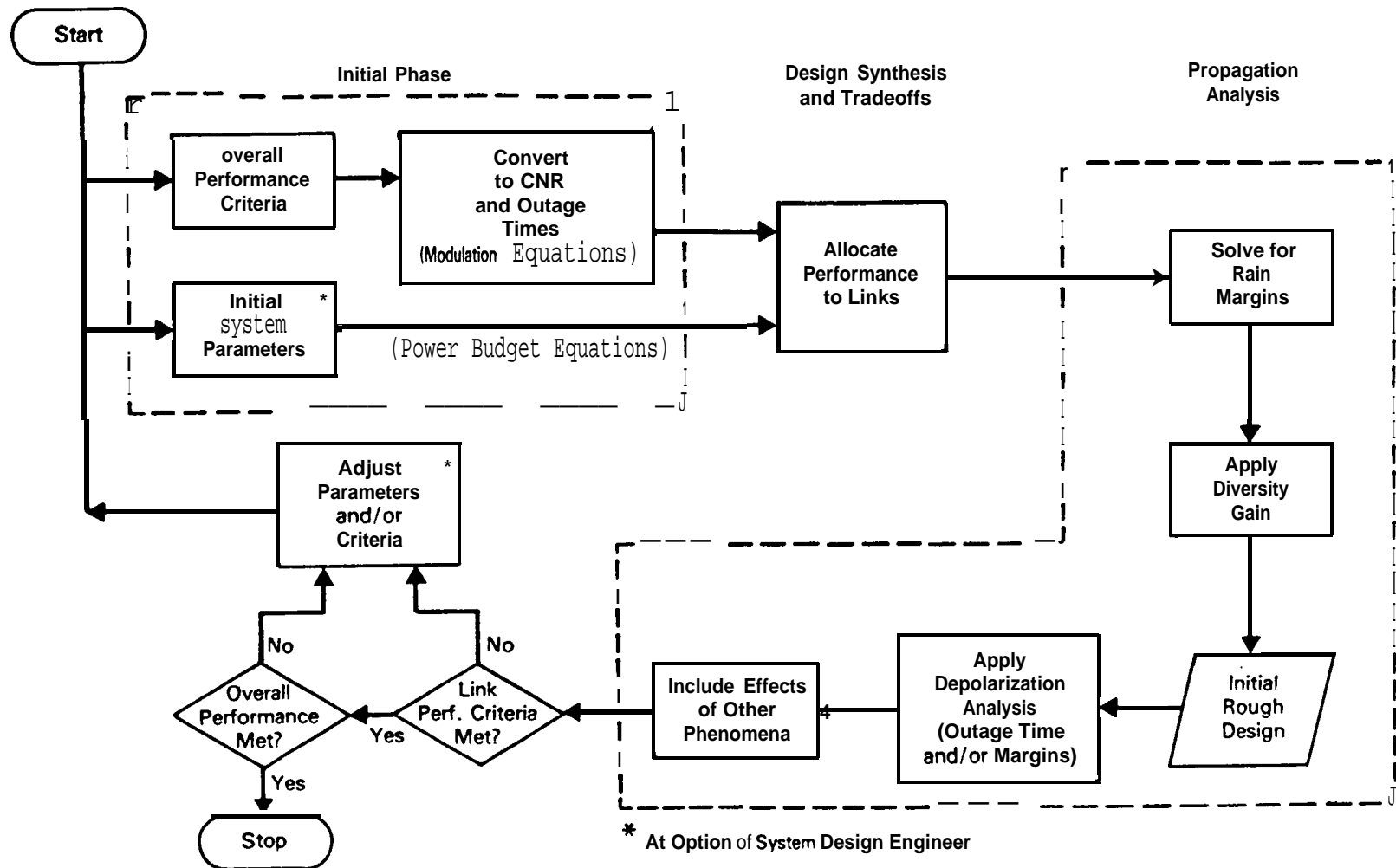


Figure 7.1-1. System Design Process

PROPAGATION ANALYSIS AND ITERATION PHASE

- 5) Compute rain margins, as reduced by diversity gain, for each path.
- 6) Adjust system parameters according to margins given by step 5. This gives a preliminary design at the feasibility concept level.
- 7) Apply depolarization analysis to adjust margins and/or increase the outage time values (% of time for the **worst-performance** level of the distributions).
- 8) Consider other propagation effects such as cloud and fog **attenuation**, signal fluctuations and antenna gain degradations and add margin to design as necessary.
- 9) Adjust system parameters to include all additive margins. Analyze **system performance**, first at the path **level**, then on the **end-to-end** performance level.
- 10) If performance meets requirements closely, stop. Otherwise, adjust design and repeat analysis. If design cannot be made to meet requirements, consider changing requirements.

Performance criteria typically deal with baseband quality, or digital error rates, whereas the power budgets relate physical system parameters to signal-to-noise **ratio, CNR**, (or equivalents such as **S/N, Eb/No, C/kT**, etc.). Therefore, the baseband or digital performance criteria must be functionally related to CNR by means of modulation performance equations.

Gross design is performed by means of elementary power budget analysis and free-space (or clear air) propagation characteristics. Basic choices are made at this point, such as selection of modulation and multiple access techniques. It is assumed that the reader is familiar with these techniques and power budget analysis (Northrop-1966) . This analysis establishes a relationship between

basic system parameters and the signal- or carrier-to-noise ratio (**CNR**) on a given transmission path.

The system performance requirements, which apply to end-to-end performance, are **suballocated** to various system components. Most important, the relationship of the end-to-end communication performance to that of each of the links must be determined. For example, the actual received CNR is a composite which may include both **uplink** and downlink noise contributions. The end-to-end availability involves availabilities of each path.

Since rain induced attenuation is the most severe propagation effect for the frequencies of interest, the next step in the procedure is to calculate a rain margin. If the system uses site diversity, some of this rain margin may be offset by "diversity gain." The remaining margin is then applied to the initial system parameters. Typically, the margin is applied as an increase in power; but it is also possible to increase antenna gains or modify the modulation parameters. At this point, a rough design has been achieved. This level of detail and accuracy may be sufficient if the objective is only to determine system feasibility. For more accurate results, the effects of other propagation phenomena must be considered. Except for depolarization, these effects are generally additive in terms of margin. Loss in **crosspolarization** isolation (usually termed "depolarization") can be accommodated as an additive term whenever the interference component is small relative to thermal noise and other interference sources. Thus, small degradations such as those due to depolarization from ice are treated as part of the system margin computation*. The more severe degradations in cross polarization such as those caused by rain cannot be counteracted by margin increases. These events will

*It is not necessary to add margins on a worst case basis. Where large margins have already been included for rain, the ice depolarization event can be assumed to "share" the same margin.

usually be severe enough to cause an outage. Therefore, in systems employing cross polarization isolation, the depolarization phenomenon may reduce or limit the system availability.

Having thus adjusted the system parameters and the performance analyses, the system design engineer can determine whether performance criteria are met, first for the individual link, and then for the overall system. If so, the design process is essentially completed*. If not, the system parameters and/or the performance criteria are modified, and the analysis procedure is repeated. To some, the idea that the criteria are subject to change is disturbing. Within physical (and economic) constraints, it is preferable to modify only the technical system parameters. **But** there may be cases where the initial performance goals are unrealistic. For example, it simply may not be worth the expense of a large increase in EIRP in order to get a circuit availability of 99.99% for small earth terminals at 44 GHz.

Section 7.2 addresses system performance criteria and examples of representative satellite communication systems, while paragraphs 7.3.1 through 7.3.3 are introductions to general system design procedures. The experienced communication system engineer will probably be familiar with the material covered in these paragraphs, and may therefore skip them without loss of continuity, and concentrate on paragraphs 7.3.4 through 7.3.6, which are addressed to the main issue at hand, namely the specific application of propagation data. Section 7.4 describes several methods for overcoming the effects of rain fades. Diversity schemes and signaling techniques are described that can significantly improve communication performance. Table 7.1-1 is a guide to specific examples contained in this chapter.

*A fine-tuning iteration may be desirable if the design exceeds requirements.

Table 7.1-1. Guide to Systems Analysis Procedures

| <u>Paragraph Number</u> | <u>Description</u> | <u>Page Number</u> |
|-------------------------|---|--------------------|
| 7.3.4 | Performance specification of digital and analog systems | 7 - 4 3 |
| 7.3.5 | Analog and digital system synthesis and tradeoffs | 7 - 4 6 |
| 7.3.6 | Analog and digital system propagation analysis and link budgets | 7-55 |
| 7.3.7 | Calculation of composite margin | 7-70 |
| 7.4.2.1.3 | Estimates of parameters required for empirical diversity model | 7-93 |
| 7.4.2.1.4 | Analytic estimate of site diversity gain | 7-102 |

7.2 COMMUNICATION SYSTEM PERFORMANCE CRITERIA AND SPECIFIC SATELLITE SYSTEMS

7.2.1 Performance Criteria

7.2.1.1 Introduction

Criteria for communication system performance represent attempts to quantify the "reliability or "quality" of the service. **Two** methods, applying different probabilistic **notions**, are generally used. The first method is to regard some indicator of communication quality (e.g., CNR) as a random variable and specify values of its inverse cumulative distribution function, or the probability that a given value is exceeded. With the second method of specifying performance criterion, the quality indicator is taken as a random process, and some statistic of this time-varying process is used. A

typical statistic in this case might be the **median**, mean, or "three-sigma" duration of the periods during which the value stays below a given threshold. If a period during which the CNR is below some threshold is regarded as an "outage", then the criterion would specify outage duration statistics.

The first type of performance criterion, which will be termed availability criterion, is generally specified as the percentage of time that a threshold value is exceeded (or not exceeded), rather than a probability. This is natural, since what we can measure is percentage of time, and not probability. (Ergodicity allows these to be assumed equivalent). Availability criteria are in wide use, and the bulk of long-term performance data analysis has been done from an availability standpoint. However, such criteria and data do not give any information about the time-variation of performance. In many situations, it is desirable to know something about how fast the performance may change. Some temporal information is given by a slightly modified availability criterion, in which a time period is specified. For example, the criterion could state that a given level of noise will not be exceeded for more than a certain percentage of any month. However, the connection between such a criterion and any quantitative temporal description is obscure.

The second type of performance criterion, which expressly describes the temporal behavior, such as mean outage duration, will be termed outage statistics. Besides the outage duration, such statistics might include the distribution function for the time until the next **outage**, given that an outage is just over. Or they might **probabilistically** describe diurnal or seasonal performance variations. In the limit, such statistics would give the **autocorrelation** function or the spectral density of the process. As yet, the available data does not cover a long enough time span to be statistically reliable. We will therefore confine our attention primarily to performance criteria that specify availability, rather than outage statistics.

There are several sources of performance criteria. Among the more generally accepted standards are those promulgated by the International Radio Consultative Committee (**CCIR**). Telecommunication systems for U.S. commercial use conform to standards similar but not identical to the **CCIR's**. These criteria are expressed in terms of a baseband noise level (analog) or an error rate degradation (digital) not to be exceeded more than some small percentage of the time in any month (typically, .001 to 0.3%). The Defense Communications Agency has more recently advanced (Kirk and **Osterholz-1976** and Parker-1977) criteria based on the probability of occurrence of outage on a five minute call (voice channels), or the error free block probability for a 1000 bit block (data channels).

7.2.1.2 Digital Transmission Performance

7.2.1.2.1 Short Term Bit Error Rate. The primary measure of circuit or transmission quality for digital systems is the bit error rate (**BER**). Semantically, we use "bit" error rate because the overwhelming majority of digital communications systems transfer binary data streams.* Bit error rate usually applies over a moderately short term, and normally does not incorporate "errors" or outages of duration longer than a few tens of bits.

For most digital systems, the bit error probability can be expressed as a function of the energy-per-bit to noise power spectral density ratio (E_b/N_0). These relationships are available for the theoretical performance of commonly used modulation and coding systems from any good communication theory reference (e.g., Schwartz, et al-1966 and **Spilker-1977** . The theoretical BEP vs. E_b/N_0 relations usually assume white, Gauss an noise. In the presence of

*We should also distinguish between bit error rate, which defines the actual performance, and must be measured by averaging over a sequence of bits communicated, and the bit error probability (**BEP**), which is a theoretical concept that can apply even to a single bit. BER will be used here, since it is more **common**, even though BEP is technically more correct.

non-white or non-Gaussian noise, or interference, these relations are not accurate. It is now becoming common to express the performance of actual systems in terms of the E_b/N_0 rather than CNR. E_b/N_0 is numerically equal to the ratio of signal power to noise power within a (noise) bandwidth equal in hertz to the digital bit rate in bits per second. (Note that bit rate is not in general the same as symbol rate.) For example, the (theoretically ideal) performance of binary PSK modulation requires an E_b/N_0 of 9.6 dB for a BER of 10^{-5} .

In the case of digital systems used to accommodate fundamentally analog requirements (e.g., PCM voice channels), there exists a threshold error rate at which circuit quality is considered unacceptable. This threshold value then determines the point at which an "outage" exists. Because error rate is a sensitive function of E_b/N_0 , circuit quality degrades quite drastically when E_b/N_0 falls below the value corresponding to the threshold error rate. **Degradation is not "graceful."**

7.2.1.2.2 Digital Transmission Performance. Data communications systems rarely **transmit uniform, homogeneous**, continuous bit streams. Rather, the data is often formatted in blocks or packets. In many cases, then, the performance requirement is specified in terms of the probability of an error free block, which might typically contain 1000 or more bits. If the only type of transmission imperfection is the randomly occurring bit error process, then the block error performance can be calculated from the bit error rate: Probability of error free block of n bits = $P(\geq 1, n) = (1 - \text{BER})^n$. However, the block error performance may be influenced by the probability of longer outages, losses of synchronization, and the like, which are not usually included in the BER.

In systems used to transfer well-defined messages, other performance criteria may be required. In the most general case where a block is composed of many messages, the system performance requirements could include a message performance **criterion**, a block transmission performance criterion and a bit error rate. Note that

consistency among the various criteria is mandatory. For **example**, a block error performance of 99% (i.e., 99 out of 100 blocks are error free) for 1000-bit blocks could not be achieved when the bit error rate is 10^{-4} .

In data communications systems where real time delivery is not **critical**, the concept of throughput is often used. It is implicit that the system involves a return channel path over which acknowledgments and/or requests for retransmission are made. The throughput is defined (Brayer - 1978) as the ratio of the number of information bits transmitted (K) to the total number of bits (including overhead and re-transmissions), n, before the block is accepted. The throughput is approximately

$$K[1-P(\geq 1, n)]/n \quad (7.2-1)$$

This approximation for throughput as a function of block error rate applies only when the return channel is error free. Brayer (1978) makes a case for using message delivery delay as the most important criterion, rather than throughput itself. However, they are related closely.

In summary it can be seen that throughput and block error rate are directly related. Bit error rate contributes a major, but not always the only, portion of the block error rate. In communication system design, the (short term) bit error rate or bit error probability is taken as a parameter of analysis and preliminary design. Final performance estimates must, however, take into account both the nominal BER performance, and some consideration of outages. The qualitative relationships among the various criteria are shown in Figure 7.2-1. Notice that the fundamental, or **user-requirement-** oriented, criteria are on the right side of the diagram, yet the correct logical path for analysis is from left to right. Thus, analysis is employed to demonstrate that a set of system and environmental conditions will meet the performance requirements.

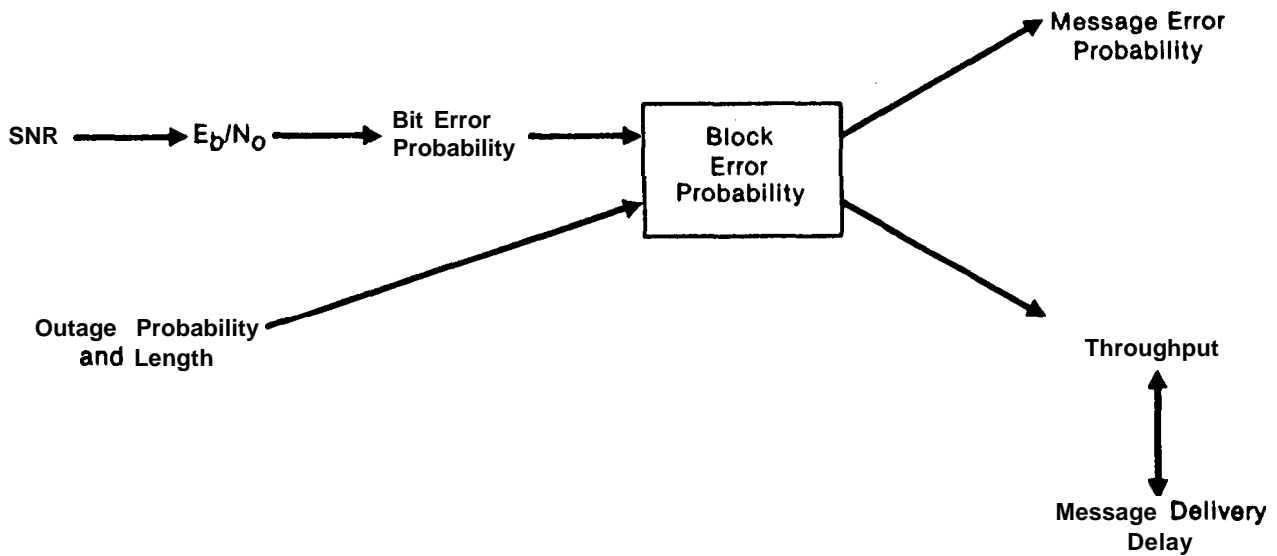


Figure 7.2-1. Data System Performance

7.2.1.3 Analog Transmission Performance

The establishment of performance criteria for analog systems is a complex issue. Transmission system criteria are usually defined on an **end-to-end**, reference circuit basis. If the satellite system is only a portion of this end-to-end path, a sub-allocation must be made to the satellite segment. Also, when the system is used for relay of multichannel voice **trunks**, the conversion from baseband (voice channel) performance criteria to the radio frequency criteria (i.e., C/N) involves assumptions about channel loading and modulation parameters. For example, for an **FDM-FM** system, the noise in picowatts, **psophometrically** weighted (**pwop**), in a voice channel is (GTE-1972)

$$pwop = \log_{10}^{-1} \left\{ \frac{1}{10} [-C - 48.1 + F - 20 \log (\Delta f / f_{ch})] \right\} \quad (7.2-2)$$

where

c = RF input power in dBm

F = receiver noise figure, dB

Δf = peak deviation of the channel for a 1 kHz test tone signal

f_{ch} = center frequency of the channel in the baseband

Similar equations apply to single channel FM voice and FM video, and to other modulation structures.

pWOp is one of many noise measures in use. Specifically,

dBrnc (dB above reference noise, C-message weighting. Reference noise is equivalent in power to a 1,000 hertz tone at -90 dBm.)

dBa (dB above reference noise-adjusted, FLA weighting. Reference noise adjusted is equivalent in power to a 1,000 hertz tone at -85 dBm.)

pwp (picowatts of noise power, psophometrically weighted.)

dBmOp (psophometrically weighted noise power in dB, with respect to a power level of 0 dBm.)

These units represent absolute values of noise. By appending a "0" to each (e.g., pWOp), the same units serve as measure of noise relative to 0 level signal (i.e., 0 dBm). Then the following approximate conversions apply (GTE-1972):

$$dBrnc0 = 10 \log_{10} pWOp + 0.8 = dBa0 + 6.8 = dBmOp + 90.8 = 88.3 - S/N$$

In general, most standards involve long term nominal objectives and short term or worst case threshold values. Below this threshold, an "outage" exists. FM links are often engineered so that the receiver FM threshold value of C/N is at or within a few dB of that value which gives the absolutely minimum acceptable

performance. That is, the receiver RF performance threshold and the baseband (acceptable) performance threshold are matched.

As an example of a long-term performance objective, the latest CCIR position (reflected in Recommendation 353-3, **CCIR-1978**) is that 10,000 pWOp one-minute mean noise power should not be exceeded more than 20% of any month. The old U.S. criterion for long **intertoll** trunks required 20,000 pWOp or less nominal (in the absence of a fade) . In the case of television signals, various criteria require a weighted baseband S/N of from 50 to 59 **dB** to exist under nominal conditions.

Noise performance requirements for small percentages can be thought of as "outage" conditions. The CCIR recommendation is that 1,000,000 pWO (unweighed) measured with a 5 ms. integration time, exist not more than 0.01% of any year. An intermediate requirement is also established: that 50,000 pWOp one-minute mean power not be exceeded for more than 0.3% of any month. In the U.S., a criterion of 316,000 pWOp for .02% of the time is often employed. DCA standards similarly require that 316,000 pWOp not be exceeded for more than 2 minutes in any month **nor** for one minute in any hour. Video threshold requirements are typically in the 33 to 37 **dB** weighted signal to noise ratio range.

Criteria are under constant revision. Indeed, there are arguments suggesting that new applications require specialized criteria. Current criteria, developed for terrestrial systems or for satellite communications systems below 10 GHz, may not be applicable for millimeter wave systems where the statistics differ appreciably.

Note that outage criteria, such as the one DCA has promulgated (probability of outage on a five minute call), are very different from nominal or long-term availability criteria. Because propagation outages in the frequency range of interest typically have durations on the order of magnitude of minutes, it is not straightforward to relate availability statistics to outage

probability statistics. Some approximations may be made from rain statistical data and limited data on fade depth vs. duration, but more theoretical and experimental work appears to be necessary before such outage criteria can be reliably applied in design. In this-Handbook, therefore, we have found it necessary to emphasize availability criteria. Where duration data is available, it may be employed as a **subsidiary**, or second **order**, check on whether system requirements are met.

7.2.1.4 Summary of Nominal Criteria and Their Application

The nominal performance criteria for digital and analog systems are substantially different. However, these can be related by analysis to corresponding values of CNR, which communication engineers prefer to work with. There is, usually, a long term or nominal performance standard, as well as some definition of short term event behavior (outage criterion). With data systems, the long and short term phenomena may be statistically combined, so that it is possible to define combined performance criteria. These similarities, differences, and relationships are shown in Table 7.2-1.

Table 7.2-1. Performance Criteria and Relationships

| System | Fundamental Quality Parameter | Nominal (Long Term) Performance | Short-Term (Outage) Criterion | Combined Criterion |
|------------------|-----------------------------------|---------------------------------|--|--|
| Analog | Baseband noise or signal to noise | Mean or Median CNR | CNR equalled or exceeded except for p% | |
| Digitized Analog | Baseband quality | Bit Error Rate | Same as above | |
| Data | Error free block probability | Bit Error Rate | Outage probability | Error free block probability Throughput Delivery Delay |

7.2.1.5 Additional Performance Criteria

In some applications, more specific control of the transmission quality is necessary and criteria such as those cited above are inadequate. In these situations a number of linear and nonlinear distortion parameters may be specified. Most of these relate to the system (hardware) components. It appears that the only significant distortion parameter introduced by the propagation path is phase fluctuation (scintillation)*. Small amounts can be accommodated in the power budget analysis as equivalent S/N or E_b/N_0 degradations. (By "small amounts," we mean values which lead to no more **than, say,** 1 dB in equivalent S/N degradation.) On the other hand, large phase scintillations that occur infrequently will add to the outage time calculation providing:

- 1) these events are not concurrent with the predominant cause of outage, namely amplitude fades (attenuation), and
- 2) the rate of phase variation is high enough that it will not be tracked by a digital system, or be filtered out in an analog system.

7.2.2 Recent Satellite Technology

The ever increasing demand for worldwide satellite telecommunication will saturate the available frequency spectrum allocated to current C-band and Ku-band services by the early 1990's. To meet future demands, the systems designer is exploring higher frequency bands (such as Ka) to relieve the congestion in orbit and developing new technologies enabling higher degrees of frequency reuse for a more efficient utilization of the orbital arc.

*A possible exception is dispersion at frequencies near the absorption bands, but these bands will usually be avoided.

Most communications satellite designs include methods for frequency reuse. Polarization isolation is currently used on most C-band and Ku-band systems to effectively double the bandwidth and capacity of a satellite system. Another attractive method is to use **multibeam** (or spot beam) antennas, provided the beams are sufficiently separated to avoid beam-to-beam interference. **Multibeam** antennas are appropriate for satellite systems operating in the higher frequency bands because narrow spot beams can be achieved with moderate antenna sizes.

The principle of **multibeam** frequency reuse and its advanced technologies will enhance satellite capacity and orbital arc/spectrum utilization.

In satellite communication employing digital modulation, **on-board** processing (demodulation/remodulation) is becoming more widely used. Benefits include improved end-to-end bit error rate performance as well as improved terminal interconnectivity.

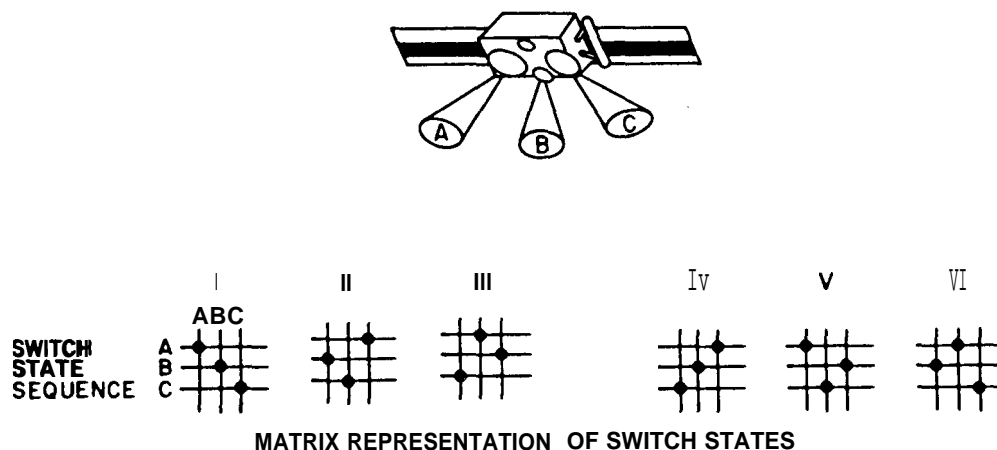
These relatively recent technologies are discussed in the following paragraphs. Section 7.3 discusses propagation considerations peculiar to the newer systems.

7.2.2.1 SS/TDMA

One way to increase the capacity of satellite communication systems is to employ multiple beams with time division multiple access (**TDMA**) techniques. This is especially attractive at **Ka-band** since the higher the frequency, the more workable the multi-spot antennas are. However, this approach makes it difficult to ensure proper connectivity between **uplink** and downlink beams that cover different geographical locations. In order to reduce the number of required transponders, satellite-switched/time division multiple access (**SS/TDMA**) can be used.

In an **SS/TDMA** system the satellite uses several spot beam antennas and a microwave switch matrix (**MSM**) to route TDMA bursts arriving on different **uplink** beams to different downlink beams.

Figure 7.2-2 shows a simplified example of an **SS/TDMA** system that will be used for NASA's Advanced Communications Technology Satellite (ACTS).



| SWITCH STATE NUMBER | | I | II | III | IV | V | VI |
|---------------------------|-------------|------|------|------|------|------|------|
| SWITCHING MODE ALLOCATION | FROM BEAM A | TO A | TO C | TO B | TO C | TO A | TO B |
| | FROM BEAM B | TO B | TO A | TO C | TO B | TO C | TO A |
| | FROM BEAM C | TO C | TO B | TO A | TO A | TO B | TO C |

Figure 7.2-2. Diagram of the MSM interconnecting the three beams

The on-board Distribution Control Unit (**DCU**) programs the switch matrix to execute a **cyclic** set of switch states, each consisting of a set of connections between the **uplink** and down link **beams**, so that the traffic from various regions is routed to designated regions without conflict. A switch state sequence is a succession of switch states during a frame period. To accommodate all of the traffic presented to a system, a sequence of different switch states occurring in a periodic frame is required. For example, for complete interconnectivity between **N beams**, a total of **N!** different switch state sequences is needed.

The switching mode allocation describes both the succession and the duration of each switch state so as to route the desired amount of traffic among the beams. The first state shown at the bottom of Figure 7.2-2 provides the connections A to A, B to **B**, and C to C; the second state provides the connections A to C, B to A, and C to B, and so on.

Figure 7.2-3 illustrates a 3-beam **SS/TDMA** frame which consists of a synchronization field and a traffic field. The first state of the synchronization field provides loop-back connections to the origination beams. This provides for synchronization between the satellite switch and a TDMA reference station. The reference station in each beam observes synchronization errors of the stations in other beams and sends them necessary corrections. Subsequent states in the synchronization field provide for the distribution of reference bursts and location of synchronization bursts from the traffic stations. The traffic field consists of a number of switching modes and a growth space. The growth space is allocated to cope with traffic pattern changes, since unbalanced traffic between pairs of uplink and downlink beams are likely to occur. The satellite transponder utilization is maximum when the traffic field is fully occupied with a number of switching modes and the growth space is zero.

The Microwave Switch Matrix (**MSM**) is the key element of **SS/TDMA** system. ACTS MSM provides connectivity for the three stationary beams. The MSM **is** a solid state (dual-gate GaAs **FET**), programmable crossbar switch with a switching time of less than **100ns**; it is a 4x4 IF switch, but only 3 input and 3 output ports are used at **any** given time (Naderi, **Campanella** - 1988). The **INTELSAT VI** satellite incorporates a 6x6 dynamic switch and a 8x8 static switch. The 6x6 switch provides interconnectivity between the two hemisphere **beams**, and the four overlaid zone **beams**, two in each hemisphere. The 8x8 static switch provides interconnectivity between the two 14/11 GHz spots and six 6/4 GHz beams. The static switch also provides

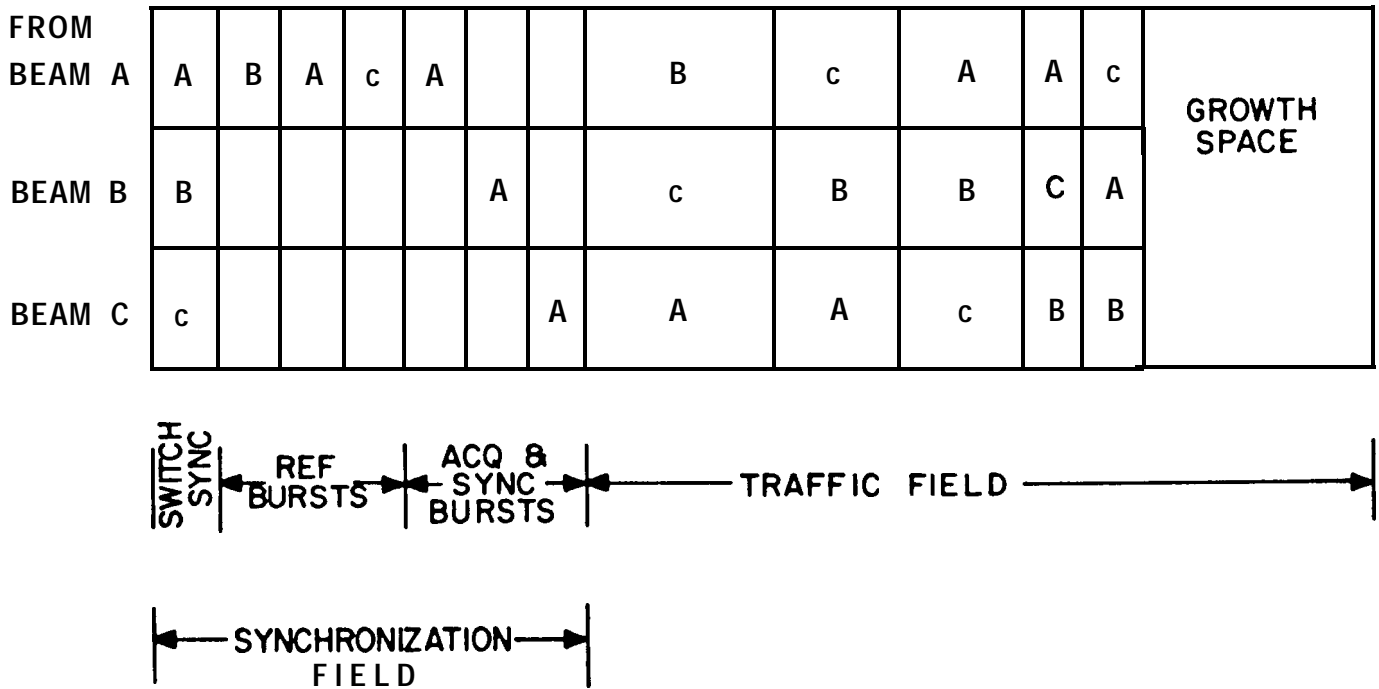


Figure 7.2-3. Typical **SS/TDMA** frame for a 3-beam system

interconnectivity between the two global beams (**Scarcella** and Abbott - 1983). The architecture the INTELSAT VI satellite switch matrix is a coupler crossbar with dual-gate GaAs FET switching elements.

7.2.2.2 On-board Processing

The difficulty with some of the more common means of satellite access, such as frequency division multiple access (**FDMA**) and-code division multiple access (**CDMA**), is that the power in each of the downlink signals is controlled by the relative power in each of the satellite **uplink** signals. Thus, downlink power cannot be allocated to user requirements independent of the uplink. Furthermore, **uplink** power from each user must be carefully controlled to prevent saturation of the satellite power amplifier. Saturation distorts the signal modulation and generates **undesired intermodulation** products.

Time division multiple access (**TDMA**) to a satellite repeater avoids saturation of the power amplifier, but there is still an effective downlink power sharing (really, time sharing) problem because of the uplink time sharing. Moreover, linear and nonlinear distortion (**intersymbol** interference and AM-to-PM conversion) still occur because of required **bandlimiting** and amplification on the satellite. In addition, all users must operate at high data rates on both the **uplink** and downlink because of the burst transmissions.

On-board processing circumvents many of these difficulties first of all because **uplink** signal distortion and interference are not retransmitted on the **downlink**, and secondly because downlink power can be allocated in accordance with downlink user needs, independent of **uplink** transmissions. This allows interconnection of terminals that use different modulation and coding schemes. In addition, all downlink users will then have a common frequency standard and symbol clock on the satellite, which is useful for network synchronization.

On the other hand, on-board processing requires carrier and clock synchronization of the uplink signals, which functions are not required on a conventional frequency translation satellite.

To get an idea of the performance improvement achievable with on-board processing, Figure 7.2-4 shows a comparison between conventional and on-board processing satellites, in terms of **uplink** and downlink carrier/noise power ratios, considering a specified bit error rate of **10e-4**. Ideal error rate ($P_e = 1/2 \text{erfc } E_b/N_o$) conditions are assumed, that is no degradation resulting from filtering or non-linear distortions.

Link analysis for an on-board processing satellite treats the uplink and downlink as two separate point-to-point analyses. To estimate the **performance**, it is necessary to determine separately the bit error probability on the uplink and downlink. The overall error rate is obtained by combining **uplink** and downlink error rates as follows:

$$BER_C = BER_U (1 - BER_D) + BER_D (1 - BER_U) \approx BER_U + BER_D \quad (7.2-3)$$

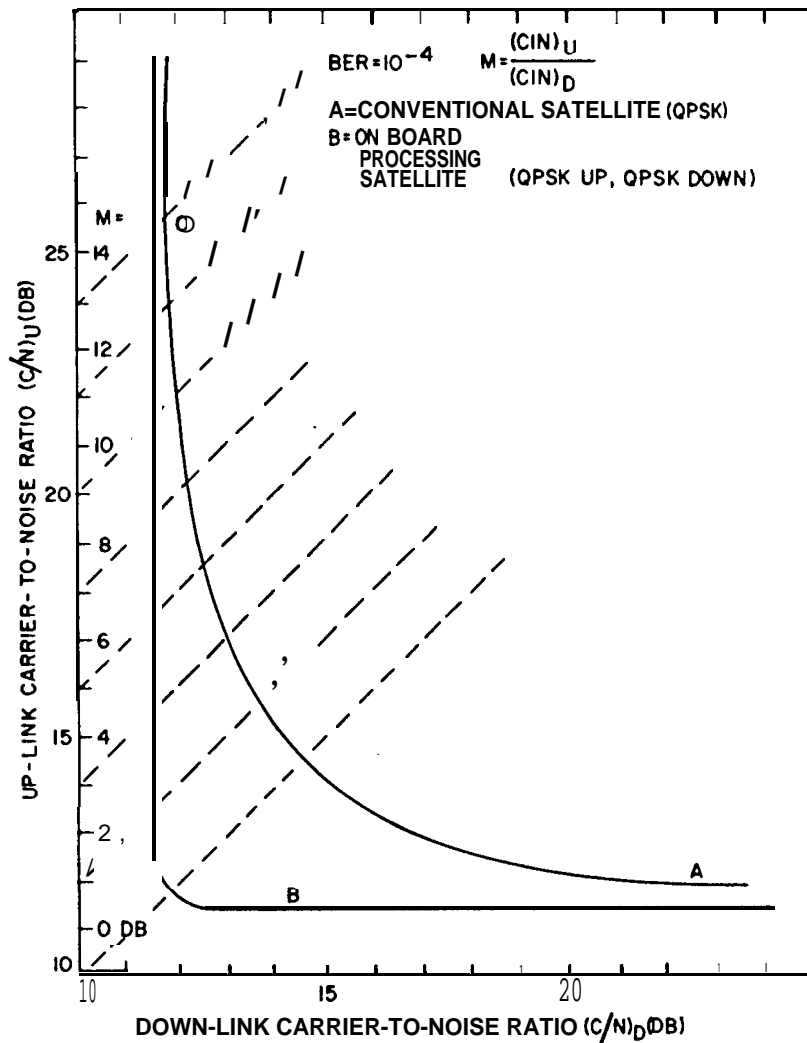


Figure 7.2-4. Comparison of conventional and processing satellite performances (linear channel)

By comparison, link analysis for a conventional satellite generally **treats** the entire "round-trip" (**uplink** transmission to the satellite and downlink retransmissions to an earth station) as a single analysis. To estimate performance, the uplink and downlink values of **Eb/No** (or C/N) are combined as follows:

$$(Eb/No)^{-1}_C = (Eb/No)^{-1}_U + (Eb/No)^{-1}_D \quad (7.2-4)$$

where the subscripts **U**, **D**, and **C** denote **uplink**, **downlink** and **composite** values respectively.

One can see from Figure 7.2-4 that the maximum power gain saving is obtained when **uplink** and **downlink** are the same. In that case the advantage of an on-board processing satellite compared with a conventional one is a saving of 3 **dB** on both **uplink** and **downlink** transmitted power. However, when the **uplink** power is much larger than the **downlink** power the saved power is much smaller (about 0.5 **dB**).

7.2.3 Representative Systems

Several systems that exploit expanded satellite capacity and efficient utilization of the orbital arc have recently been developed. These systems generally use higher carrier frequencies, such as Ka-band. This leads to the possibility of smaller earth stations, but at a cost of larger rain attenuation. Many of these systems use multiple beams, on-board processing and switching, and intersatellite links, as discussed in paragraph 7.2.2.

The proliferation of microterminals and VSAT systems provides a means for bypassing terrestrial communication networks. The Ku- and **Ka-bands** are particularly suitable for the VSAT application. Typical examples of current U.S. and European satellite communication systems are discussed in the following paragraphs.

7.2.3.1 VSAT Networks. The capability of satellite data communication networks has improved significantly because of recent advances in technology, especially in the area of microwave integrated circuits. This includes the development of solid-state power amplifiers (**SSPA**) with up to 5 watts of output power at C-band and 2 watts at Ku-band, low cost **up-converters**, and low noise **down-converters**. Current digital technology, which allows significant processing power in a small size and at low cost, led to the introduction of Very Small Aperture Terminal (**VSAT**) Networks for data communications.

VSAT networks are rapidly gaining *in* importance as a means of providing private voice and data communications for corporations that operate in widely dispersed sites. Currently two frequency bands are being used for VSAT networks: C-band and Ku-band. In general, VSAT networks operate at Ku-band because the higher frequency provides about 7 **dB** more gain than C-band for the same aperture size. On the other hand, Ku-band suffers significant rain attenuation, so consequently more system outages occur (Lyon-1985).

The networks are configured as hub-based systems, with a large earth station commonly referred as "hub," located at or near corporate headquarters and numerous small terminals (**VSATs**) located at remote sites. Since terminals are small, typically between 1.2 meters and 1.8 meters in diameter, it is usual to use a large earth station to receive and regenerate the transmitted data signals before distribution to other terminals. Hence, VSAT'S communicate with the hub over the **VSAT-to-hub** satellite link and the hub station communicates with the VSAT usually by terrestrial links." Consequently, such communication involves double hops, which can present considerable difficulty for voice communication and is not used except in extreme cases.

With the use of a baseband processor on the satellite, the function of the major earth station can be replicated and the double hop eliminated. With this technology, voice communication would also be **acceptable**, because of the smaller time delays. This concept was recently proposed as an application of the NASA ACTS baseband processor technology (Naderi, **Campenella-1988**). The ACTS baseband processor will provide small customer premise' services, allowing low data rate users direct and efficient access to the satellite. The use of spot beams and switching technologies will provide multiple voice channels to **VSATs** in a single satellite hop, neither of which is possible with current VSAT networks.

The range of possible applications for VSAT networks is. . . widespread, particularly since rapid one-and two-way communications can be supported. Typical VSAT network applications include:

inventory management between retail stores and **head-quarters**, express mail and facsimile? travel and financial related services, meteorological data **gathering**, and corporate video distribution. Such variety in applications for VSAT technology is one force behind the growing number of companies installing **VSAT** networks to satisfy their ever increasing telecommunications needs. The emergence of these networks was stimulated by the U.S. industry investment in **DBS-TV** technology, the success of Equatorial Communications with over 25,000 receive-only and **1,000** transmit/receive VSATS installed, and the decision of Federal Express to purchase 50,000 small two-way earth stations for networking their field centers.

7.2.3.2 **ACTS**. The Advanced Communications Technology Satellite (ACTS), currently under development by NASA, will contain several new technologies and features which have the potential to dramatically enhance the capabilities of future satellite systems. ACTS will be one of the first satellites to operate a **K_a-band** (30 GHz **uplink/20** GHz downlink), and will include electronically hopping multiple spot-beam antennas, on-board processing with baseband message routing, and adaptive rain fade compensation. These capabilities enable ACTS to provide multiple voice/data channels to VSAT type ground terminals in a single satellite hop, which is not possible with current VSAT networks at C- and Ku-bands (Naderi and **Campanella-1988**) .

The ACTS system has two modes of access and operation:

- 1) On-board stored baseband switched **TDMA, OSBS/TDMA**, and
- 2) A **SS/TDMA** system based on IF switching, with no on-board processing. System access and control is accomplished by the network's master control station, located at NASA Lewis Research Center, in Cleveland, Ohio.

The **OSBS/TDMA** (on-board processor) mode demodulates and stores the received signal, reroutes data from input to output storage locations, then demodulates and transmits on the downlink beam.

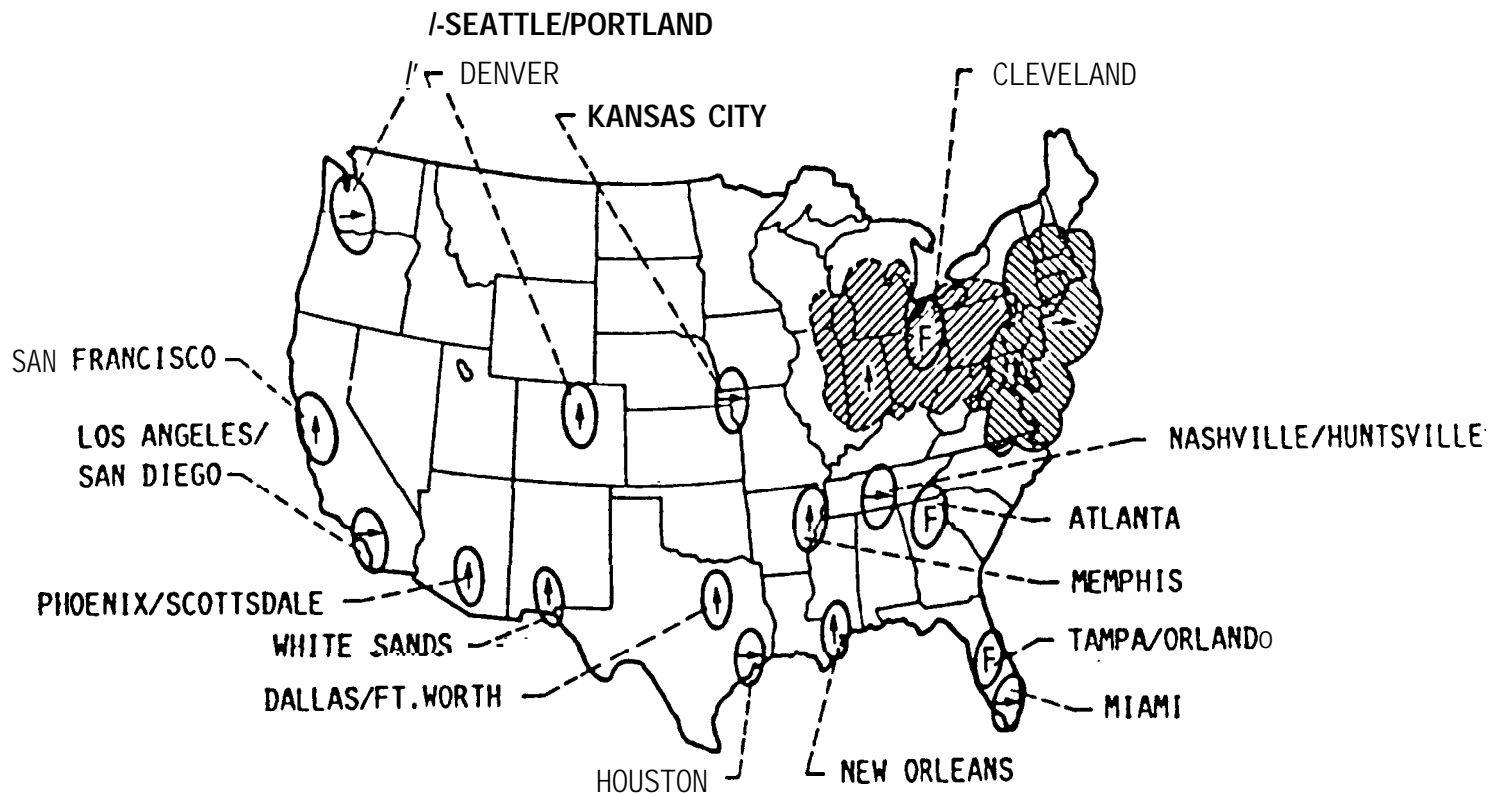
Serial minimum shift keying (**SMSK**) modulation is employed, with transmission rates of 110 or 27.5 Mbps on the **uplink** and 110 Mbps on the downlink

The **SS/TDMA** mode has no on-board storage or processing, other than switching. The system is designed to operate at a nominal burst rate of 220 **Mbps**, but other rates are possible. Since this mode is non-regenerative, ground terminals are not restricted in the modulation technique utilized for transmission.

Figure 7.2-5 shows the antenna beam coverage areas for ACTS. There are three fixed beams, focused on Cleveland, Atlanta, and Tampa, and two hopping beams. One of the hopping beams (vertically polarized) can hop to anywhere in the west sector (cross-hatched area on the figure indicated by a vertical arrow), or to any of the six fixed beam locations indicated by the vertical arrows. The second hopping beam (horizontally polarized) covers the east **sector**, and any of the seven fixed beam locations shown with horizontal arrows. A mechanically steerable antenna, not represented *on* the figure, is also included, which will provide a spot beam to anywhere in the disk of the earth as seen from the 100° West longitude location of ACTS.

Propagation measurements are an important element in the ACTS program, and will be accomplished both through the communications channels and with a set of three beacons available on the satellite. Table 7.2-2 summarizes the characteristics of the beacons on ACTS. The 27.5 GHz beacon and 20 GHz beacon pair operate through CONUS coverage antennas, providing a nominal **E.I.R.P.** of 13 dBw at edge of beam. The 27.5 GHz beacon is unmodulated, while one of the 20 GHz beacons will contain low rate telemetry data. The beacons will allow measurements of the classical propagation **parameters**, such as rain attenuation, depolarization, gaseous and cloud attenuation, diversity, and fade rate/duration.

Links operating in "the **OSBS/TDMA** mode are designed for about-a 5 **dB** clear weather margin, but terminals experiencing a fade can be



- SPOT BEAM
- F FIXED BEAM
- ↑ POLARIZATION

ACTS AT 0° LATITUDE, 100° W

STEERABLE ANTENNA WILL COVER ALL OF U.S. including ALASKA & HAWAII

Figure 7.2-5. ACTS Antenna Beam Coverage Areas

Table 7.2-2. ACTS Beacon Parameters

| Item | 27.5 GHz Beacon | 20 GHz Beacons |
|-----------------------------|--|--|
| Number of Beacons | 1 | 2 |
| Frequency (Polarization) | 27.505 GHz ±0.5 MHz (Vertical) | 20.185 GHz ±0.5 MHz (Vertical) 20.195 GHz ±0.5 MHz (Horizontal) |
| Modulation | None | FM and PCM (telemetry) |
| R.F. Power | 20.0 dBm | 23.0 dBm |
| Operating Temperature | -10 to +55 °C | |
| Frequency Stability | ±10 PPM over 2 yrs at constant temperature ±1.5 PPM over 24 hrs for -10 to +55°C | |
| Output Power Stability | ±1.0 dB over 24 hrs ±2.0 dB over full mission | |

provided an additional 10 **dB** margin by a dynamic rain fade compensation method incorporated in the processor. Fade levels are monitored at the terminals either by the ACTS **beacons**, or by direct monitoring of the communications signal. Once a predetermined fade threshold is exceeded and the master control station is informed, two corrective actions are implemented; forward error correction (**FEC**) coding and burst rate reduction. **Viterbi** convolutional coding with a reduction of the burst rate to 1/2 is employed.

Fade compensation in the **SS/TDMA** mode is accomplished by a dual mode traveling wave tube amplifier (**TWTA**), which can operate with output powers of 11 or 46 watts. Locations undergoing a fade can be switched to the high power **mode**, resulting in over a 6 **dB** improvement in margin.

ACTS, scheduled for launch in 1992, will be used for a series of technology verification experiments over a period of two to four years. NASA has issued information on the requirements for participation as an experimenter with ACTS and has encouraged participation in a wide range of technology areas (NASA-1987).

7.2.3.3 INTELSAT VI The first commercial satellite, Intelsat I, initially known as the Early Bird, was launched in a geosynchronous orbit above the Atlantic in 1965, providing 240 two-way telephone circuits and one TV transatlantic channel. It weighed only 38 Kg in orbit and was spin **stabilized**. Since 1965 over 100 commercial communications satellites have been launched to provide both domestic and international communications.

The latest addition to Intelsat's fleet of satellites will be the **Intelsat VI**. **Intelsat VI** is a dual-spin stabilized spacecraft, compatible for launch **by** either the Space Shuttle or Ariane IV. The major technological advancements of Intelsat VI include a sixfold reuse of the 6/4 GHz bands, the dynamic interconnection of six of the satellite's antenna beams for use with satellite-switched TDMA (paragraph 7.2.2.1), and a 10 year design life. The spacecraft provides a capacity of approximately 40,000 two-way telephone circuits plus two color-TV channels.

The antenna system consists of a 2 m diameter receive (6 GHz) and a 3.2 m diameter transmit (4 GHz) reflector; 1.12 m and 1.0 m diameter east and west spot beam steerable reflector antennas (14/11 **GHz**); and transmit and receive global horn antennas (6/4 **GHz**). The repeater system consists of 48 distinct transponders operating over the 6/4 GHz and 14/11 GHz bands. Frequency reuse through beam isolation and orthogonal polarization is employed at both frequency bands. The spacecraft thus has available a useful bandwidth of 3,200 MHz. Two 150 MHz, six 72 MHz, and two 77 MHz channels are assigned to 14/11 GHz. Twenty-six 72 MHz, two 41 MHz, and a maximum of ten 36 MHz channels are assigned to 6/4 GHz. Four of the 6/4 GHz, 36 MHz channels, as well as the two 41 MHz channels, provide permanent global coverage. Additional bandwidth of up to 72 MHz may

be switched to global coverage. Finally, considering the availability of the **hemi**, zone, spot, and global **coverages**, up to 1,389 MHz of bandwidth can be assigned to earth stations in the geographic areas of highest traffic density (A. Ghais, and et. al., 1982) .

The Intelsat VI provides static and dynamic interconnection capabilities to achieve the required signal paths from the receive to the transmit **coverages**. The spacecraft incorporates a 6x6 dynamic switch matrix which switches through a sequence of modes each frame and an 8x8 static switch which maintains a constant configuration for relatively long periods of time until changed by a new set of ground commands. The 6x6 dynamic switch provides full interconnectivity between two hemisphere beams and four overlaid zone beams. The 8x8 static switch provides full interconnectivity between the two 14/11 GHz spots, the six 6/4 GHz beams, and the two global beams.

The communications capability from Early Bird through Intelsat VI represents an increase in capacity by a factor of more than 150. The Intelsat system has maintained an amazing reliability factor of greater than 99.9 percent. Furthermore, it has achieved significant reduction in utilization charges.

7.2.3.4 DoD Missions The major role of t'he military in space activities today is for communication, navigation and observation. The Defense Satellite Communications Systems (**DSCS**) III and the Fleet Satellite Communication (**FLTSATCOM**) satellites are currently operational in worldwide military communications missions.

The DSCS III satellites consist of four synchronous satellites that provide reliable world wide communications to the United States defense forces throughout the 1980's and 1990's. Each three-axis stabilized satellite contains a Super High Frequency (**SHF**) communication payload consisting of multi-beam antennas and a six channel transponder **designed** for both FDMA and TDMA operation and real-time commendable uplink and downlink. By the early 1990's new

payloads enhancing mission capabilities are feasible. Possibilities include advanced wideband user and AFSATCOM payloads. The new wideband payload features **EHF links**, adaptive **nulling**, on-board respreading, and an active transmit array giving higher capacity and jammer protection. The AFSATCOM payload includes EHF and UHF links plus multichannel digital demodulation to give higher jamming protection and capacity in a **MILSTAR** backup role and to provide **EHF** telemetry/commanding. Both payloads will utilize satellite **crosslinks** to improve global netting.

The Fleet Satellite Communications (**FLTSATCOM**) satellites are a powerful addition to the world-wide Navy, Air Force, and Department of Defense (DoD) network for communications between naval aircraft, surface ships, and **submarines**, ground stations, Strategic Air Command and the Presidential command networks. Each satellite provides twenty-three communication channels in the 240 to 400 MHz UHF band and at SHF. The communications transponder features **channelized**, limiting repeaters to facilitate access to low-power users and on-board processing for anti-jam protection. Four **FLTSATCOM** satellites are needed in geosynchronous orbit to provide visible-earth coverage for the DoD strategic and tactical users. FLTSATCOM 7 and 8 are modified with additional EHF transition packages to upgrade anti-jam protection. **FLTSATCOM** 6, 7, and 8 now provide world wide service until the early 1990's, at which time the new **MILSTAR** spacecraft will take over strategic and tactical service, both at UHF and at EHF.

The trend in DoD satellite communications systems, as with commercial and international **systems**, is to higher operational frequency bands. The EHF bands, (44 GHz up/20 GHz down), will see extensive service commence in the early 1990's, with **MILSTAR**, **DSCS** III, **FLTSATCOM**, and **SDI** (Strategic Defense Initiative) baseline communications elements.

7.2.3.5 OLYMPUS-1 Olympus-1, formerly known as L-SAT (Large Satellite), is an experimental 3-axis stabilized satellite being developed by the European Space Agency (**ESA**) for advanced satellite

communications applications. It is a very large satellite, with a total span of 60 meters between solar panels, a transfer orbit mass of 2,300 kg, and a solar array power of **2.9 kW**. Satellite location is at 19° W **latitude**, with its control center at **Fucino**, Italy.

Olympus-1 consists of four separate payloads:

- 1) 12/20/30 GHz Propagation Package - for propagation measurements and experimenter
- 2) 14/12 GHz Specialized Services Payload - for business services experiments involving small customer premises earth terminals,
- 3) 17/12 GHz Direct Broadcast Satellite (**DBS**) Payload - for two channels of direct broadcasting services, and
- 4) 30/20 GHz Communications Payload - for point-to-point and **multi-point** communications applications.

Table 7.2-3 summarizes the characteristics of the Olympus-1 beacon package. All three beacons are coherently derived from a single frequency source. The 12.5 GHz beacon is transmitted through a full earth coverage antenna, which provides a signal to the entire earth sphere as observed from the satellite location. This provides coverage to all of Europe, South America and Africa, and to the east coast of North America. The 20 and 30 GHz beacons provide coverage through regional spot beams to Europe and North Africa only.

The 14/12 GHz Specialized Service Payload consists of four 30 watt transponders with an EIRP of 44 dBW. Each transponder can be subdivided into two TDMA data streams of 25 Mbps each, serving five spot beams covering most of Europe. Four of the five beams can be utilized in an IF switched **SS/TDMA** mode of operation.

The DBS Payload provides two channels, one for use by Italy, the other for the European **Broadcasting Union (EBO)**. A 230 watt TWTA is employed, with a peak EIRP of 63 dBW available.

Table 7.2-3. OLYMPUS-1 Propagation Beacons

| Frequency | 12.502 GHz | 19.770 GHz | 29.656 GHz |
|---|---|--|--|
| Polarization | Vert. | Vert. or Her. or switched (1866 Hz rate) | Vert. |
| EIRP (min.) | 10 dBW | 24 dBW | 24 dBW |
| Frequency Stability: Over 24 hrs Over any 1 yr Over 7 yrs | ±1.2 KHz ±36 KHz ±120 KHz | ±2 KHz ±60 KHz ±200 KHz | ±3 KHz ±90 KHz ±300 KHz |
| EIRP Stability: Over 1 sec Over 24 hrs Over any 1 yr Over 7 yrs | ±0.05 dB ±0.5 dB ±1.0 dB ±2.0 dB | | |

The 30/20 GHz Payload consists of two 40 MHz transponders and one 700 MHz transponder operating through two independently steerable 0.6° spot beams. Each TWTA is 30 watts, resulting in an EIRP of **51 dBW** for each of the spot beams. Videoconferencing, tele-education and wideband communications experiments? both **point-to-point** and **multipoint**, are planned.

Olympus-1 is scheduled for launch in 1989 on an Ariane launch vehicle, with an expected mission life of 5 to 10 years.

7.2.3.6 ITALSAT ITALSAT, the first satellite to be launched by the Italian Space Agency (ASI), is a wideband regenerative SS/TDMA system to be integrated into the existing Italian terrestrial telephone network, to improve performance and provide advanced access and routing techniques (**Morelli**, et al-1988). The satellite, to be located at 13° E latitude, is three-axis stabilized, with a payload mass of 255 kg, prime power of 1.565 Kw.

ITALSAT consists of three payloads:

- 1) 30/20 GHz **Multibeam** Payload - employing on-board baseband processing, for point-to-point and point-to-multipoint communications?
- 2) 30/20 GHz Global Payload - three non-regenerative transponders, for video and digital user services, **and**,
- 3) 20/40/50 GHz Propagation Beacon Package - for propagation measurements and experiments.

The **multibeam** package provides on-board demodulation at 12 **GHz**, and direct 4 phase **QPSK** demodulation at 20 GHz. The data rate is 147.5 Mbps, and the system operates with six 0.5° spot beams providing coverage throughout Italy and its islands. Six active repeaters provide a total capacity of 885 **Mbps**, equivalent to about 12,000 digital telephony circuits. 20 watt TWTA'S are employed, resulting in an EIRP for each beam of 57 dBW.

The global payload consists of 3 frequency translation transponders, each with a 36 MHz useable bandwidth, operating through a single 1.8° x 1.3° beam. EIRP is 46.2 dBW, with 20 GHz **TWTA's** also employed.

Table 7.2-4 summarizes the characteristics of the ITALSAT propagation beacon package. All three beacons are generated from the same master oscillator. The 18.7 GHz beacon is used as a telemetry relay, and is radiated on the global antenna. The 40 GHz beacon is phase modulated at 505 MHz to provide two sidebands for differential attenuation and phase measurements over a 1.01 GHz bandwidth. The 50 GHz beacon is switched between polarizations at an 1866 Hz rate, similar to OLYMPUS-1, to measure **cross-**polarization characteristics. The 40 and 50 GHz beacons are radiated from 3° horns, to provide coverage over most of Europe.

Table 7.2-4. ITALSAT Propagation Beacons

| Frequency | 18.685 GHz | 39.592 GHz | 49.490 GHz |
|---|---------------|--|---|
| Polarization | Vert. | Vert. | Vert or Her. or switched @ 1866 Hz rate |
| Modulation | PSK (512 bps) | PM (505 MHz) | None |
| EIRP (rein) | 23.7 dBW | 27.8 dBW 24.8 dBW (mod.) | 25 dBW |
| Frequency Stability: Over 24 hrs Over 5 yrs | | $\pm 3 \times 10^{-7}$ $\pm 3 \times 10^{-6}$ | |

The ITALSAT propagation measurements program is an ambitious effort involving a wide range of experiments and **experimenters**, and it will provide the first direct satellite path measurements at frequencies above 40 GHz (**Giannone, et al-1986**). **ITALSAT** is scheduled for launch in early 1991 on an Ariane 4 launch vehicle.

7.2.3.7 ATDRSS The current Tracking and Data Relay Satellite System (**TDRSS**) has for its main purpose the relaying of digital data from low-orbiting satellites to a single ground station, from where the data is distributed to the users that require it. The TDRS satellites themselves are geostationary bent-pipe satellites that will eventually replace the existing ground network of tracking and data relay stations. The Advanced TDRSS (**ATDRSS**) will upgrade the current system to satisfy user data relay requirements into the next century. This upgrade will include the capability of **TDRS-to-TDRS crosslinks** either at 60 GHz or at optical **frequencies**, together with the capability of relaying data directly to several ground **stations**, using **K_A** band links.

The capability of downlinking data to more than one ground station provides the opportunity to mitigate downlink rain fades by

the use of site diversity (paragraph 7.4.2.1), thereby **improving** system availability. In addition, other fade mitigation techniques such as adaptive FEC coding (paragraph 7.4.3.2) are being investigated for use with ATDRSS. The goal is to achieve a 99.9 percent system availability. This will involve consideration of service scheduling (Schwartz and **Schuchman-1982**) that will allocate downlink power in accordance with user needs rather than simply the transmission of fixed power levels. Because of the multiple ground stations, on-board beam switching will be used for downlink data transmission, which, together with downlink power control, provides an opportunity for significant downlink rain fade mitigation (paragraph 7.4.3.1.2) not possible with the current **TDRSS**.

7.3 DESIGN PROCEDURE

7.3.1 Introduction

The procedure presented in this Section is a general one, applicable to satellite communication systems of conventional design and application. Special purpose systems, unusual variants, or unusual system architectures will require modifications to the procedure. For example, those systems which employ adaptive power control or adaptive antenna beam control fall into the "unusual" category. Power budgets for some of the newer satellite communication systems are, presented at the end of this section.

The procedure is based on time percentage availability or outage as the primary and initial design criterion. Emphasis on this approach is necessitated by the fact that the largest amount of reliable propagation data is presented in time percentage terms. Where other criteria are important, different procedures may be necessary. But even where other criteria are employed, it is expedient to perform initial gross sizing calculations according to time percentage criteria.

As previously noted, the system design process is not a true synthesis. It consists rather of iterative analyses. The designer

begins with some rough "guesstimates" of parameters such as earth terminal antenna size, satellite RF power, along with a set of system requirements (coverage area or locations, **capacity**, connectivity, and service criteria). By employing analytic (not synthetic) **procedures**, the designer determines whether the initial parameters and the requirements/criteria are consistent. If not, additional iterations are made, with adjustments either to the parameters or to the requirements. This last point is not trivial: if there is a large disparity between calculated system performance and the **requirements**, it may be necessary to consult with the source of the requirements and agree to a change (e.g. , lower capacity **or** availability) . The final system design parameters should always be verified in as many variables as possible according to available data. Thus, although the initial design may have been performed using an availability criterion, it may be of interest and importance to predict outage duration **statistics**, if the **necessary** data are available.

7.3.2 Path Performance Versus Overall Channel **Performance**:. Availability Allocation

The typical satellite communication application involves two or four distinct links. For example, a telephone trunk system between Los Angeles (LA) and New York (NY) will involve these **links**:.:

LA to **Satellite**

Satellite to NY

NY to Satellite

Satellite to LA

If the performance requirements for this example specify the availability of a duplex telephone circuit between NY and LA, the system designer may be faced with a difficult problem. In general, finding the simplex, duplex, or (worst of all) system-wide availability with multiple earth terminal locations is a problem of considerable statistical complexity. Significantly, this problem is

unique to satellite **systems**, and is particularly aggravated at the higher frequencies. Also, symmetry applies in these systems. Statistical assumptions made and procedures developed for terrestrial systems, and for satellite systems below 10 GHz, may not be adequate for the applications to which this Handbook is directed.

Some sort of availability allocation is necessary, since most of the propagation data and procedures for applying them are oriented towards single path availability. The composite availability calculations involved are similar to multiple and redundant part reliability calculations. Each application will involve its own special considerations in the allocation process. Often, a worst case philosophy is applied in an attempt to simplify the problem. The following factors are relevant:

- . One end (terminal location) often has considerably worse rain statistics than the other.
- . **Satellite systems** are limited in downlink power; uplink power **margin** at the **earth** terminal is more readily obtainable.*
- . **Uplink** and downlink effects are quantitatively similar except for widely separated uplink/downlink frequencies (e.g., **30/20**, **43/20**), where attenuation factors in particular can differ substantially.
- . The **uplink** and downlink connecting to a given earth terminal have highly correlated propagation outage statistics.
- The propagation effects on paths between the satellite and two different earth terminals are uncorrelated.

Because of the variety of system concepts and frequency bands possible, general rules for allocation of availability cannot be given. The following may be of help in many cases of interest:

*A **very** important exception involves mobile or portable **terminals**.

- In a one-way (simplex) system, availability can be **suballocated** or **split** between the **UP** and **downlink** with considerable freedom.

Frequently, however, the downlink is the dominant (weaker) link. In other words, the working assumption is that the **uplink** non-availability is an order of magnitude smaller than the **downlink's**.

- . For a two-way (duplex) system, one of the following simplifications may be **applied**:

One end has much worse rain statistics than the other. Then, this duplex circuit can be treated as two simplex circuits with the majority of the outages on that end. On each of these simplex circuits, either the **uplink** **or** the **downlink**, whichever is worse, dominates the availability.

Assume initially that **uplink** margin is liberally available. The duplex link availability is then determined by the composite availability of **both downlinks** (**or**, the circuit outage time is the sum of the outages of each of the two downlinks).

Because the designer is forced by the procedure to iterate the design, errors introduced by simplifying assumptions made during the availability **suballocation** phase are corrected when performance verification analyses are made. For example, suppose the initial downlink design parameters were selected under the assumption that ample **uplink** margin **exists**, and that the **uplink** parameters were chosen to be as good as possible within economic constraints. In the final performance computation, the slightly less than perfect availability of the uplink is factored into the overall availability. Any shortfall relative to requirements can then be met by a small adjustment to the downlink parameters? in the next iteration of the design.

7.3.3 Summary of Procedures for Application of Propagation Data

The system design procedure presented here is based on criteria that take the form of discrete cumulative probability distribution functions of performance. In practice, three, two, or just one point on this distribution are given, for example, 99.9% probability that the baseband signal to noise ratio exceeds 20 dB. The worst (lowest probability) point of this set is usually considered to be the outage point or the non-availability threshold. In addition, a statement might be made about the time characteristics of the outage **events**, for **example**, the maximum acceptable value for the average duration. These criteria are usually for the baseband (e.g., voice channel) noise performance, or for the digital channel performance (e.g., error rate). The steps necessary to go from this set of requirements and propagation statistics to a system design are (see Figure 7.3-1):

INITIAL PHASE

- 1) Establish system performance requirements (discrete distribution of baseband/digital performance)
- 2) Apply modulation equations to convert system performance requirements to discrete distribution of the received composite CNR
- 3) Prepare initial design with parameters sized according to free space propagation conditions (apply power budget equations).

DESIGN SYNTHESIS AND TRADEOFF PHASE

- 4) Employ
 - a) Composite CNR distribution from step 2
 - b) System Architecture
 - c) **Multiple Access** Equations

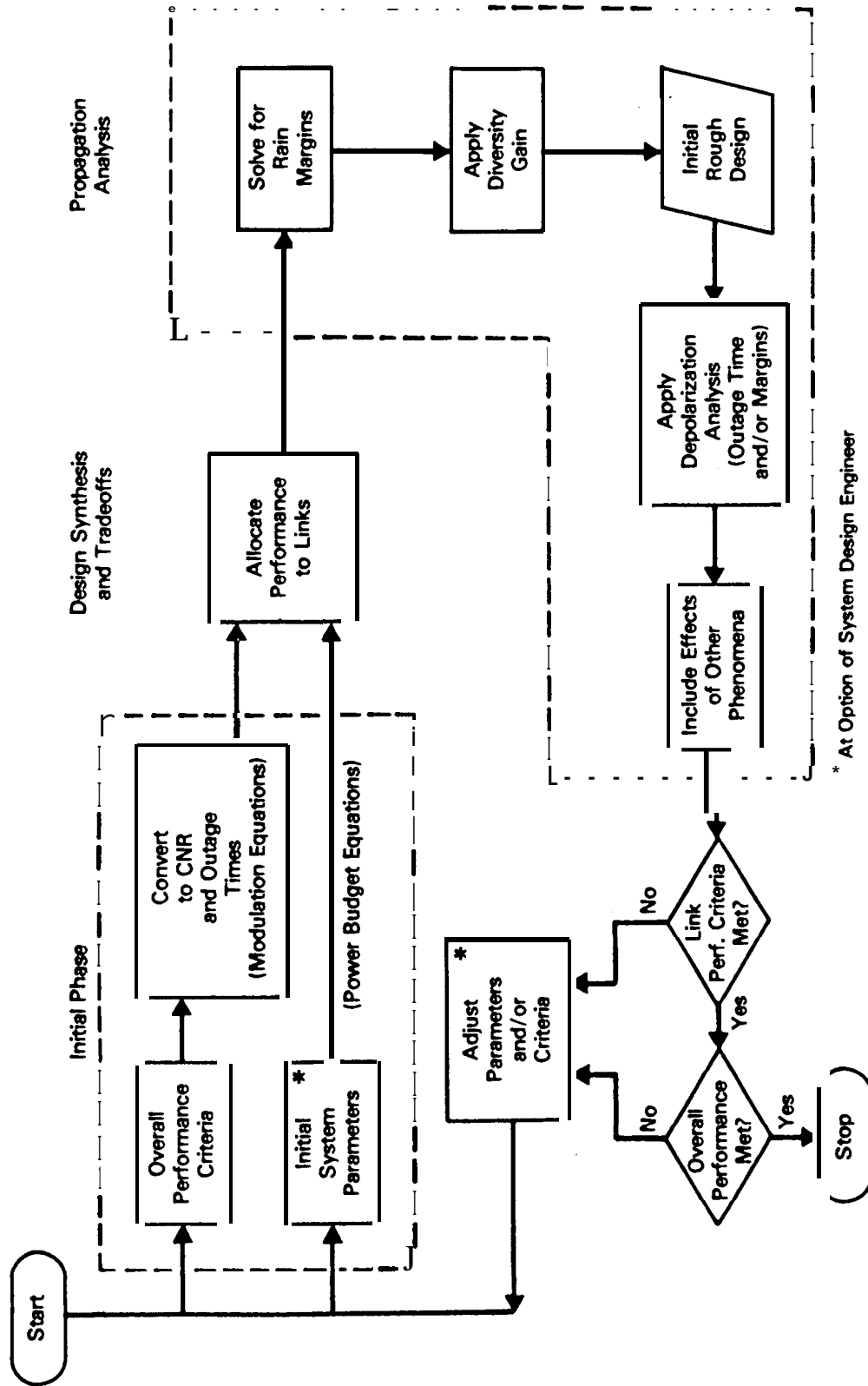


Figure 7.3-1. System Design Process

- d) Availability sub-allocation philosophy to develop distribution functions for CNR on each path.

PROPAGATION ANALYSIS AND ITERATION PHASE

- 5) Compute rain margins, as reduced by diversity **gain**, for each path.
- 6) Adjust system parameters according to margins given by step **5**. This gives a preliminary design at the feasibility concept level.
- 7) Apply depolarization analysis to adjust margins and/or increase the outage time values (% of time for the **worst-**performance level of the distributions).
- 8) Consider other propagation effects, adding margin to design as necessary.
- 9) Adjust system parameters to include all additive margins. Analyze system performance, first at the path level, then at the end-to-end performance level.
- 10) If** performance meets requirements closely, stop. Otherwise, adjust design and repeat analysis. If design cannot be made to meet requirements, consider changing requirements.

These steps will be considered in more detail in the remainder of this chapter. The most difficult step is 4 above. It is not possible to define a step-by-step "**cookbook**" procedure for this phase of the design process.

As indicated above, these steps may be grouped into three major phases. It is in the third phase that propagation phenomena and data are explicitly considered. Since the emphasis of this Handbook is propagation, a detailed exposition of the first two phases is not appropriate. However, some discussion is **required** because both performance criteria and the system **engineering** are profoundly

influenced by the pronounced propagation effects which apply above 10 GHz.

7.3.4 Specifics of Applications Initial Phase - Performance Specification of Digital and Analog Systems

The initial phase contains three steps:

- 1) performance requirements
- 2) conversion to received CNR requirement
- 3) initial design choices

Two examples will be used to illustrate the design procedure. The first step, to specify performance requirements, is now carried out for the examples. Additional information will be given for the systems in the example as they are developed further.

EXAMPLE 1 (Digital transmission system)

Requirement: One-way bit error rate of 10^{-6} or better for at least 80% of the time, and 10^{-4} or worse for a maximum of 1% of the time.

EXAMPLE 2 (Analog, duplex telephone trunking **system**)

Requirement: No more than 10,000 pWOp for at least 80% of the worst **month**, and no more than 100,000 **pWOp**, except for 0.3% of the time or less. (More than 500,000 pWOp is outage condition.)

The second and third steps are performed in parallel. Conversion from the basic performance criteria to receiver CNR requirements involves application of modulation equations. To apply the equations, the type of modulation* and other system parameters such as total link capacity need to have been selected. For the above two examples:

*"Modulation" is used in a generic sense **here**, to include **coding**, baseband processing, and the like.

- 1) The digital system is considered to operate, at a link data rate of 40 Mbps, employing quaternary phase shift keying (QPSK) and Rate 3/4 convolutional encoding with Viterbi decoding. This combination is assumed to operate with an E_b/N_0 of 10.3 dB for a BER of 10^{-4} , and 12 dB for 10^{-6} . The values of C/kT required are 86.3 and 88 dB-Hz, respectively. Because of the rate 3/4 coding, the symbol rate is $4/3 \times 40 = 53.5$ Ms/s and the CNR values in the symbol rate bandwidth are 9 and 10.7 dB for 10^{-4} and 10^{-6} BER, respectively.
- 2) The analog system is assumed to use FDM-FM with 120 channels and CCIR pre-emphasis characteristics. The following is a simplified version of the FM modulation performance equation (see Section 7.2.1.3):

$$(C/kT)_{dB} = 125.8 - 20 \log(\Delta f/f_{ch}) - 10 \log(pWOp)$$

From this, and the typical parameters $\Delta f/f_{ch} = 1.22$, the required values of C/kT are:

| <u>pWOp</u> | <u>C/kT</u> | <u>ξ</u> |
|-------------|-------------|-------------------------|
| 10,000 | 84.1 | 80 |
| 100,000 | 74.1 | 99.7 |
| 500,000 | 67.1 | N/A (defines outage) |

Note however that the FM equation only applies above "threshold." The threshold values of C/kT must also be determined. Since this system has a bandwidth of about 62 dB-Hz, the threshold values of C/kT and the threshold C/kTB are related:

$$(C/kTB)_{dB} = C/kT - 62$$

Thus, if this system is implemented with a conventional FM receiver of 12 dB C/kTB threshold, a C/kT of 74 dB will be at threshold, and this becomes the outage point. With an extended threshold demodulator (6 dB threshold), the 500,000 pWOp outage noise level and the demodulator threshold occur at about the same point, which is desirable.

To complete the first phase of design, it remains to select initial **values, ranges,** or limits of system parameters. Many of these may be implied by overall system requirements, such as coverage area or total number of channels. Others may be constrained by cost considerations or achievable levels of hardware performance. The primary parameters that must all eventually be specified are the frequencies of operation and the receive and transmit antenna gain, transmitted power, and receiver noise temperature of both the satellite and the earth terminal. We start by specifying as many of these as possible. In the subsequent design synthesis and trade-off phase, the parameter values are adjusted for consistency and the missing parameters are determined.

The initial parameters assumed for the digital example are the **following:**

- 1) 12 **GHz** downlink, 14 GHz uplink
- 2) 3-meter earth terminal antenna, if possible, but no greater than 5 meters in any case
- 3) Satellite EIRP (equivalent isotropic radiated power, power times gain) on the order of 40 dBW
- 4) Ground terminal *noise* temperature no less than 300K
- 5) Satellite antenna receive gain - 33 dBi
- 6) Satellite **receiver** noise temperature - 1000 K.

For the analog example, we start with the following parameter values:

- 1) 30 GHz **uplink**, 20 GHz downlink
- 2) Ground terminal figure of merit (G/T: ratio of antenna gain over noise temperature) = 40 dB/K
- 3) Earth terminal receiver noise temperature = 200 K
- 4) Satellite antenna transmit gain = 36 dBi

- 5) Satellite antenna receive gain = 33 dBi
- 6) Satellite figure of merit (G/T) = **3.dB/K.**

7.3.5 Design Synthesis and Tradeoff Phase

A general method of translating overall performance objectives into individual link objectives does not exist at this time for satellite systems operating above 10 GHz. Techniques have been developed for line-of-sight systems (Parker-1977 and GTE-1972), and satellite systems at lower frequencies (**CSC-1971**), but these have limited application in the present case. We present here some design tools that have been used in millimeter-wave system design. They include rules-of-thumb and simplifications that often apply, and more detailed procedures useful when the simplifying assumptions cannot be made.

At this point in the design procedure we have two functionally related parameters: a required composite C/N value, and the percentage of time for which this C/N applies. There may be several points of this function (the cumulative probability distribution function of C/N) specified. At some small percentage of time, the system is considered to be unavailable. At some larger percentage of time, a form of "degraded" operation might be **defined**, corresponding to a higher C/N value than the outage C/N. The present problem is one of assigning to each link of the system values of C/N and corresponding time percentages for which the values must be exceeded. Practically, this usually reduces to allocating outage time *or* availabilities among the links comprising the system, and allocating C/N values to the links in a way that is both compatible with the link outage time allocation, and achieves the required overall system performance.

7.3.5.1 Suballocation of Outages and Signal-to-Noise Ratio. One important element in this phase is the sub-allocation of outages. We have a specification on the permitted outage time for a service

or **circuit**, which comprises **2, 4,** or perhaps more **links**. It is clear that in general

$$\text{Outage}_{\text{total}} = \sum \text{link outages} + \left(\begin{array}{c} \text{jointly} \\ \text{determined} \\ \text{outages} \end{array} \right) \quad (7.3-1)$$

The definitions of link outages are usually obvious once the system architecture has been defined. If the permitted total outage time is small (**<1%**), the jointly determined outages are extremely small and can be ignored. For example, if **(S/N)_{composite} < 10 dB** is an outage, then for a bent pipe repeater either **(S/N)_{up} < 10 dB** or **(S/N)_{down} < 10 dB** would constitute link outage events. Now, a variety of combinations (e.g., **(S/N)_{up} = 13 dB** and **(S/N)_{down} < 13 dB**) can also result in an outage condition. However, assuming **uncorrelated** statistics and a small percentage of time **criterion**, these joint contributions can be ignored with only slight error, *since* they are very small. Therefore it is reasonable for the initial design, even with bent pipe repeaters? to **suballocate** the total outage time to **up-** and downlinks according to the rule

$$\left(\begin{array}{c} \text{total} \\ \text{outage} \\ \text{time} \end{array} \right) = \left(\begin{array}{c} \text{uplink} \\ \text{outage} \\ \text{time} \end{array} \right) + \left(\begin{array}{c} \text{downlink} \\ \text{outage} \\ \text{time} \end{array} \right) \quad (7.3-2)$$

Using this outage time **suballocation** is particularly appropriate in digital systems where only a few **dB** separate nominal and barely acceptable performance. The nominal performance analyses (not syntheses) are performed in iterations subsequent to the initial design. These performance analyses must not be neglected, however, since a system design that meets a particular outage or availability criterion does not necessarily meet its other performance criteria (e.g., nominal performance). This is particularly important in analog systems where there can be a wide gap between what is considered an outage and what is required most of the time. Since it appears that most satellite systems being designed for above 10

GHz are digital, this difficulty is perhaps academic. In **practice**, the use of availability **alone**, or in conjunction with **outage** duration characteristics, is prevalent in the design of such systems.

In Table 7.3-1, we give the simplifying rules of thumb which may usually be employed for **suballocation** of outage **time, T_{OUT}**. In the duplex case, the exact value of **T_{OUT}** relative to its upper and lower bounds depends on the type of repeater and on the joint statistics of outage (**i.e.**, the correlations between outages). The lower bound will apply if a perfect correlation of outages exists on the up- and downlink to a single terminal.

In general, the allocation of carrier-to-noise ratios among the several links is a more difficult problem. For the case of a **bent-pipe** repeater used for simplex **service**, the composite **carrier-to-noise ratio (C/N)_C** for the circuit is given by

$$(C/N)_C = \left[(C/N)_U^{-1} + (C/N)_D^{-1} \right]^{-1} \quad (7.3-3)$$

where **(C/N)_U** and **(C/N)_D** are the individual carrier-to-noise ratios on the uplink and **downlink**, respectively. Figure 7.3-2 illustrates the trade-off between **uplink** and **downlink** C/N defined by the equation. The combination of C/N values for a digital circuit through a processing (**demodulating-remodulating**) satellite repeater is different. In that case, it is the errors on the **uplink** and downlink rather than the noise power that are added. The C/N trade-off curve for a regenerative repeater would be similar to that in Figure 7.3-2, but with a sharper **"knee"** because of the high sensitivity of error probability to C/N.

Curves such as Figure 7.3-2 allow convenient selection of **uplink** and downlink C/N **values**, but in the absence of propagation **statistics**, there are no other criteria for **selection**. At the first

Table 7.3-1. Outage Time Allocation

Allocation Relations:

Simplex Circuit Outage

$$\tau_{OUT} = \tau_{AS} + \tau_{SB}$$

Duplex Circuit Outage Bounds

$$\tau_{AS} + \tau_{SB} + \tau_{BS} + \tau_{SA} \geq \tau_{OUT} \geq \text{Larger of } \left\{ \begin{array}{l} (\tau_{AS} + \tau_{SB}) \\ \text{or} \\ (\tau_{BS} + \tau_{SA}) \end{array} \right\}$$

Definition of Terms:

Total Outage Time : τ_{OUT}

Uplink outage, Terminal A to Satellite : τ_{AS}

Downlink outage, Satellite to Terminal B : τ_{SB}

Uplink outage, Terminal B to Satellite : τ_{BS}

Downlink outage, Satellite to Terminal A : τ_{SA}

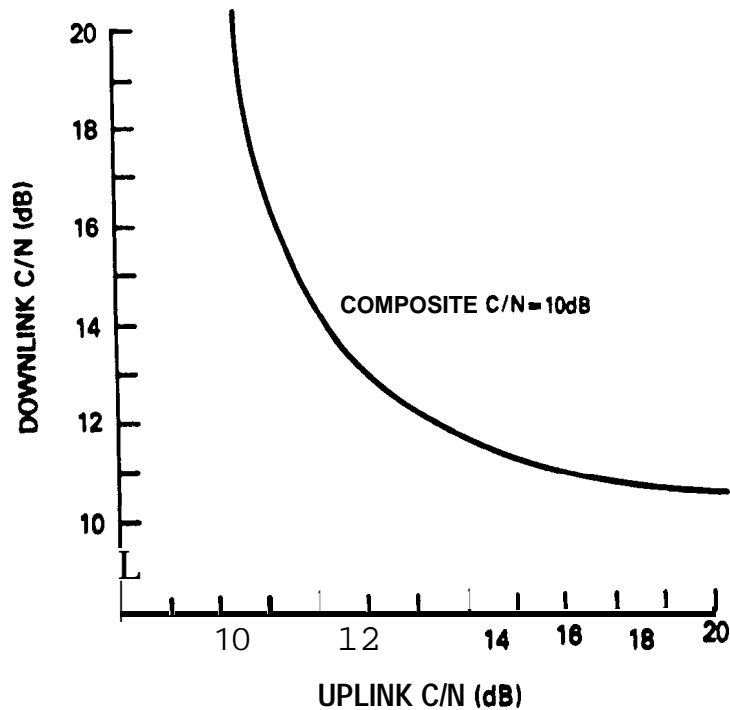


Figure 7.3-2. Uplink and Downlink Carrier-to-Noise Ratio (C/N) Trade-Off

iteration of the design synthesis **phase**, the selection is somewhat arbitrary. It will be refined in subsequent iterations. A good starting point may be equal C/N on both links. In this case, the link C/N must be 3 dB greater than the composite C/N. If allowed by system architecture? the **uplink** may be assigned a C/N value several dB more than that of the downlink because resources for achieving a high C/N (**e.g.**, high-power amplifiers) are more readily available on the ground.

7.3.5.2 ~~Power Budget Equation~~ The power budget equation relates the values of C/N or C/kT for individual uplinks or downlinks to physical system parameters. It defines the trade-offs possible between system components performance levels and is the basis of the

current phase of system design. In decibel form, the downlink power budget equation is:

$$C/N = P_t + G_t + G_r - L_{fs} - L_1 - L_{rain} - 10 \log_{10} [kB (T_r + T_{sky})] \quad (7.3-4)$$

where:

- P_t** = satellite transmitter power, dBW
- G_t** = satellite antenna gain, dBi
- G_r** = ground receiving terminal antenna gain, dBi
- L_{fs}** = free space path loss, dB
- L₁** = attenuation losses which are constant, especially gaseous absorption, dB
- L_{rain}** = attenuation from rain, dB
- k** = Boltzmann's constant, 1.38×10^{-23} J/K
($10 \log_{10} k = -228.6$ dB-K⁻¹-Hz⁻¹)
- B** = bandwidth, Hz
- T_r** = receiving terminal noise temperature, K
- T_{sky}** = sky noise temperature K

To calculate **C/kT**, the bandwidth **B** is simply left out of the equation. The equation for the **uplink** is the same except the satellite and earth terminal parameters are interchanged and **T_{sky}** is replaced with **T_{earth}**, the satellite antenna noise temperature increase due to the earth (discussed in Section 6.8.5). In these first phase iterations, one assumes **L_{rain}=0dB**, **L₁=0dB**, **T_{sky}=0** K or some small clear air value. Note that **(P_t + G_t)** is the satellite **EIRP**, and that **(G_r - 10 log T_r)** is often given as a single parameter, the terminal's Figure of Merit or **G/T**.

7.3.5.3 Further Development of Design Examples. For the digital system example, the following assumptions are made:

- 1) The system will be assumed to operate in a simplex (one-way) mode for purpose of availability calculation (the necessary acknowledgments of data are assumed to occur at much lower data rates, therefore much higher availability).
- 2) TDMA is assumed. Therefore power sharing in the repeater is not a problem.
- 3) For initial system design, we will assign the same **carrier-to-noise** ratio to both the uplink and the downlink.
- 4) Nominal (long term) propagation characteristics will be assumed to apply, on the average, on both up and downlinks at the same times. Outage level fades in up and down directions will be assumed **uncorrelated**.
- 5) No terminal diversity will be employed.

We now apply the power budget equation to the downlink for the digital example. From the initial system parameters given in Section 7.3.4, we have

- . Satellite EIRP = $P_t G_t = 40$ dBW
- . Earth terminal antenna receive gain = G_r
 $= 18.2 + 20 \log (\text{freq.}-\text{GHz}) + 20 \log (\text{diam.}-\text{m})$
 $= 18.2 + 20 \log (12) + 20 \log (3) = 49.3$ dBi
- . Bandwidth = symbol rate = 53.5×10^6
- . Free space loss = L_{fs}
 $= 92.4 + 20 \log (\text{range}-\text{km}) + 20 \log (\text{freq.}-\text{GHz})$
 $= 92.4 + 20 \log (35,780) + 20 \log (12) = 205.1$

The value of composite C/N used for the nominal (clear sky) condition will be that which must be exceeded at least 80% of the time, or **10.7dB**. From assumption 3) above and the C/N **allocation** formula of Section 7.3.5.1, we select downlink C/N = 13.7 dB.

Substituting into the power budget equation, we find the required ground terminal noise temperature:

$$13.7 = 40 + 49.3 - 205.1 + 228.6 - 10 \log_{10} (53.5 \times 10^6) - 10 \log_{10} T_r$$

$$T_r = 152 \text{ K}$$

We note that this violates the minimum value restriction of 300 K assumed at the outset. Suppose we determine from spacecraft design considerations that it is possible to double the output power of the satellite. Doing this, we have the compatible initial values,

- $T_r = 300 \text{ K}$

- $G_t + P_t = 43 \text{ dB}$

For the uplink in the digital example, we note from the initial parameter values assumed in Section 7.3.4 that everything is specified except ground terminal transmit power. We now use the power budget to find what value is required. First, we compute

- . Free space loss for 14 GHz downlink = $L_{fs} = 206.4 \text{ dB}$

- . Ground terminal transmit gain = 50.6 dBi

The power budget equation, again assuming a link C/N of **13.7dB** is required, gives the following

$$13.7 = P_t + 50.6 + 33 - 206.4 + 228.6 - 77.3 - 30$$

$$P_t = 15.2 \text{ dBW (approx. 30W)}$$

For the analog system example, we will proceed on the following assumptions:

- 1) Initial system sizing will assume equal carrier-to-noise density on the uplink and downlink. A better allocation for the duplex link, which cannot be made at this time, would be such that both the uplink and downlink at a given **terminal reach the outage**

threshold simultaneously (since there is no need to be capable of transmitting when one cannot receive).

2) **Outage** time will be split evenly between **uplink** and downlink.

3) Dual site diversity will be used if necessary to enhance availability on the downlink. We assume **uplink** diversity will not be necessary.

For the downlink, at 20 **GHz**, we have

- . Free space loss = $L_{fs} = 209.5 \text{ dB}$
- . Nominal (clear air) **C/kT** required is **3dB** more than the" composite **C/kT** that must be exceeded at least 80% of the time. Thus, downlink **C/kT** = 87.1 dB.
- . From Section 7.3.4, ground terminal G/T = 40 dB/K and satellite transmit gain = 36 dB.

We use the power budget equation to find the missing parameter, the satellite transmitted power P_t .

$$C/kT = P_t + G_t + G_r - L_{fs} - 10 \log_{10} K$$

$$87.1 = P_t + 36 + 40 - 209.5 + 228.6$$

$$P_t = -8.0 \text{ dBW}$$

The 30 **GHz** uplink power budget requires the ground terminal transmit gain, which is $20 \log(30/20) = 3.5 \text{ dB}$ greater than the receive gain. The receive gain is found from the specified G/T (**40dB**) and noise temperature (**200K**) to be $40 + 23 = 63 \text{ dBi}$ so the transmit gain is 66.5 dBi. Other parameters are

- . Satellite G/T = 3 dB
- Free space loss = $L_{fs} = 213 \text{ dB}$

We again solve for the" required ground terminal transmit power: -

$$87.1 = P_t + 66.5 + 3 - 213 + 228.6$$

$$P_t = 2 \text{ dBW}$$

It should be evident by now that, even prior to explicitly incorporating the various propagation elements, the system design process involves an iterative and interactive series of choices of parameter values. Each choice must be tempered by pragmatic considerations. There are in the above examples numerous unstated assumptions. For example, for the 12/14 GHz digital system, the earth terminal antenna diameter of about 3 meters is appropriate for a direct user-to-user application. Subsequent tradeoffs might influence a change to, say, 5 meters **at most**. It is not feasible, nor appropriate, to set down all of these system engineering considerations in this Handbook.

7.3.6 Propagation Analysis and Iterations Phase

7.3.6.1 Compute Rain Margin (less diversity gain) and Adjust System Parameters Accordingly. The rain margin is the increase in system transmission parameters (such as power or gain) needed to offset the attenuation caused by rain and other precipitation. Note that since precipitation also increases the effective noise temperature on downlink paths, the margin should include this effect as well. If the system employs diversity (particularly, but not exclusively, space diversity), there is an effective "diversity gain" which can be obtained. This diversity gain can be subtracted from the rain margin. These calculations are described in detail in Chapter 6 for rain and section 7.4 for diversity. The (possibly adjusted) rain margins must be applied on the up and downlinks in accordance with the performance **suballocation** decisions made in the previous phase. Once again, this is best illustrated through the examples.

We address the digital system example first. We will assume no measured attenuation or rain rate statistics are available, and will use the analytic estimation technique of Figure 6.3-1 (the Global Model). The location of the ground terminal is in climate region D3 at 35° N latitude and sea level, and the path elevation angle is 20°.

We are interested in the attenuation at 12 and 14 GHz exceeded 0.5% of the time. For this case, we calculate the horizontal projection distance of the path to be 9.9 km. The point rain rate exceeded in region D3 for 0.5% of the time is 7.8 mm/hr. The attenuation values exceeded for this time are predicted at 2.9 dB for 12 GHz and 4 dB for 14 GHz. The composite C/N for the circuit can be less than 9 dB for 1% of the time or less. Using an equal allocation philosophy, the carrier-to-noise ratio not exceeded on either link for 0.5% of the time should be 12 dB. With the current initial parameter values, the downlink clear air C/N is 13.7 dB. The rain attenuation expected would drop this to 9.7 dB, so at least 2.3 dB of downlink rain margin is needed. In a similar manner the required uplink margin is found to be 1.2 dB. The **uplink** margin could easily be provided by increasing the ground terminal transmitter power. The **downlink** margin can be gained either through an increase in satellite EIRP or ground station G/T. Rather than attempting to again increase the satellite **EIRP**, we shall exercise our option for 5-meter ground station antennas, which provides 4.4 dB more gain. (Note that ground stations located in drier climates may **meet** the availability requirements with 3-meter antennas.) Since a given ground terminal will presumably be used for transmitting as well as *receiving*, the antenna size increase also increases the ground station EIRP by 4.4 **dB**, providing more than ample uplink margin without increasing **the** transmitter power.

For the analog example, assume the same ground station location and path elevation **angle**. The outage time percentage of interest in this case is 0.15% for each link. The attenuation exceedance curves given by the computation of Figure 6.3-1 are shown in Figure 7.3-3. On the **downlink**, the attenuation exceeded for 0.15% of the time is 17.2 dB. From Figure 7.4-4, we see that up to 12 dB of diversity gain may be obtained at large separations. Here, we will assume that 10 dB can be achieved, so the attenuation exceeded is effectively 7.2 dB. Accompanying 7.2 dB of attenuation, there is (by Section 6.7.4) a sky noise increase of 220K. The noise temperature of the ground station (**200K** in **clear** air) increases by this **amount**, so the

downlink C/N is reduced by a total of 10.4 dB. Recall that the composite C/N was allowed to be 10 dB worse than the nominal value for 0.3% of the time. Thus, provided we can limit the uplink degradation to less than 10 dB for at least 0.15% of the time, the downlink is nearly sufficient as is. We shall increase the satellite transmitted power by 2 dB to -6 dBW to guarantee its adequacy.

We can now determine how many 120 channel trunks may share the satellite repeater passband. Given that FDMA requires that the power amplifier be "backed off" from saturation for intermodulation noise reduction, and that solid state transmitter technology is limited to a few watts, we may decide that about 8 trunk-paths should be established per transponder channel. Following established practice for lower frequencies, these transponder channels will be 35 or 40 MHz wide.

For the 30 GHz uplink, Figure 7.3-3 shows that the attenuation value exceeded 0.15% of the time is 38.2 dB. Recall that under clear air conditions, a 2 dBW ground terminal transmitter yielded $C/kT = 87.1$ dB on the uplink. For $C/kT = 77.1$ dB with 38.2 dB of rain attenuation, the transmitter power would need to be increased to 30.2 dBW, or more than 1 kW. Considering the losses in transmitter output components and waveguide runs, this may require a power tube of several kilowatts, which is not now technologically feasible at 30 GHz. To provide the required uplink margin, then, either the satellite G/T must be drastically increased, or we must abandon our original assumption of no uplink diversity. We choose the diversity route as the more feasible. (Uplink diversity presents a technological problem of its own: the switchover of uplink transmissions between diversity sites is more difficult and potentially more disruptive to circuit integrity than diversity switching of downlink signals.) See Section 7.4 for a more detailed discussion of diversity problems.

Let us assume that 100W or 20 dBW of output power is readily achievable in the ground station. This means that the effective

attenuation exceeded for 0.15% of the time cannot exceed 28 dB. This would require a diversity gain of at least 10.2 dB. Alternately, we may specify a diversity advantage (see Section 7.4.1). Figure 7.3-3 indicates that an attenuation of 28 dB is exceeded for about 0.3% of the time on the 30 GHz link. The required diversity advantage is therefore 2, which most available data (**Engelbrecht-1979** and Hogg and **Chu-1975**) indicates is easily obtained. With some foresight, we will stipulate **that 13 dB** of diversity gain is required for the uplink (or the diversity advantage must be 2.3). See Figure 7.4-1 for definitions of diversity gain and diversity advantage.

7.3.6.2 Apply Depolarization Analysis. The transmission of two orthogonally polarized signals from one satellite is employed to double the spectrum utilization by frequency reuse. Not every system, of **course**, will need to employ this **technique**, in view of the additional complexity and the added potential contribution to propagation caused outages.

The term "depolarization" is commonly employed to designate the reduction in cross-polarization discrimination seen at the receiving location under some propagation conditions. When this occurs, each of the two received channels (polarizations) contains an interference signal from the other polarization. Therefore, this signal is similar to interference which may occur from other satellites, terrestrial systems, or other beams **of** the same satellite.

Depolarization is caused by rain, as well as by ice layers, in the troposphere. The rain can cause strong depolarization events, in which the cross-polarization discrimination drops to 20 or 15 dB. Ice depolarization is quantitatively milder, but appears to occur more often. It is therefore convenient to treat two cases of depolarization effects, strong and weak.

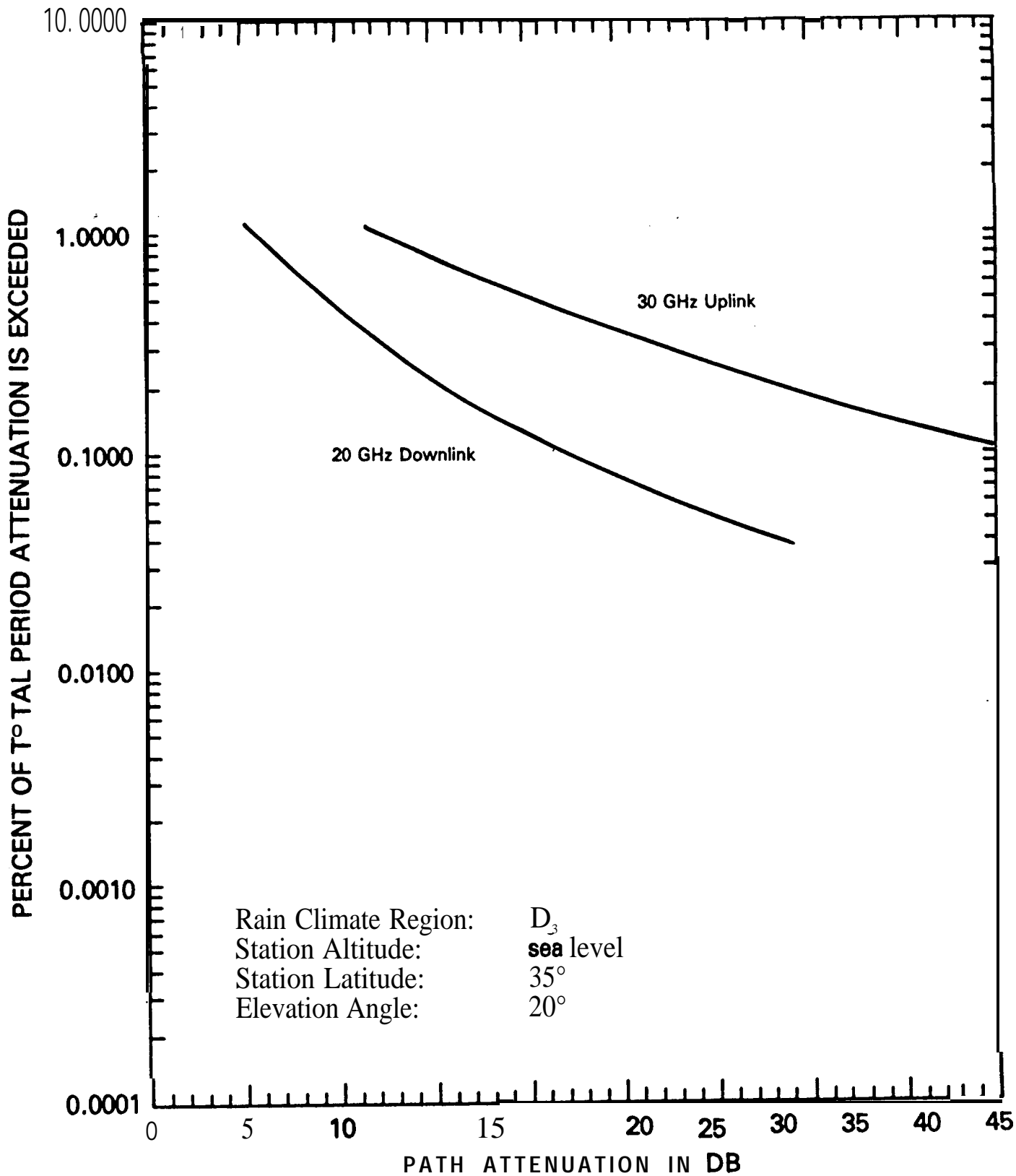


Figure 7.3-3. Analytic Estimate of Attenuation for 20 and 30 GHz Links of Example

Strong depolarization events should be correlated with deep attenuation **events**, since both stem from the same physical **cause**, namely rain. Both the deep attenuation fades and the strong depolarization intervals can cause outages. In order to perform a composite outage **analysis**, it is convenient to have joint statistical **data**, for example in the form introduced by Arnold, et. al. (1979). In Figure 7.3-4, we show a hypothetical version of such a joint outage plot. The parameter on the curves represents the threshold value of depolarization above* which the given system is **inoperable, i.e.**, an outage exists. It can be seen that there may be many combinations of attenuation and depolarization that will result in any given probability of outage. Typically, the threshold depolarization is not an independent variable, but is fixed by the modulation parameters. Then, it can be immediately determined whether the previously computed rain margin is sufficient for the desired system availability.

In most cases, such joint statistics are not available. Section 6.6 presents methods for prediction of depolarization statistics, including functional relationships between attenuation and depolarization statistics. Using these prediction methods, it is possible to approximate curves like those in Figure 7.3-4, though the exact shape of each curve will not be mathematically precise. For example, the curve for "percent of time attenuation or depolarization exceeded" for the depolarization parameter equal to -10 **dB** is essentially the same as the attenuation versus percent exceeded curve alone (since depolarization is effectively "never" so large). For intermediate values of the depolarization parameter such as -25 dB, the appropriate curve is horizontally asymptotic to the percentage of time that depolarization alone exceeds the percentage. Each such horizontal asymptote then smoothly curves

*Here depolarization **in dB** is given a minus **sign** so that the term "exceeded" can correctly **apply**.

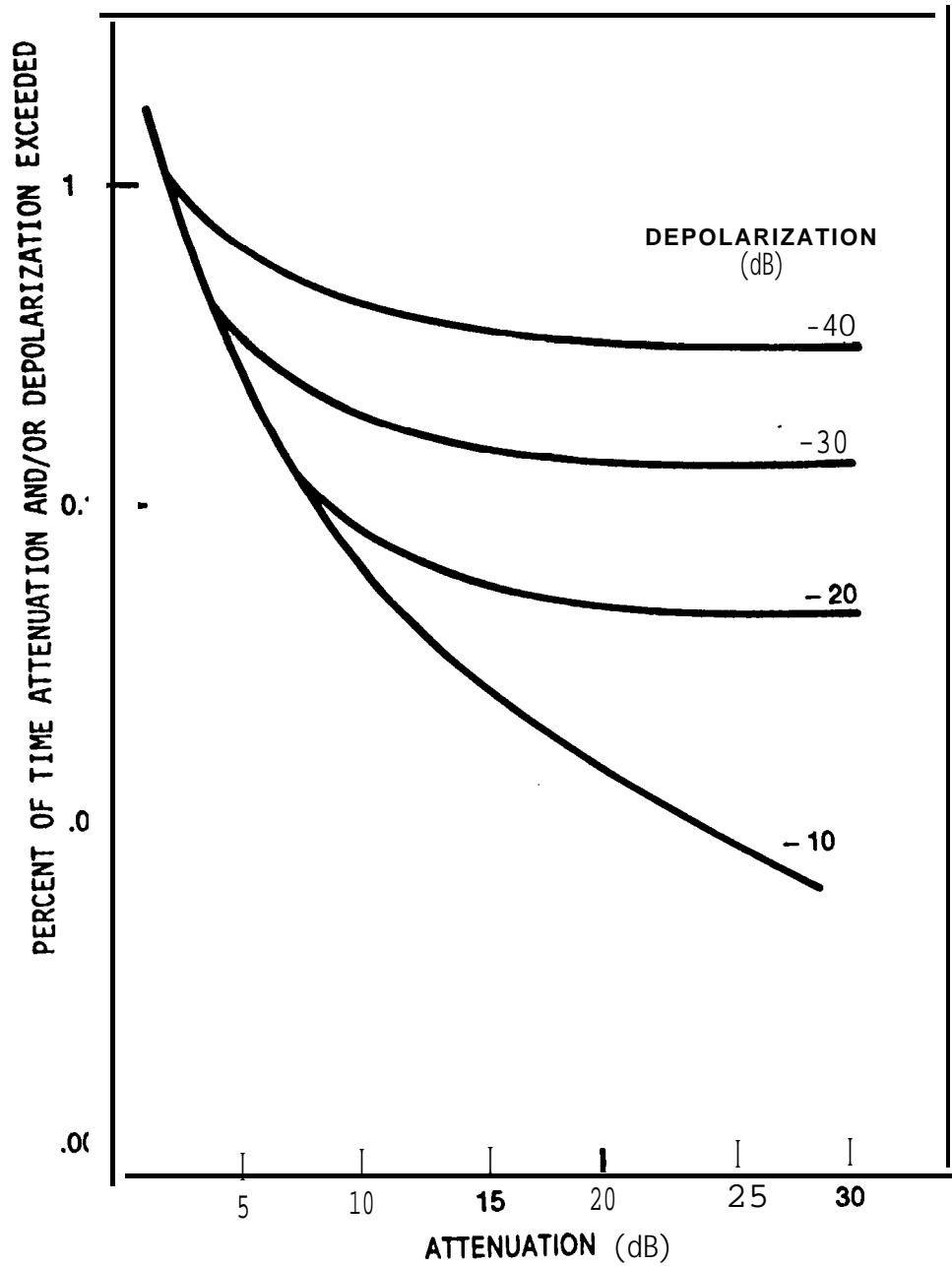


Figure 7.3-4. Composite Outage Versus Attenuation with Depolarization as a Parameter (Hypothetical Case)

into the attenuation only curve. Only this curved portion involves estimation by eye, and will introduce negligible error for initial design purposes.

The effect of diversity in reducing depolarization outage has received little attention to date (see Wallace-1981). The procedure outlined above applies to single-terminal attenuation and depolarization. When outages from attenuation and depolarization are each of the same order of magnitude, it is not clear that the concept of diversity gain (Section 7.4.1) is appropriate, since diversity should reduce depolarization outages as well.

In contrast to the "outage" values of depolarization, the smaller but more frequent values of depolarization can be accommodated in the system power margins. In almost all satellite communications systems, the thermal noise is the dominant portion of the **total** noise and interference. Small cross-polarized components may therefore be treated like any other interference. **Castel** and **Bostian** (1979) **point** out that depolarization on **digital** systems can be regarded as an equivalent C/N degradation. The equivalent degradation D due to depolarization for a **n-ary** PSK system is bounded by

$$D(\text{db}) < -20 \log [1 - (\log_{10} x/20) / \sin(\pi/n)] \quad (7.3-5)$$

where x is minus the cross polarization discrimination (**XPD**), in decibels. The effect of crosspolarization (and interference in general) on digital systems is considered more precisely by **Rosenbaum** (1970) and **Rosenbaum** and **Glave** (1974). The determination of link availability considering the equivalent degradation in combination with rain attenuation is discussed by **Wallace** (1981).

Similar procedures apply in analog systems. In practice, the equivalent noise powers from all thermal noise and interference **sources**, including intermodulation and depolarization are **added** together, in P_{WOp} for example, to produce a total link noise power

which must meet the appropriate performance criterion (e.g. , 10,000 pWOp). This adjustment to the system noise budget results in a further modification to the previously calculated system parameters. For example, the INTELSAT V system has been designed to meet a 10,000 pWOp criterion (Gray and Brown-1979). The composite received downlink must meet 7500 pWOp, with the remaining 2500 allocated to terrestrial and intersystem interference. This 7500 pWOp corresponds to a C/N of about 14 dB, yet the composite downlink thermal noise C/N is about 5 to 8 dB larger than this value, to allow for intermodulation products and for frequency reuse interference.

We do not consider here the employment of adaptive techniques to cancel cross-polarized components and to enable systems to operate at high levels of depolarization (e.g., 10 dB). By using such techniques, one pushes the outage threshold level of depolarization back to a value which effectively "never" occurs, so that the outages stem from attenuation alone.

7.3.6.3 Apply Lesser Propagation Effects. Attenuation effects from other than precipitation generally are of "second order" for system design purposes. Indeed, they may not need to be considered in the first iteration. They will be needed, however, for later, more accurate, estimates of performance.

"Clear air" attenuation, in excess of free space path loss, will typically be less than one or two dB except at the shortest millimeter wavelengths (greater than 50 GHz) or near absorption bands. These values may be calculated as shown in Figure 6.2-3. Adjustments are then made to the nominal performance power budgets (previously computed on a free-space-loss basis).

Cloud, fog, and dust attenuation factors may be very difficult to incorporate unless adequate statistics for their occurrence are available. These phenomena have significant effect only in unusual system designs, because the amount of attenuation is generally much less than that of rain. In general, a system with a fair amount of

rain margin will also have sufficient margin to operate through clouds . In addition, clouds and fog are not likely to occur so often as to influence the nominal performance value (50 or 80% of the time). Where appropriate, however, the system designer may incorporate an additional margin to allow **for** these attenuation effects. Similarly, signal fluctuations and antenna gain degradations, as treated in Paragraph 6.5, are relatively small and need be considered only in later iterations of performance **analysis**, at which time the effect can be accounted for through small margin adjustments to the nominal path loss.

7.3.6.4 Adjust System Parameters and Analyze System Performance.

In the foregoing, adjustment of system parameters has been carried out simultaneously with the development of the examples. The system designer may choose to use this approach, or to defer these adjustments until this point in the process. To do this in an organized manner, one should accumulate all propagation impairments which are (or can be equated to) attenuations or losses into a composite margin. Increases in sky noise, and the interference components? can be equated to losses in signal **power**, as previously discussed. This composite margin will be offset by power or gain adjustments. These margins and consequent system parameter adjustments are applied to the nominal system performance budget. In the analog example, this was the 10,000 pWOp criterion. Separately, the more severe effects which cannot be offset by (reasonable) margin are treated according to an outage criterion, **i.e.**, by addition of outages contributed by each. Adjustments to system parameters resulting from a deficiency in meeting this criterion often involve fundamental changes in qualitative system design rather than simply margin changes. As an **example**, if the outage time is excessive because the system concept is very sensitive to mild **depolarization**, it may be necessary to use a different type of polarization, adaptive polarization techniques or a different modulation technique.

In order to illustrate this step of the design process using the **examples**, a recapitulation of the constraints and parameters determined up to this point is in order. This is done in Table 7.3-2 for the digital system, and in Table 7.3-3 for the analog system.

The parameters for the digital system example from Table 7.3-2 are *now* used to carry out a detailed link power budget **analysis**, shown in Table 7.3-4. Here the power budget equation is applied to determine the C/N on the uplink and downlink separately. The individual C/N values are then combined to give the composite C/N. This is done for both the clear air *or* nominal case and the degraded case. The clear air budget includes an allowance of 0.5 **dB** for clear air attenuation (estimated using the data of Section 6.2.2), antenna pointing **error**, and other minor degradations. The degraded budget includes the rain attenuation exceeded for 0.5% of the time, as estimated earlier, and the increase in ground terminal noise temperature that is expected during the 0.5% **downlink** rain. This "sky noise" contribution was neglected earlier.

The nominal composite C/N for the digital *system* clearly exceeds the minimum required for at least 80% of the time (10.7 dB). When rain attenuation and sky noise have been included, however, the composite C/N is 0.4 **dB** less than the required value for 99% of the time (9.0 dB). We note that this deficiency can be easily made up by increasing the **uplink** transmitted power to 40W (**16dBW**), shown in parentheses in the Table 7.3-4 budget table.

The corresponding power budget calculations are carried out for the analog example in **Table** 7.3-5. In this case, the nominal composite C/N exceeds the minimum by nearly 4 dB, and the degraded value is 0.8 **dB** better than required. The 4 **dB** "overkill" under nominal conditions suggests that **uplink** power control would be advisable in this case to decrease the disparity in power level between the nominal and faded carriers in a transponder's passband.

Table 7.3-2. Digital System Summary

| | |
|--|--|
| <p><u>Specified Performance Criteria</u></p> | <p>Bit Error Rate $\leq 10^{-6}$ $\geq 80\%$ of the time $\leq 10^{-4}$ $\geq 99\%$ of the time (outage time $\leq 1\%$)</p> |
| <p><u>Modulation and Performance</u></p> | <p>Data Rate: 40 Mb/s Modulation: QPSK Coding: Rate 1/2, Convolutional Required C/N (in symbol rate bandwidth) BER = 10^{-4}: 9.0 dB BER = 10^{-6}: 10.7 dB</p> |
| <p><u>System Parameters</u></p> | <p>14 GHz uplink, 12 GHz downlink TDMA (no power sharing <i>or intermodulation</i> in satellite repeater)</p> |
| <p><u>Satellite Parameters</u></p> | <p>EIRP = 43 dBW G/T = 3 dB</p> |
| <p><u>Ground Terminal Parameters</u></p> | <p>Receive noise temperature = 300K Receive antenna gain = 53.7 dBi Transmit antenna gain = 55 dB Transmitted power = 15.2 dBW</p> |

Table 7.3-4. Digital Example Power Budgets

| | Uplink (14GHz) | Downlink (12GHz) |
|---|-------------------|--------------------|
| Transmit Power (dBW) | 15.2 (16)* | |
| Antenna Gain (dBi) | 55 | |
| EIRP (dBW) | 70.2 | 43 |
| Free Space Loss (dB) | -206.4 | -205.1 |
| G/T (dBK ⁻¹) | 3 | 28.9 |
| Boltzmann's Constant (dB) | -(-228.6) | -(-228.6) |
| Clear Air and Other Propagation Losses (dB) | <u>-0.5</u> | <u>-0.5</u> |
| Nominal Link C/kT(dB-Hz) | 94.9 (95*7)* | 94.9 |
| Reference Bandwidth, 80MHz (dBHz) | 79 | 79 |
| Nominal Link C/N (dB) | 1509 (16.7)* | 15.9 |
| Nominal Composite C/N (dB) | | 12.9 (13.3)* |
| Rain Attenuation, ≤0.5% of Time (dB) | -4 | -2.9 |
| Sky Noise Increase, 134K (dB) | <u> </u> | <u>-1.6</u> |
| Degraded Link C/N (dB) | 11.9 (12.7)* | 11.4 |
| Degraded Composite C/N, ≤1% of Time (dB) | | 8.6 (9.0)* |

* 40 Watt transmit power case

Table 7.3-5. Analog Example Power Budgets

| | Uplink (30GHz) | Downlink (20GHz) |
|---|-------------------|------------------|
| Transmit Power (dBW) | 20 | -6 |
| Antenna Gain (dBi) | 66.5 | 36 |
| Free Space Loss (dB) | -213 | -209.5 |
| G/T (dBK ⁻¹) | 3 | 40 |
| Boltzmann's Constant (dB) | -(-228.6) | -(-228.6) |
| Clear Air and Other Propagation Losses (dB) | <u>-1.5</u> | <u>-1.2</u> |
| Nominal Link C/kT (dB-Hz) | 103.6 | 87.9 |
| Nominal Composite C/kT (dB-Hz) | 87.8 | |
| Rain Attenuation, ≤0.15% of Time (dB) | -38.2 | -17.2 |
| Diversity Gain | +13 | +10 |
| Sky Noise Increase, 220K (dB) | <u> </u> | <u>-3.2</u> |
| Degraded Link C/kT (dB-Hz) | 78.4 | 77.5 |
| Degraded Composite C/kT, ≤0.3% of Time (dB-Hz) | 74.9 | |

The power budget shown for the analog system does not include some noise contributions that should be considered in the next iteration of the design. Those contributions include **self-interference**, interference from other satellite and terrestrial **systems**, and intermodulation in the satellite repeater. **Self-interference** may arise from crosstalk between frequency bands, orthogonal polarizations, antenna patterns, or combinations of the three, as determined by the system architecture.

7.3.6.5 Iterate System Design and Analysis. This phase needs little explanation. If the **initial** design does not, per **analysis,deliver** the level of performance required, the design must be changed in some way. Various trade-off techniques may be used to assist the design engineer in deciding what to change. The next section describes some of these techniques. In some cases, a critical look at the system requirements themselves must be taken. The examples that have been presented here were simplified in several respects, so that the several modifications to initial design assumptions could be made as the design proceeded. In an actual, real-world design, more refined analyses and iterations would be needed. Both of the examples used a particular terminal rain rate and elevation angle assumption. For a real system with a distribution of terminals in various locations, considerable refinement of the approaches would be possible, and could have significant impact in reduction of power requirements and/or outage times. Also, the examples did not illustrate the consideration of criteria other than long term (outage percentage) statistics.

7.3.7 Supplementary Design Tools

Techniques are available for assigning rain margins and allocating link performance parameters with more precision than has been used in the examples. We describe two of them here and provide references to others.

The first technique incorporates rain attenuation, sky noise temperature increase due to rain, and satellite repeater non-linearity into the carrier-to-noise trade-off relation given earlier. The composite carrier-to-noise ratio $(C/N)_c$ on a satellite circuit with rain effects is given by the formula

$$(C/N)_c = \left[(C/N)_U^{-1} L_U^{-1} + (C/N)_D^{-1} L_D^{-1} n(L_D) b^{-1}(L_U) \right]^{-1} \quad (7.3-6)$$

where

$(C/N)_U$ = clear air value of **uplink** carrier-to-noise ratio

L_U = uplink rain attenuation

$(C/N)_D$ = clear air value of downlink carrier-to-noise ratio

$n(L_D)$ = downlink noise power increase factor due to sky noise temperature

$b(L_U)$ = satellite repeater output power reduction factor due to decrease in input power

All the parameters in the formula are expressed as numerical values, rather than decibels. The factor $n(L_D)$ is the fractional increase in noise temperature (and therefore downlink noise power) corresponding to the downlink rain attenuation L_D . For example, by the formulas in Section 6.7.4, the increase in antenna noise temperature accompanying a rain producing a 5 dB fade is about 188K (assuming surface temperature = 290K). If the ground terminal clear sky noise temperature was 300K, then the temperature increase factor $n(5dB)$ would be $488/300 = 1.6$ (2.1 dB). The factor $b(L_U)$ is a function of the nominal operating point and the characteristics of the satellite repeater (typically a TWT operating near saturation). If the fractional output power reduction corresponding to an input power reduction (**uplink** loss, L_U) of 5 dB were 3 dB, then $b(5dB) = 0.5$.

Figure 7.3-5 shows the trade-off curve defined by the equation for three conditions. (All parameters are shown in decibels for convenience.) Curve A corresponds to the clear-air condition and is the same as Figure 7.3-2. For curve B we assume **uplink** rain only. It is curve A shifted up by the factor $b(L_U)$ (in decibels) and to the right by the uplink attenuation L_U . Curve C assumes downlink rain only, and it is curve A shifted up by the downlink rain attenuation L_D plus the noise temperature increase factor $n(L_D)$ (in decibels). If L_U is the uplink attenuation exceeded for P_D % of the time, then curve B gives the corresponding values of $(C/N)_U$ and $(C/N)_D$ that will achieve at least the required $(C/N)_C$ except for P_U % of the time, assuming no downlink rain. Likewise if L_D is the downlink attenuation exceeded P_D % of the time, then curve C gives the corresponding C/N combinations assuming no uplink rain. The intersection of the two shifted curves B and C is the combination of C/N values that gives at least the required composite $(C/N)_C$ except for $P_U + P_D$ % of the time, assuming uplink and downlink rain do not occur simultaneously. Since the probability of jointly determined outages is much less than that of uplink or downlink outages (see Section 7.3.5.1), this technique gives a good approximation to the values of $(C/N)_U$ and $(C/N)_D$ needed to achieve the required outage time percentage $P_U + P_D$. The method requires an initial allocation of outage time to the **uplink** and downlink. To optimize system parameters, it could be carried out for a range of allocations.

This technique, since it does not consider carrier **suppression**, interference or intermodulation **noise**, is most applicable to single carrier operation as in TDMA systems. The method is discussed by **Calo**, et. al. (1978) who carry out the computation of optimum uplink and downlink system parameters for a 12/14 GHz TDMA system. It is also used by McGregor (1981) in an example system design.

The second method of analysis to be described was used by Kittiver and Westwood (1976) in supporting the satellite-ground system design of the Satellite Business Systems network. This method, termed the Composite Margin Plane (**CMP**) analysis, permits a

precise calculation of link availability (or alternately, outage time percentage) given the rain attenuation statistics for the uplink and downlink and the "system performance parameters. The CMP analysis is based on the equation for composite carrier-to-noise ratio given earlier, but takes the **uplink** and downlink rain attenuations as the independent variables. Satellite repeater non-linearity and downlink sky noise are not considered explicitly, but may be allowed for. The equation for $(C/N)_c$, disregarding these terms, can be plotted on the L -L coordinates as shown in Figure 7.3-6. The region contained within the curve represents the combination of uplink and downlink attenuation values that will result in a composite carrier-to-noise ratio less than $(C/N)_c$, taken as the outage value. The **CMP** plot is dependent on the clear-air values of $(C/N)_u$, $(C/N)_d$, and $(C/N)_c$ assigned, so requires an allocation of these parameters at the outset. Its utility lies in the fact that the independent variables coincide with those of the measured (or predicted) attenuation statistics. To determine circuit availability (1-outage probability) we must calculate the integral

$$P_{avail} = \int \int P_{xy}(x, y) \, dx dy \quad (7.3-7)$$

$$(C/N)_c > \min(C/N)_c \quad (7.3-8)$$

where

- P_{avail} = availability
- x = uplink attenuation
- Y - downlink attenuation
- P_{XY} = Joint probability density function of X, Y

The CMP defines the boundary of the region of the X-Y plane over which the integral is carried out. On the boundary the "composite" rain margin is zero. Outside the boundary the margin is negative

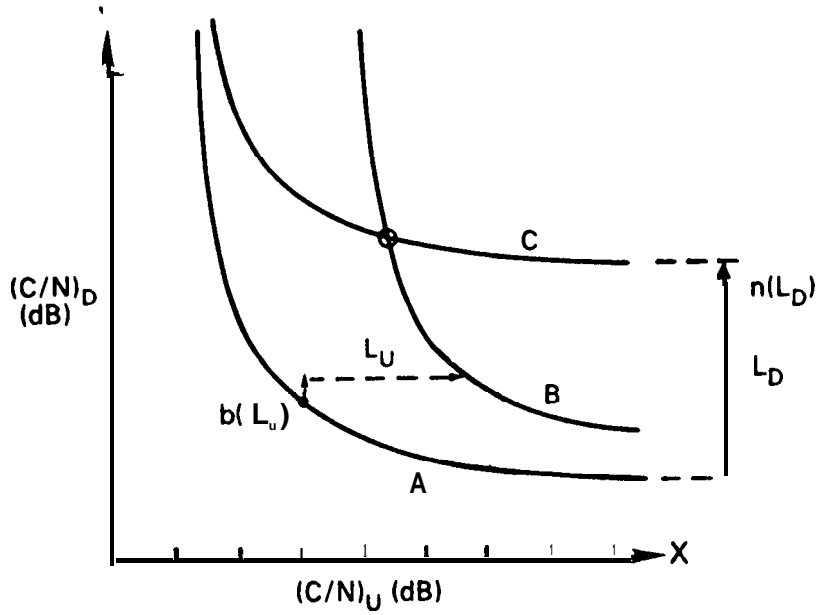


Figure 7.3-5. Uplink and Downlink Carrier to Noise Ratio Tradeoff

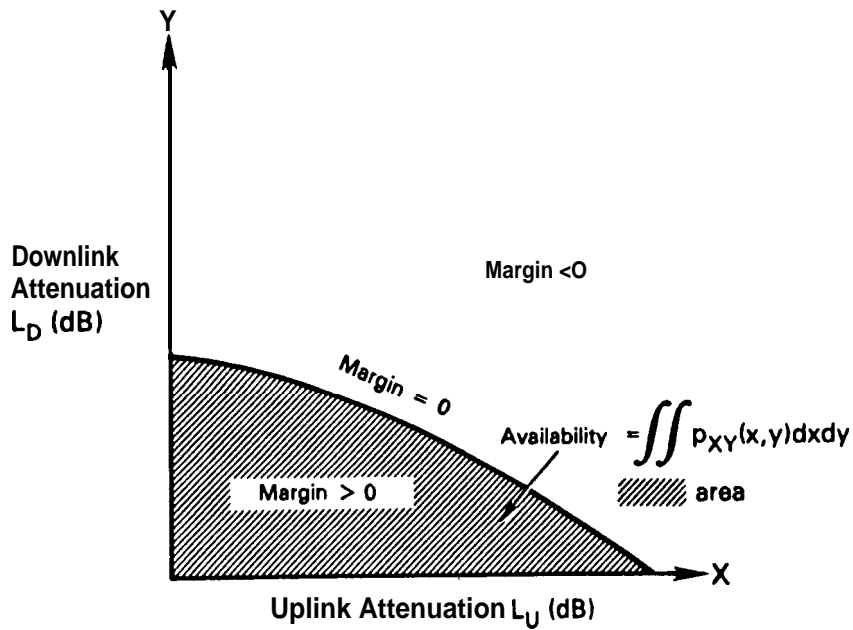


Figure 7.3-6. Composite Margin Plane

or the circuit is unavailable. The probability density function P_{xy} is given by the product of the **uplink** and downlink probability density functions (**pdf's**), which are in turn determined from the attenuation exceedance statistics plots for the **uplink** and downlink ground terminal locations. Since the joint **pdf** is taken as the product of the individual **pdf's**, we are implicitly assuming that the **uplink** and downlink attenuations are statistically independent, which is usually a reasonable assumption.

Kittiver and Westwood (1976) carried out the availability calculation by this method for 12/14 GHz circuit between Washington, **D.C.** and Atlanta, Georgia. The steps are illustrated in Figure 7.3-7, reproduced from the referenced paper. The **CMP** is shown in part (a) for the selected clear air values of $(C/N)_U$ and $(C/N)_D$. The dotted lines indicate that the C/N on each link is considered to be reduced by an implementation margin of 1.5 dB. The **CMP**, adjusted by this margin, is again modified by the downlink sky noise contribution. Part (b) shows the effect of downlink sky noise as an equivalent increase in downlink attenuation. Using part (b) to revise the ordinate of the **CMP** yields part (c). Part (d) shows the attenuation exceedance statistics measured for the up- and **downlink** locations at the respective frequencies. This is used to label the axes of the **CMP** with the **exceedance** percentages, as shown in part (e). Using the data in part (e), it is possible to graphically integrate the joint **pdf** and arrive at a value for the availability. Further details are given in the references.

A simplification of the **CMP** graphical integration is used by **Calo**, et. al. (1976) and **McGregor** (1981). The simplification consists of finding the sum of the integrals over two regions of the **CMP**, $L_U > L_{UMAX}$ and $L_D > L_{DMAX}$, as indicated in Figure 7.3-8. The approximate value of availability obtained in this way does not include the integral over the region bounded by the zero margin line and the L_{UMAX} , L_{DMAX} rectangle, but includes twice the integral over $L_U > L_{UMAX}$, $L_D > L_{DMAX}$. The unavailability (1-availability) given by this is equal to the probability that **uplink** rain reduces the margin

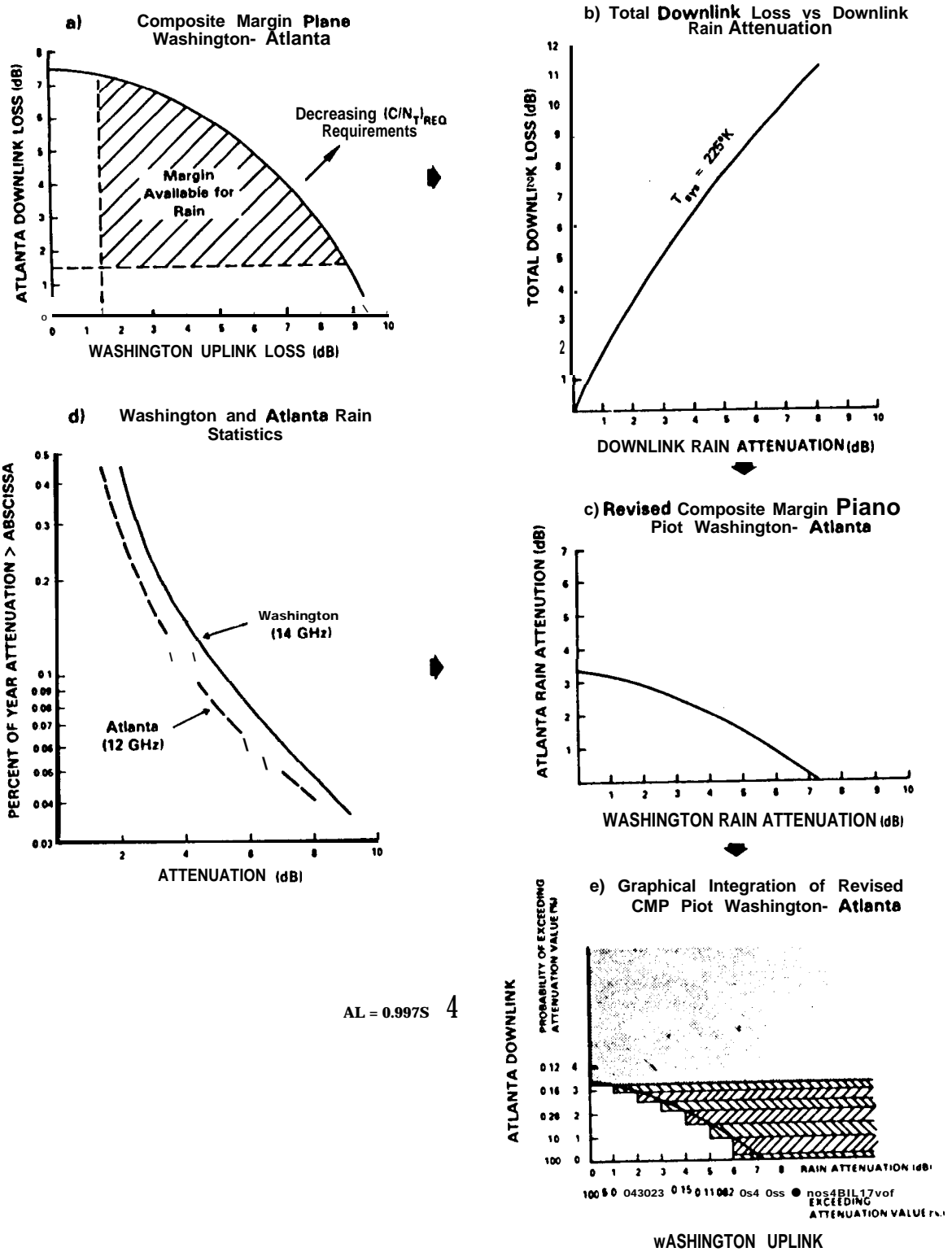


Figure 7.3-7. Composite Margin Plane Availability Analysis .
(from Kittiver - 1976)

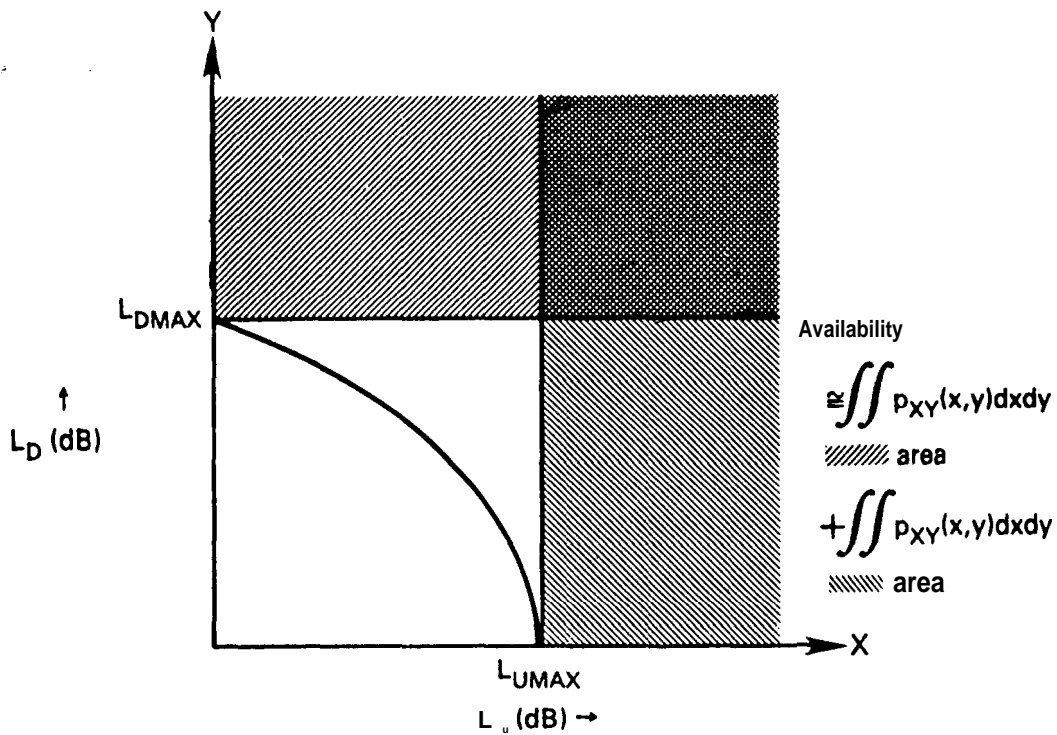


Figure 7.3-8. Approximate Composite Margin Plane Analysis

to zero with no downlink rain, or, that the downlink rain reduces the margin to zero with no **uplink** rain. Thus the approximation is the same as that used in the C/N trade-off analysis of Figure 7.3-4.

Other techniques for calculating system availability have been described in the literature. Lyons (1974, 1976) has performed statistical availability analyses including the effects of repeater non-linearity and limiting, intermodulation **noise**, and uplink power control in FDMA systems. Bantin and Lyons (1978) studied the effects of rain, scintillation, 'ground terminal antenna pointing error, and satellite station-keeping on system availability statistics. Because they require complex computer evaluation, the techniques described in these papers are not easily applied. Also ,

their use is limited to one or two multiple access configurations. McGregor (1981) presents a method of finding system availability that is general in its approach and does not require computer evaluation. The method allows one to find the **pdf** of the composite carrier-to-noise ratio for a satellite circuit, considering the characteristics of the multiple access **configuration**, the propagation effects statistics, and the statistical characteristics of the body of users accessing the satellite. In the referenced report, the method is applied to the availability analysis of a code-division (spread-spectrum) multiple access system.

7.4 RAIN FADE MITIGATION

There are, of course, several brute-force methods that can be used to combat **rain** attenuation. One method is simply to operate at as low a carrier frequency as possible. However, for reasons already discussed, satellite communication is going to higher rather than lower frequencies. Another method of combatting rain attenuation is to increase either the transmitter EIRP or the receiver G/T, or both, in order to improve the performance margin. However, because of technological, **regulatory**, and radio interference considerations, one can go only so far in raising system EIRPs and **G/Ts** to improve performance margins. In fact, rain attenuation statistics presented in Chapter 3 of this Handbook indicate that highly reliable satellite communication systems operating in the millimeter-wave bands above 20 GHz would need excessive power margins to mitigate rain fades. So other, more clever, means for mitigating rain fades are clearly needed for good system performance.

With a view toward commercial utilization of the 20/30 GHz satellite bands, researchers are investigating techniques for dealing with the problem in elegant and cost-effective ways. Much of this work (**Bronstein - 1982**) is sponsored by NASA as part of the Advanced Communication Technology Satellite (ACTS) program, which

has the goal of making the 20/30 GHz bands technologically accessible to U.S. industry (NASA - 1987).

The amount of rain attenuation is, of course, extremely time and space sensitive. For example, in many densely populated areas on the eastern seaboard of the United States, propagation impairments due to rain are especially acute because of the timing of thunderstorm activity. Thunderstorms occur predominately during the peak in communication traffic between the east and west coasts. Nevertheless, one can overcome this extreme spatial sensitivity by using various space diversity techniques to combat rain fades. Space diversity involves the use of two or more spatially separated links for redundancy. If, at some instant, one of the redundant links experiences a fade, a spatially separated link may not experience a fade at the same instant. So we can switch to the link that provides the better performance. Careful timing of link switchovers can overcome the time sensitivity of rain fades. Examples of appropriate space diversity techniques for combatting rain fades are:

1. Site diversity (multiple transmitting and/or receiving terminals), and
2. Orbit diversity (multiple satellites).

In a similar vein, one can combat rain fades either by adaptively adjusting certain signal parameters to existing propagation conditions, or by using redundant signals. For example, a link experiencing a fade at one frequency may not experience fading at another (lower) frequency. So one can switch to a frequency that provides acceptable performance whenever a severe rain fade occurs. Examples of appropriate signaling techniques for combatting rain fades are:

1. Transmitter power control
2. Adaptive forward error correction

3. Frequency diversity

4. Data rate reduction.

In this Handbook these signaling techniques are considered as possible implementations of "signal diversity" schemes.

These and other approaches (**Ippolito** - 1986, Brandinger - 1978, and **Engelbrecht** - 1979) have been suggested as techniques for significantly improving communication reliability in the presence of rain attenuation. More experimental results have been obtained for site diversity than for any other form of rain fade mitigation. However, system designers will want to consider combinations of all diversity options. Complexity and cost will play major roles in the ultimate decision to use any diversity technique.

The following sections discuss each of these techniques for rain mitigation.

7.4.1 Measures of Diversity Performance

To characterize the performance of diversity systems, one must establish suitable performance parameters. One such parameter in common use is "diversity gain". Suppose the rain attenuation on a single diversity branch (a single propagation path or a single carrier frequency, for example) is A dB at some instant. The attenuation will vary with time, so let $A(T)$ be the value of A that is exceeded T percent of the time. To obtain good fade statistics (and therefore an accurate estimate of T), we must assume that the attenuation has been measured over a sufficiently long time period. Now suppose additional diversity branches (site diversity or frequency diversity, for example) are introduced to reduce the effective rain attenuation. Let $A_{div}(T)$ be the value of A that is exceeded T percent of the time after diversity has been introduced. As illustrated in Figure 7.4-1, we can define the diversity gain (Hedge - 1974a) to be the difference between $A(T)$ and $A_{div}(T)$ at the value of T that has been selected:

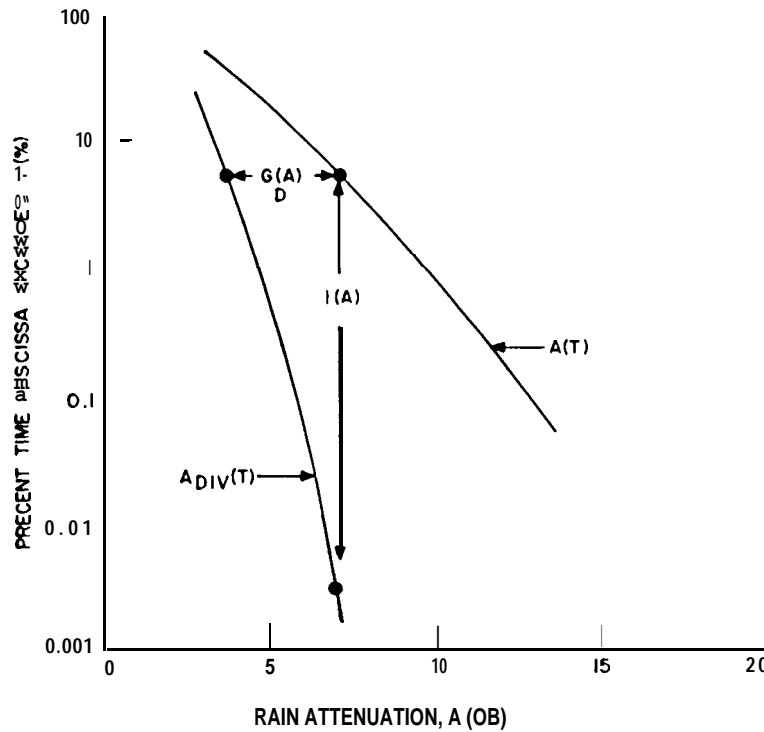


Figure 7.4-1. Definition of Diversity Gain and Advantage

$$G_D(A) = A(T) - A_{div}(T) \quad (7.4-1)$$

Another measure of diversity performance is "diversity advantage" (Wilson and Mammel - 1973). Let $T(A)$ be the percentage of time that some attenuation A (in dB) is exceeded when there is no diversity. Similarly, let $T_{div}(A)$ be the corresponding value of T when diversity is employed. As illustrated in Figure 7.4-1, we can define diversity advantage as the ratio of these two quantities at the selected value of A :

$$I(A) = \frac{T(A)}{T_{div}(A)} \quad (7.4-2)$$

If the system designer specifies that a given attenuation A (with or without **diversity**) may not be exceeded more than T percent of the time, then the diversity gain turns out to be the reduction in EIRP or G/T that the introduction of diversity **permits**, while maintaining the specified value of T . On the other hand, suppose instead that the system designer wants to specify the value of the

attenuation above which a rain-induced system outage is considered to occur. Then the diversity advantage is the factor by which the outage duration can be reduced by introducing **diversity, while** maintaining other system parameters such as EIRP and G/T constant. Clearly, these two parameters (diversity gain and diversity advantage) are not independent descriptors of diversity performance because Figure 7.4-1 shows that when one of the two parameters is known, the other is readily determined.

Up to now we have implicitly assumed that the fade statistics associated with each diversity branch are identical. In practice this is seldom the case. Attenuation statistics differ on the two branches either because of measurement uncertainty or because of real differences that exist among the diversity branches. A quantitative description of this effect would require more than one parameter to characterize diversity performance. But the use of only a single parameter is very convenient, and furthermore there is little reason a priori to assign more weight to one branch than to another. One way to get around this difficulty is to use average values for the single-branch attenuation and time **percentage, and to** define the diversity gain and diversity advantage as

$$G_D(A) = A_{ave}(T) - A_{div}(T) \quad (7.4-3)$$

$$I(A) = \frac{T_{ave}(A)}{T_{div}(A)} \quad , \quad (7.4-4)$$

which are simple generalizations of **eqs.** 7.4-1 and 7.4-2. The averages in **eqs.** 7.4-3 and 7.4-4 are over the possible diversity branches.

Allnutt (1978) used both diversity gain and diversity advantage to compare diversity data. He showed that the use of diversity gain allows trends and similarities to be readily observed, while the use of diversity advantage with the same data produces results with a large amount of scatter. In explaining these **observations,** Hedge (1982) pointed out that the use of diversity advantage requires

measurements over widely different time intervals. "Uncertainties in the values of $T_{ave}(A)$ and $T_{div}(A)$ being compared are therefore very different, which apparently accounts for the widely fluctuating values. A second drawback to using diversity advantage as a performance parameter is that it often cannot be defined when deep fades occur because the estimate of $T_{div}(A)$ for large A requires excessively long measurement times. These arguments suggest that data analysis and comparison are better done on the basis of diversity gain than diversity advantage. If required, diversity advantage can then be determined later, when the analysis in terms of diversity gain is complete.

7.4.2 Space Diversity

At carrier frequencies exceeding 10 GHz, rain attenuation often degrades earth-space propagation paths so seriously that the requirements of economical design and reliable performance cannot be achieved simultaneously. To overcome this problem, Hogg(1968) proposed the use of site diversity on earth-space paths to achieve the desired level of system reliability at reasonable cost. This proposal was based on the hypothesis that the intense rain cells that cause the most severe fading are rather limited in spatial extent. Furthermore, these rain cells are usually separated from one another, which means that the probability of simultaneous fading on two paths to spatially separated earth terminals is less than that associated with either individual path. Wilson (1970) first tested this hypothesis, using radiometric noise emission measurements to determine the rain attenuation on separated paths. Hedge (1974a) later tested the hypothesis, using actual earth-space paths. These and other ensuing experiments have demonstrated that site diversity is an effective technique for improving system reliability in the presence of rain attenuation.

Figure 7.4-2 shows a typical configuration employing site diversity. Also indicated are definitions of the following parameters, which are needed in later discussions:

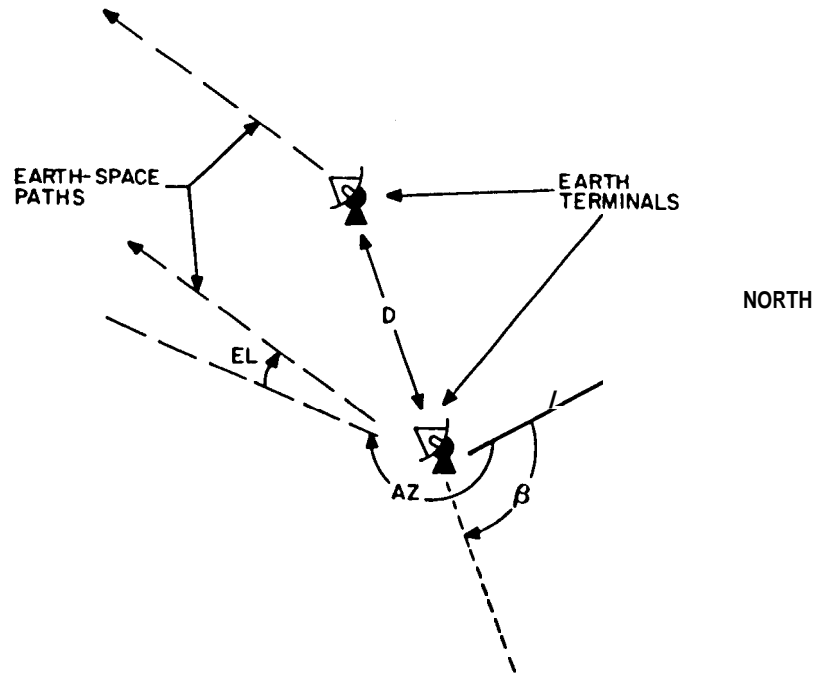


Figure 7.4-2. Site Diversity Configuration

AZ = azimuth of earth-space path (degrees)

EL = elevation of earth-space path (degrees)

d = distance between earth terminals (km)

β = orientation of earth terminal baseline (degrees)

Orbit diversity, on the other hand, uses only one ground site to communicate via two or more earth-space paths with satellites located in separated orbital positions, as illustrated in Figure 7.4-3. If a rain cell is far from the terminal, so that the cell is not likely to intercept more than one path to the **terminal**, the result will be similar to that for site diversity. However, if a rain cell is near the terminal, little improvement results because

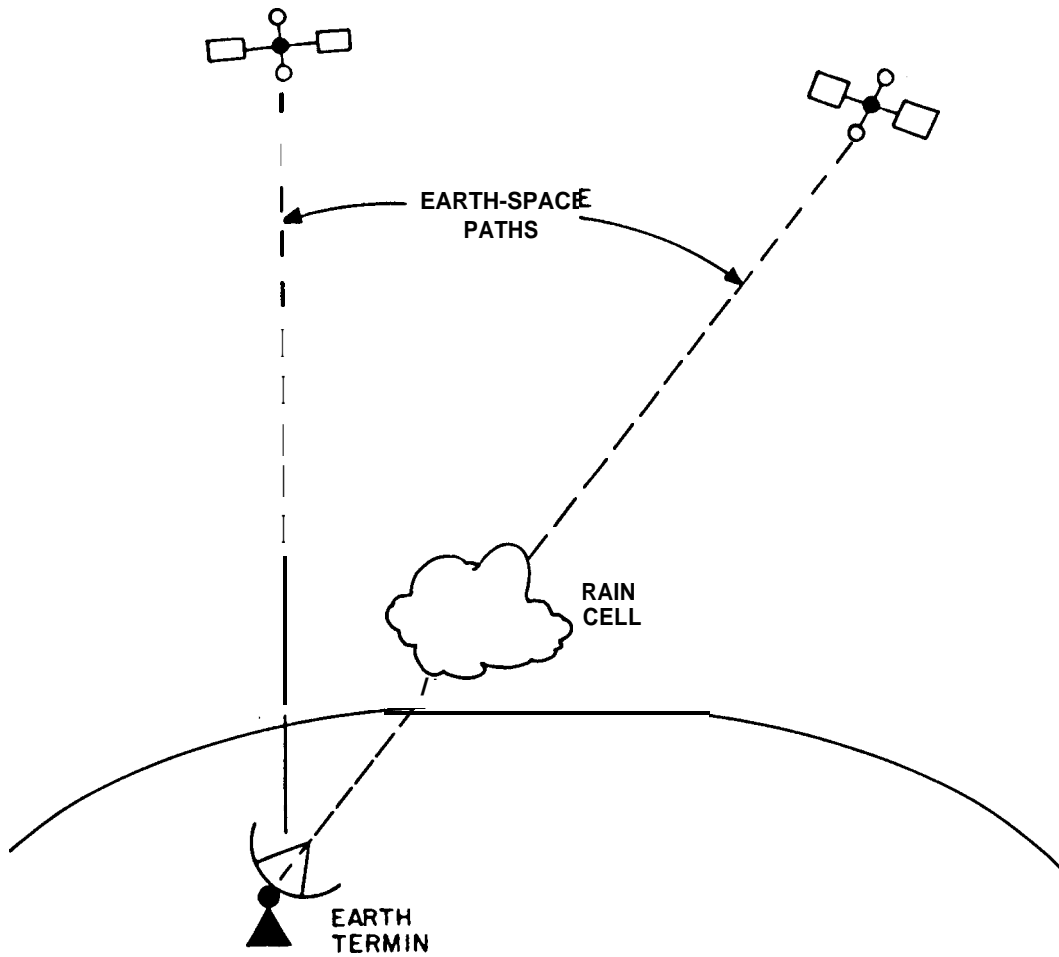


Figure 7.4-3. Orbit Diversity Configuration

all paths to the terminal pass through the same cell. **Orbit** diversity is therefore not as effective as site diversity in some cases. Nevertheless, in other situations orbit diversity can provide significant rain fade mitigation whenever multiple satellites are available.

7.4.2.1 Site Diversity

The following discussion of site diversity begins with a summary of numerous site diversity experiments that have been performed. Then, after discussing the various design factors that are required to quantitatively describe site diversity, some mathematical models for estimating the diversity **gain** that is achievable from site diversity are presented. The first model to be discussed is empirical in the sense that measured diversity data are fitted to simple equations in order to obtain formulas for the diversity gain. The second model is analytical in the sense that a definite statistical distribution for the rain attenuation is used to estimate the diversity gain.

7.4.2.1.1 Site Diversity Experiments

Table 7.4-1 presents a list of experimental diversity measurements available in the literature provided by Hedge (1982). [Additional information on diversity measurements can be found in Figures 4 and 5 of Annex I to Report 564-3 of **CCIR(1986)**.] This table includes the results reported for each of the four methods -- direct measurement of satellite beacons, radiometric measurement of the sky temperature, radar measurements of rain structures and radiometric measurements of **solar** emission. In each case the reference is cited along with the location of the **experiment**, the frequency, station separation distance, baseline orientation, path azimuth, and path elevation. In cases where multiple measurements are reported, the range of the appropriate parameters is indicated. A fifth method, rapid response raingauges, has been attempted, but has not been accurate "for predicting diversity gain. The two - reasons cited (**Allnutt-1978**) are: 1) the rainfall rate on the

Table 7.4-1. Summary of Diversity Experiments

1. SATELLITE EXPERIMENTS

| REFERENCE | LOCATION | FREQ. | SEPARATION(d) | BASELINE ORIENTATION (°) | AZ | EL |
|----------------------|---------------------|----------|---------------|--------------------------|----------|---------|
| Hedge (1974) | Columbus, Ohio | 15.3 6HZ | 4.0-8.3 km | 159-164° | 210° | 38° |
| Westinghouse (1975)+ | Washington, DC area | 20, 30 | 27.9 -75.8 | Several | ≈ 206° | ≈ 40° |
| Hodge (1976b) | Columbus, Ohio | 20, 30 | 13.2 -14.0 | 33-1510 | 197° | 40° |
| Vogel, et al (1976) | Austin, Texas | 30 | 11.0 | 0° | 172° | 55° |
| Hyde (1976) | Boston, Mass. | 18 | 6.7-35.2 | 74-93° | 212° | 36° |
| | Columbus, Ohio | 18 | 5.1-38.9 | 91-95° | 196° | 42° |
| | Starkville, Miss. | 18 | 8.3-40.0 | 105-113° | 190° | 51° |
| Hosoya, et al (1980) | Yokohama, Japan | 20 | 19 | 164° | 18B° | 48° |
| Suzuki, et al (1982) | Kashima, Japan | 20 | 45 | 0° | 190° | 48° |
| Tang, et al (1982) | Tampa, Florida | 19, 29 | 11, 16, 20 | 157, 244, 210 | 196-205° | 310-57° |
| Towner, et al (1982) | Blacksburg, Va. | 11.6 | 7.3 | 160° | 106° | 10.7° |

II. RAO10METER EXPERIMENTS

| | | | | | | |
|------------------------|-----------------------------------|---------|------------|----------|------|-----|
| Wilson (1970) | Crawford Hill, N.J. | 16 | 3.2-14.4 | 135° | 226° | 32° |
| Wilson & Mammel (1973) | Crawford Hill, N.J. | 16 | 11.2 -30.4 | 135° | 226° | 32° |
| Gray (1973) | Crawford Hill, N.J. | 16 | 19.0-33.0 | 4s.1350 | 226° | 32° |
| Funakawa & Otsu (1974) | Kokubunji, Japan | 35 | 15.0 | --- | 180° | 45° |
| Hall & Allnutt (1975) | Slough, England | 11.6 | 1.7-23.6° | 20-106° | 198° | 30° |
| Allnutt (1975) | Slough, England | 11.6 | 1.7-23.6° | 20-106° | 198° | 30° |
| Strickland (1977) | Quebec, Canada | 13 | 18.0 | 11° | 122° | 19° |
| | Ontario, Canada | 13 | 21.6 | 1° | 116° | 16° |
| Bergmann (1977) | Atlanta, Georgia | 17.8 | 15.8 -46.9 | 141-146° | 228° | 38° |
| | Denver, Colorado | 17.8 | 3301 | 86° | 197° | 43° |
| Rogers (1981) | Graz-Michelbachpers. Austria | 11.4/12 | 10.9 | --- | 164° | 33° |
| | Etam-Lenox, WV | 11.6 | 35 | --- | 114° | 18° |
| | Kurashiki City - Shimotsul, Japan | 12 | 17 | --- | 260° | 6° |

111. RADAR EXPERIMENTS

| | | | | | | |
|----------------------------|---------------------|--------|------|--------|----------|--------|
| Goldhirsh & Robison (1975) | Wallops Island, Va. | 13-18 | 2-20 | 0-180° | 0-360° | 45° |
| Goldhirsh (1975) | Wallops Island, Va. | 13-100 | 2-20 | 0-180° | 0-360° | 45° |
| Goldhirsh (1976) | Wallops Island, Va. | 18 | 2-20 | 0-180° | 0-360° | 45° |
| Hedge (1978) | Montreal, Quebec | 13 | 4-42 | 0-180° | 122-240° | 19-40° |

IV. SUNTRACKER EXPERIMENTS

| | | | | | | |
|------------------------|------------------|----|-----------|---------|-----|-----|
| Wulfsburg (1973) | Boston, Mass. | 35 | 11.2 | 158° | --- | --- |
| Funakawa & Otsu (1974) | Kokubunji, Japan | 35 | 15.0 | --- | --- | --- |
| Davies & Croom (1974) | Slough, England | 37 | 10.3 | 67° | --- | --- |
| Davies (1976) | Slough, England | 37 | 10.3-18.0 | 67-110° | --- | --- |

i Long-Baseline Site Diversity Experiment

ground cannot be accurately converted to a rainfall rate on the path, and 2) the rainfall-rate model giving the drop-size distribution is not accurate enough to calculate the attenuation on the path.

In the radar-based diversity experiments, an S-band radar was used to accumulate detailed reflectivity measurements of the space surrounding the radar during rain events. These data were then used to calculate the rain attenuation along hypothetical Earth-space paths through the rain volume by applying the observed relation between reflectivity and attenuation. Diversity results were obtained by hypothesizing parallel paths, with their endpoints separated by a given distance. Results from a large number of different path pairs and a number of rain events were used to derive attenuation statistics and diversity gain. Because this method does not actually require a pair of diversity **terminals**, it is **simple** to vary the terminal spacing and baseline orientation.

7.4.2.1.2 Site Diversity Design Factors

7.4.2.1.2.1 Separation Distance. Diversity gain depends strongly upon the earth terminal separation **distance**, d . The diversity gain increases rapidly as d is increased over a small separation **distance**, i.e., up to about 10 km; thereafter the gain increases more slowly until a maximum value is reached, usually between about 10 and 30 km. This maximum value is generally quite close to that value associated with uncorrelated fading at the individual earth terminals. Radar-based results, showing the variation of diversity gain with separation, are given in Figure 7.4-4.

In contrast to the **uncorrelated** case, one may argue that correlated fading may occur for paths separated by distances associated with typical rain cell separation distances. Such an effect may be inferred from the rainfall statistics of Freeny and Gabbe (1969); however, these statistics are associated with Point rainfall rates rather **than** path average rainfall rates. No definitive report of this effect has been published to date.

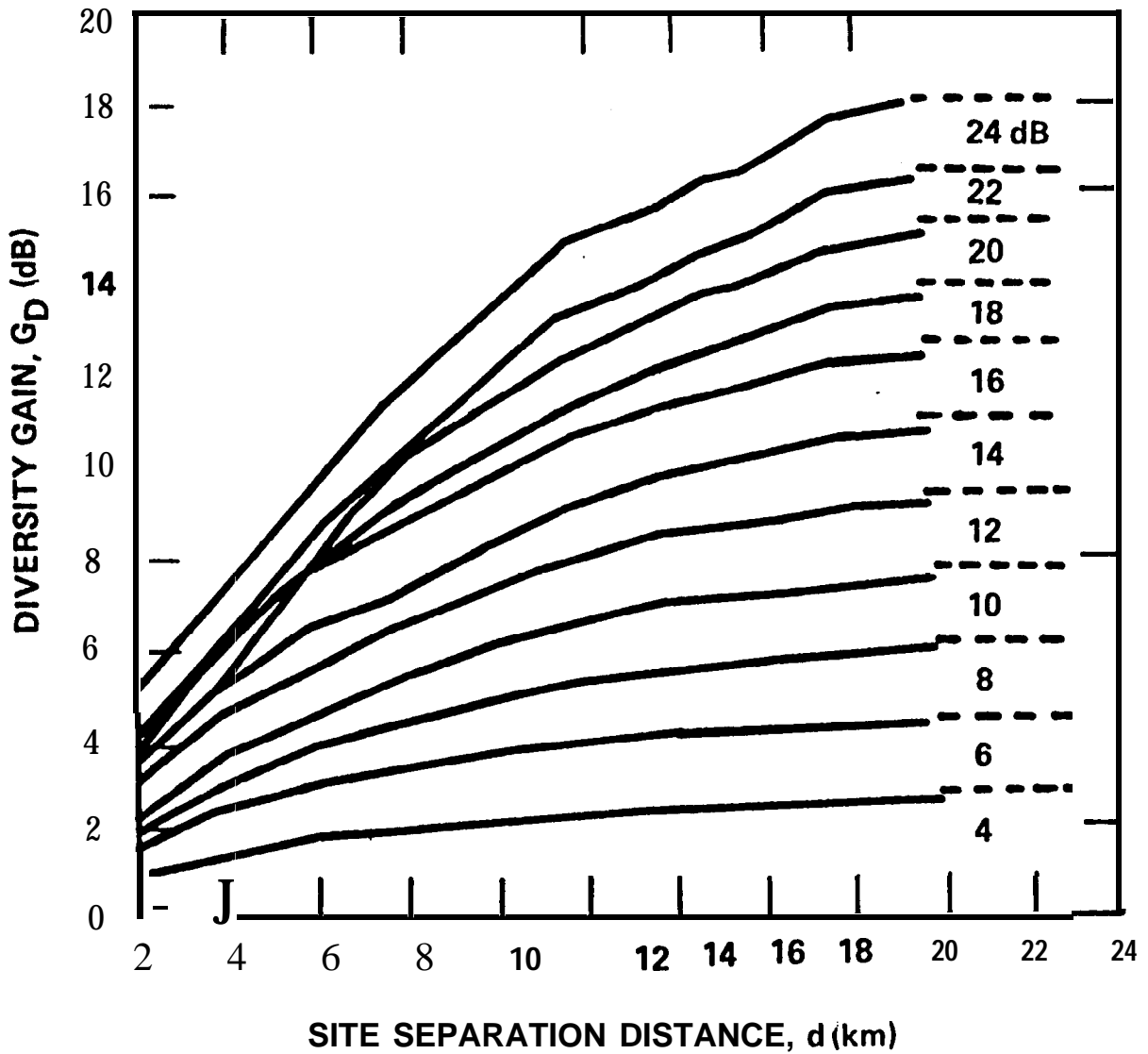


Figure 7.4-4. Diversity Gain, G_D , versus Separation Distance, d , for 18 GHz. (Horizontal Dashed Lines Represent Optimum Levels) (Goldhirsh and Robison-1975)

7.4.2.1.2.2 **Baseline Orientation.** The perpendicular separation between parallel paths is greatest when the earth terminals are located on a baseline perpendicular to the projections of the paths on the earth's surface. This arrangement minimizes the possibility of both paths passing through the same rain cell. Nevertheless, the dependence of diversity gain on baseline orientation is quite weak except, possibly, for very short separation distances.

Mass (1979) has shown analytically for circular rain cells over two ground station sites alternately positioned transverse and parallel to the earth-space path, that only a small (0.3 to 0.4 db) difference in diversity gain is to be **expected**. It is anticipated that the orographic effects will overshadow these orientation effects.

The baseline orientation problem is further complicated if spatial **anisotropy** of the rain **cells, i.e.,** a preferred direction of rain cell elongation, is known to exist in the region of interest. In this case, a baseline orientation perpendicular to the preferred axis of rain **cell** orientation would be desirable if the direction of the propagation path were ignored.

Considering both factors together, it appears that the most desirable baseline orientation is that which bisects the larger of the two angles between the projection of the propagation path and the preferred axis of rain cell orientation.

7.4.2.1.2.3 **Path Elevation Angle.** The separation distance required to achieve a given level of diversity gain increases as the path elevation angle decreases (Hedge-1978). This is due to the increased likelihood of path intersections with rain cells at lower elevation angles. This effect is coupled to the problem of rain cell anisotropy and path azimuth as noted below. Stated differently, the diversity gain decreases with decreasing elevation angle (**Allnutt-1978**).

7.4.2.1.2.4 Path Azimuth Angle. For synchronous satellites the path azimuth and elevation angles are not independent, and, thus, the dependence of diversity performance on these variables cannot be fully separated. If all rain cells were isotropic, one would expect no variation in diversity performance with azimuth angle other than that associated with the elevation angles. However, when rain cell anisotropy is considered, there appears to be a weak improvement in diversity performance for path azimuths in the southerly compass quadrant (in the northern hemisphere) that do not contain the preferred axis of rain cell orientation.

7.4.2.1.2.5 Link Frequency. Experimental measurements to date have shown a slight inverse dependency of site diversity gain on the link frequency for a given single-site attenuation over the 10-35 GHz frequency range (Hedge-1982). For link frequencies above 30 GHz, attenuation on both paths simultaneously due to uniform rain systems can be significant. This results in an apparent frequency threshold to the diversity gain (Kaul-1980) and will be discussed later.

7.4.2.1.2.6 Anisotropy of Rain Cells Along a Front. There is a tendency for convective rain cells associated with frontal activity to occur in bands nearly perpendicular to the direction of movement of the front. The direction of motion of the cells within such a band tends to be along or slightly ahead of the direction of the front. Furthermore, the more intense cells tend to elongate in their direction of motion (Harrold and Austin-1974). Thus, two types of **anisotropy** are evident. The first is associated with the elongation of individual cells and is related to the probability of parallel paths passing through the same cells. The second is associated with the statistics of the vector separation between rain cells and is associated with the probability of parallel paths simultaneously intersecting two different rain cells. Fortunately, these two preferred orientations are nearly parallel, and thus the same corrective action is required in each case. Namely, the baseline orientation should be nearly perpendicular to these preferred directions.

7.4.2.1.2.7 Local Climatology. To a first order of approximation it is commonly assumed that the probabilities of rain cell occurrence are uniformly distributed over rather large regions of the earth's surface. This assumption may be invalidated by the presence of any one of the following **features**: mountains, large valleys, large bodies of water, or urban heat "islands". These features can give rise to nonuniform spatial distributions of rain cell probabilities.

Spatial distributions of rainfall accumulation are readily available in the meteorological literature; however, it is not currently known whether the use of these data is applicable to the question of earth terminal siting. For example, it may be argued that these rainfall accumulations are dominated by low rainfall rates and thus do not reflect the spatial distributions of intense rain cells that produce high attenuation levels on earth-space, paths.

7.4.2.1.2.8 Switching Rates. The rate of change of attenuation on a single path is relatively slow. The highest rates reported are on the order of 0.6 dB/S at 11.8 GHz (Dintelmann, 1981) and 0.4 dB/S at 11.7 GHz (Nakoney, 1979), as reported in CCIR Report 564-3, Annex I (CCIR-1986). This implies that the decision and switching process for diversity paths may be quite slow and should pose no significant problem in the system design.

7.4.2.1.2.9 Connecting Link. The implementation of a path diversity system must incorporate a connecting link between the two earth terminals. If this link is closed, i.e., waveguide, coax, etc., its performance will be independent of meteorological variables and will not directly influence the reliability improvement provided by the use of path diversity. If, however, the connecting link operates above 10 GHz in the atmosphere, the joint fading statistics of the connecting link with the earth-space paths must be considered. This degrading effect appears to be small except for-

cases of very long baselines or baseline orientations parallel to the earth-space propagation paths (**Ferguson** and Rogers-1978).

7.4.2.1.2.10 Multiple Earth Terminals. Substantial link reliability improvements result from the use of two earth-space propagation paths. Thus one may conjecture that further improvement might result **from** the addition of additional diversity paths. Determination **of** diversity gain for N diversity terminals shows that most of the gain is realized for two terminals with very little further increase in gain for additional terminals (Hedge-1974b).

7.4.2.1.3 Empirical Model for Site Diversity Gain

7.4.2.1.3.1 Description of the Model. The data available from early diversity experiments in New Jersey and Ohio (Hedge-1974a, Wilson-1970, Wilson and **Mammel-1973**, Gray-1973) were used to develop an empirical model for the dependence of diversity gain on separation distance, **d**, and single site **attenuation, A** (Hodge-1976a) . The resulting model is of the form

$$G_D = a' (1 - e^{-b'd}) \quad (7.4-5)$$

where the coefficients a' and b' depend upon the single site attenuation according to

$$a' = A - 3.6 (1 - e^{-0.24A}) \quad (7.4-6)$$

$$b' = 0.46 (1 - e^{-0.26A}) \quad (7.4-7)$$

The empirical diversity gain model has been improved (Hedge - 1982) to include other factors besides single-site attenuation and separation distance. Based on data from thirty-four diversity experiments, the improved model takes into account the following variables, listed in decreasing degree of dependence

| | |
|-------------------------|---|
| Separation distance | d |
| Single-site attenuation | A |
| Link frequency | f |

Elevation angle EL

Baseline-to-path angle A

The variable **A** is the angle between the intersite baseline and the ground projection of the Earth-space propagation path, measured in such a way that $\Delta \leq 90^\circ$. Using the definitions of Figure 7.4-2,

$$A = |\alpha - \beta| \quad (7.4-8)$$

The improved model also eliminates the implication of the earlier model that diversity gain approaches a constant (3.6 dB) for very deep fades. This has been found to be incorrect in more recent experiments.

The model gives the diversity gain as

$$G_D = G_d G_f G_E G_\Delta \quad (7.4-9)$$

where each **factor** contains the dependence of the variable denoted by its subscript. The first factor is the same as the gain of the earlier model:

$$G_d = a(1 - e^{-bd}) \quad (7.4-10)$$

The regression **coefficients** are given by

$$a = 0.64A - 1.16 (1 - e^{-0.11A}) \quad (7.4-11)$$

$$b = 0.585 (1 - e^{-0.98A}) \quad (7.4-12)$$

The remaining factors are

$$G_f = 1.64 e^{-0.025f} \quad (7.4-13)$$

$$G_E = 0.00492(EL) + 0.834 \quad (7.4-14)$$

$$G_\Delta = 0.00177 A + 0.887 \quad (7.4-15)$$

In these formulas, d is in kilometers, A is in decibels, f is in gigahertz, and EL and Δ are in degrees. Figure 7.4-5 gives graphs of a , b , G_f , G_E and G_Δ to assist in application of the model.

The improved model predictions were compared with the original data set and produced an rms error of 0.73 dB. The data set used consisted of the results of thirty-four diversity experiments (including most of those listed in Table 7.4-1), covering a wide range of variable values.

Use of the empirical model is illustrated in Figure 7.4-6. It shows measured diversity gain as a function of average single-site attenuation for the VPI and **SU SIRIO** Diversity Experiment (Towner, et al - 1982). As indicated, the curve applies to one full year of data at 11.6 GHz. The figure also shows the predictions of the empirical model. The improved version of the model appears to give a better agreement with experimental measurements than the original version. However, the measured diversity gain falls well below that predicted for single site attenuation values above **about 11 dB**. The reason for this typical behavior is not **known**, but it could be attributed to the limited time period (one year), or to the especially low elevation angle (10.70).

7.4.2.1.3.2 Extension of the Empirical Model. Kaul (1980) has introduced meteorological considerations to the original empirical model which establish practical limits on the diversity gain depending on A , f , EL and other system parameters.

The extended empirical model considers that diversity gain is only realized when spatially nonuniform rain rates occur near the ground station. (A ground system imbedded in a uniform rain experiences zero diversity gain.) Convective (thunderstorm) rains are assumed to represent these non-uniform rain systems. Rice and **Holmberg** (1973) described rain types analytically as Mode 1 (thunderstorm) and Mode 2 (**stratiform**) rains (see Section 3.2). Using the Rice and **Holmberg** model, the cumulative distributions of

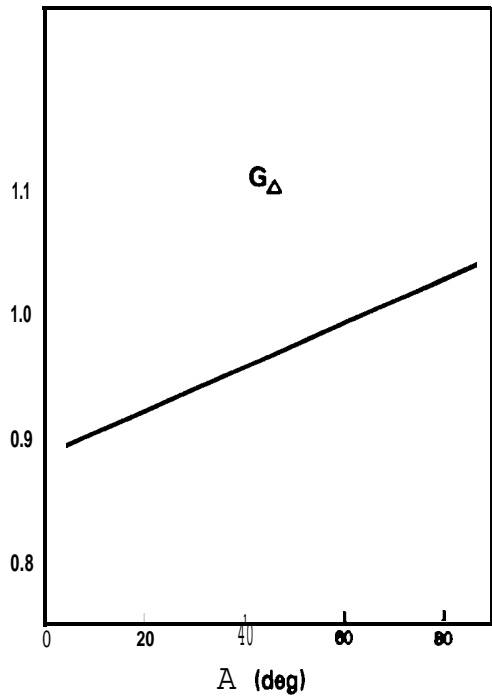
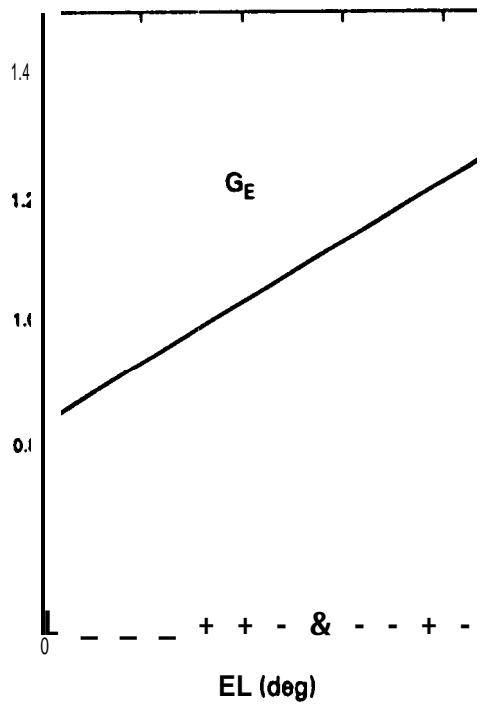
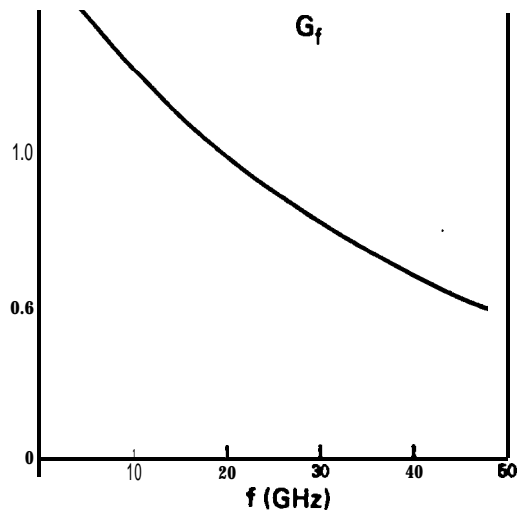
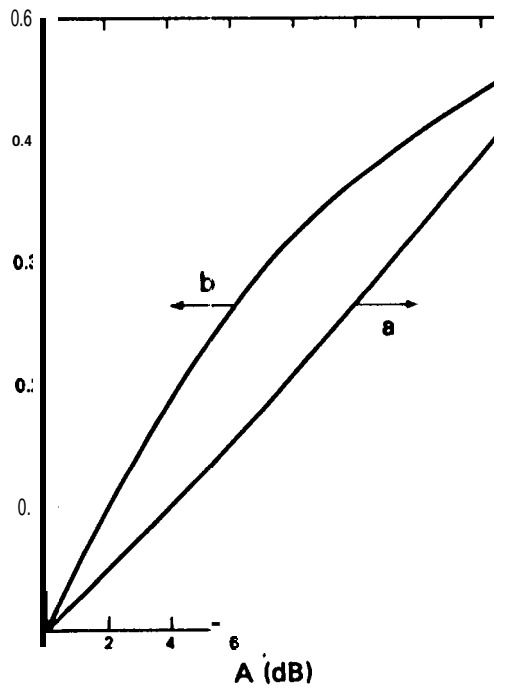


Figure 7.4-5. Parameters of Improved Diversity Model

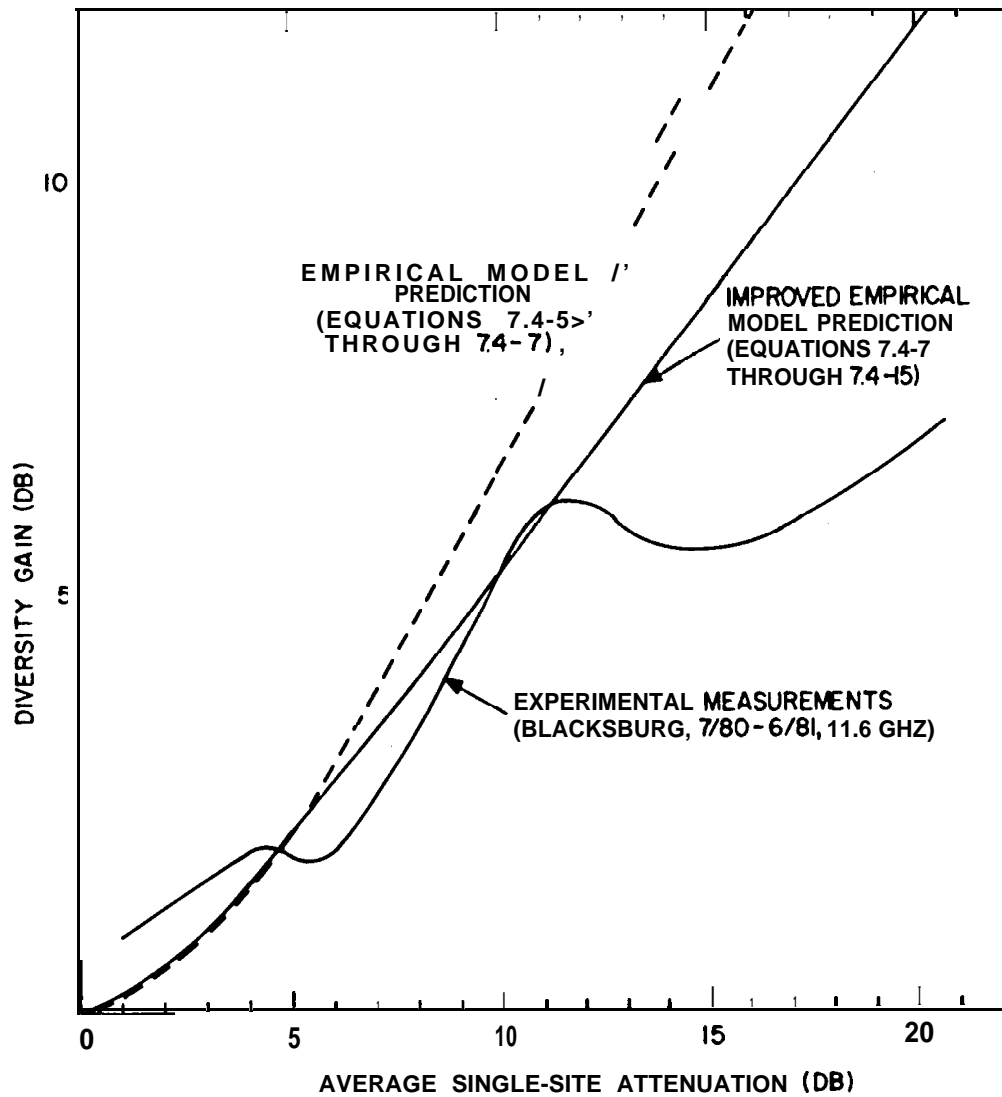


Figure 7.4-6. Comparison of Diversity Models and Experimental Results

total rain rate and uniform (Mode 2) rain rate may be developed as shown in Figure 7.4-7. Diversity gain will be obtained only for that portion of time between the stratiform and total rain curves. For $\beta = 0.3$ and $R < 10$ mm/h, this time is small (7.6 h/yr) and decreases (increases) as β and M decrease (increase). Therefore diversity gain will be large in Florida ($M \approx 1000$ mm and $\beta = 0.7$; $M\beta \approx 700$ mm) but will be small in Los Angeles ($M \approx 250$ mm and $\beta = 0.1$; $M\beta \approx 25$ for a given percentage of time. It appears that the $M\beta$ product is a good measure of the available diversity gain.

The amount of diversity gain available is also a function (to first order) of frequency, elevation angle and other meteorological parameters (height of the zero degree isotherm, etc.) as described in the attenuation model of Crane (1980). The results for a 30 GHz earth-space signal to a 40 degree elevation angle station located at sea level are shown in Figure 7.4-8. The difference between the attenuation arising from all rain events and uniform (**stratiform**) events is the maximum gain available for a diversity system. The time has been normalized to the amount of time the rain rate exceeds 0.25 mm/h (0.01 inch/h) in a year (**350h**). This same threshold value was selected by Lin (1973).

The total diversity gain available (see Figure 7.4-8) is the difference between the attenuation associated with all rain events and the attenuation attributed to stratiform (uniform) rain events. The maximum diversity gain available for one additional earth station (total of two identical earth stations) is G_1 and is computed from the cumulative distribution determined by the relation (Hodge-1978)

$$\text{pen}(A) = \{PC(A)\}^n \quad (7.4-16)$$

where:

n = the number of (identical) earth stations,

Figure 7.4-7. Cumulative Distribution of Rain Rate for Uniform and All Rain Events

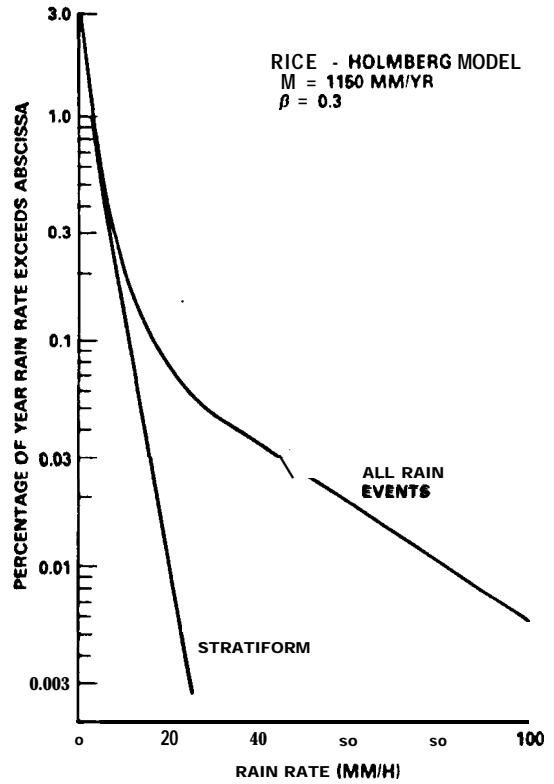
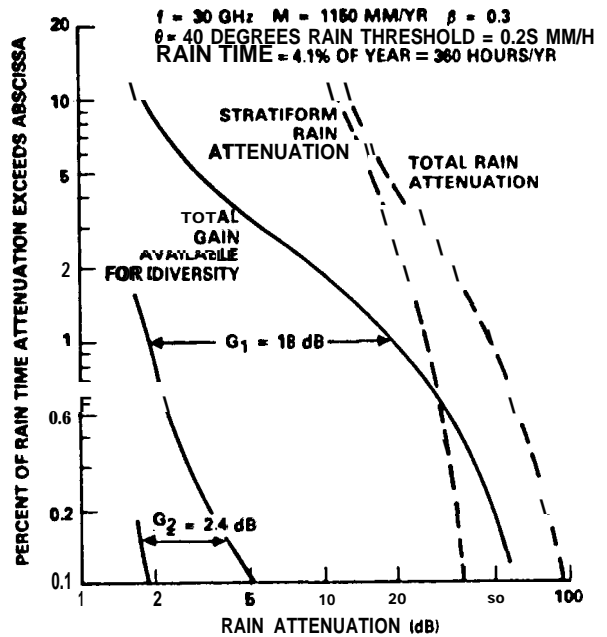


Figure 7.4-8. Cumulative Distribution of Total and Stratiform Rain Attenuation Plus Gain Available for Diversity Systems



PC(A) = the percent of time the attenuation A is exceeded for a single site, and

Pen(A) = the percent of time the attenuation A is exceeded for n identical sites.

G_1 and G_2 (the gain added by a third station) are shown in Figure 7.4-8. Plots of G_1 and G_2 versus the total attenuation on the worst path are given in Figure 7.4-9 for the region with $M = 1150$ and $\beta = 0.3$. The corresponding plots for a region with $\beta = 0.7$, such as Florida, are also given. Note the shift off zero which arises due to the effect of the uniform rains. For the case of $\beta = 0.7$ the gain G_1 saturates. This saturation prevents unrealistic system gains from being estimated as shown earlier. The saturation effect is believed to exist whenever the Mode 1 rain term dominates, but this has not been proven.

The maximum diversity gain G_1 for a two-station diversity system at selected frequencies is shown in Figure 7.4-10. Here the effects of stratiform rain at higher frequencies are clearly evident. For example at 45 GHz the zero diversity gain intercept occurs near 40 dB attenuation which will be observed about 0.4% (35 hours) of each year. Therefore for 45 GHz system links which can accommodate outages in excess of 35 hours per year, a diversity system will reduce the outage time or reduce the link margin required for 0.4% availability by only a small amount.

Based on the experimental results (Goldhirsh- 1979) and the analytic results (Morita and Higuti- 1978 and Wallace - 1981) the term G_1 may be related to the empirical a' multiplier by the approximate relation

$$a' \approx 0.9 G_{D1} \quad (7.4-17)$$

Also the station separation dependence may be retained as before so that

$$G = 0.9 G_1(1 - e^{-b \cdot d}) \quad (7.4-18)$$

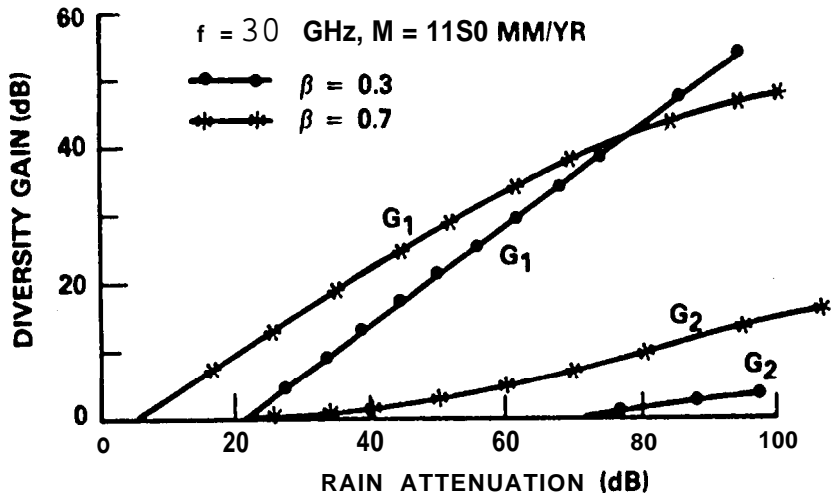


Figure 7.4-9. Maximum Diversity Gains G_1 (Two Stations) and G_2 (Three Stations) Versus Single-Site Attenuation

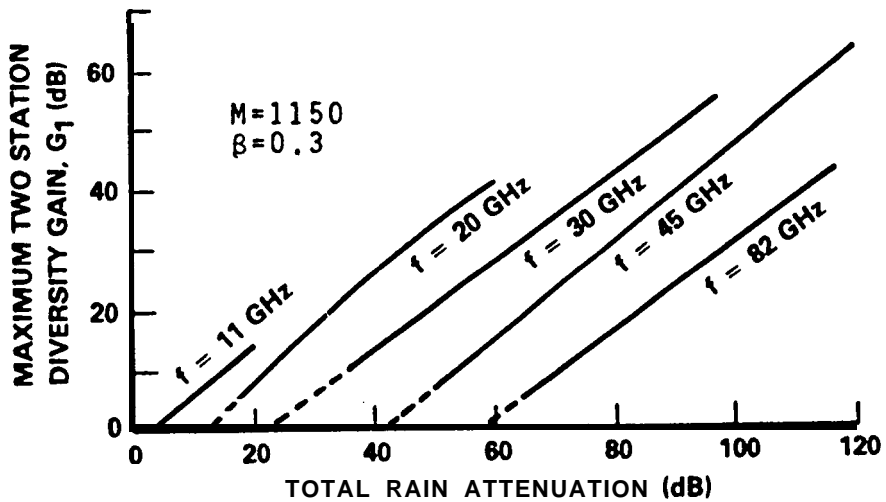


Figure 7.4-10. Maximum Diversity Gain, G_1 Versus Attenuation for Selected Frequencies

except that

$$b'' = 0.46 (1 - e^{-0.24(A-A_i)}), A > A_i \quad (7.4-19)$$

which accounts for the frequency dependent intercept attenuation A_i as shown in Figure 7.4-10.

The observation that diversity gain is obtained only for nonuniform rains has been used to devise a very simple approximation to diversity gain versus single-site attenuation (**Allnutt & Rogers - 1982**). As shown in Figure 7.4-11, the relation is assumed to be approximated by two straight line segments. One line is parallel to the "ideal diversity gain" curve (**diversitygain=attenuation**). The second line joins the origin and the first line at a point called the "knee." The single-site attenuations at the "knee" and the "offset" determines the relation for a particular location, frequency, and elevation angle. Site spacing and baseline orientation are assumed to be such that, to first order, site separation effects are removed. The value of the "offset" attenuation is the single-site attenuation exceeded for 0.3% of the time, which is assumed to correspond to uniform rainfall. The "knee" attenuation is the single-site attenuation corresponding to a 25 mm/hr rain rate, considered to be the breakpoint between stratiform and convective rain. This simple model provided a good fit to one year of radiometric measurements obtained in West Virginia, at 11.6 GHz. However, the **fit** to data from Austria and Florida was poor. A subsequent refinement to the model (**Allnutt & Rogers-1983**) **utilized** the CCIR **rain** attenuation model as modified by **CCIR** Interim Working Party 5/2 in May 1982. These predictions were much more consistent, and a clear trend of increasing diversity performance with elevation angle and rain connectivity was established.

7.4.2.1.4 An Analytical Diversity Model

An alternate model of site diversity has been proposed (Wallace-1981) that is derived from analytical representations of the joint

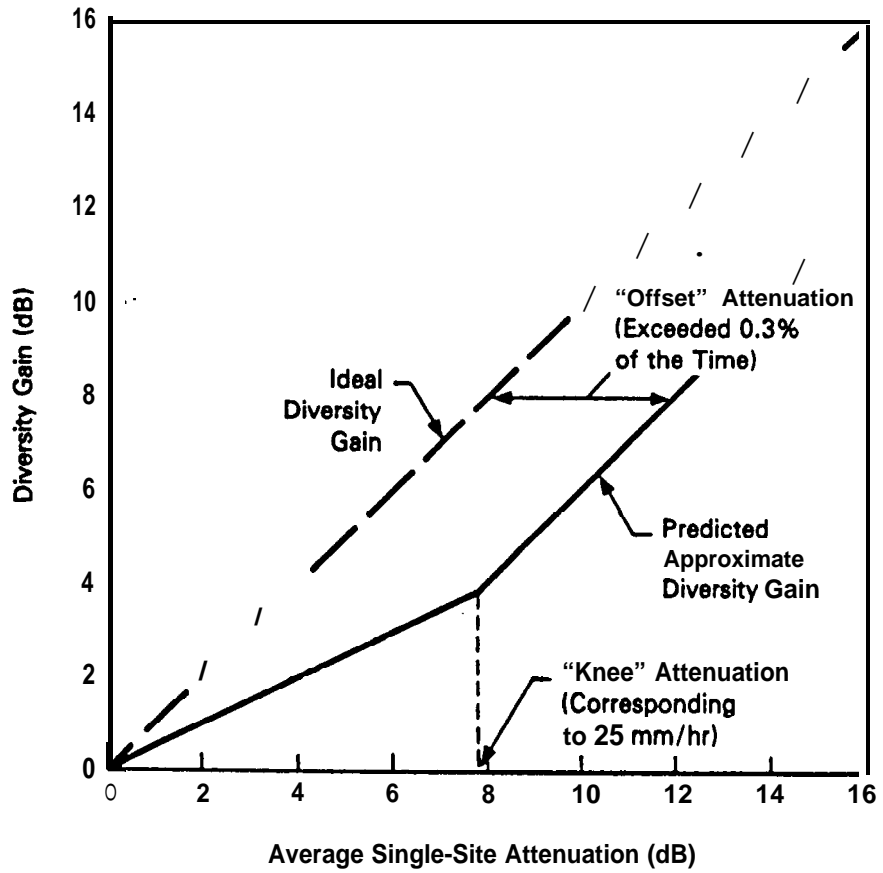


Figure 7.4-11. Construction of Approximation to Diversity Gain Prediction

site rain attenuation statistics. It is based on the well-known observation (Lin-1973) that rain attenuation in **decibels**, conditioned on the presence of **rain**, is approximately log-normally distributed. This is expressed analytically by the following:

$$\text{Prob } (A < a) = F_A(a) = P_0 K \Phi(Z, m, 0) \quad (7.4-20)$$

where

A = attenuation in decibels, a random variable

a = a particular value of A

$F_A(a)$ = cumulative distribution function (CDF) of A

P_0 = probability of rain

K = $\log_{10} e$, a scaling factor

$$\Phi(z, m, \sigma) = \frac{1}{\sqrt{2\pi} \sigma} \int_0^z \exp \left[-\frac{1}{2} \left(\frac{x-m}{\sigma} \right)^2 \right] dx \quad (7.4-21)$$

m = mean of $\log A$

σ = variance of $\log A$

The "exceedance probability" or "time percentage of exceedance" customarily used as the abscissa in presenting attenuation or rain rate statistics is the inverse, or one minus, the CDF (see Section 6.3.1.1). The factor P_0 expresses conditioning on the presence of rain mentioned above. This conditioning effectively reduces the time during which the log-normal distribution applies to the fraction of time that it is raining. The parameter m is the same as the logarithm of the median attenuation during the time it is raining, or the value that is exceeded for half the raining **time**. σ is a measure of variability of the attenuation. It is large if the attenuation is much greater or much less than the median value for significant **periods** of time. Typical values of median attenuation,

or 10^m , lie in the 0.3 to 0.5 dB range for 16 GHz links (Lin-1973), and understandably increase with frequency. σ is typically 0.5 to 0.8 and is highly dependent on the nature of the rain in a given location.

Given a log-normal estimate of the rain attenuation at a single ground station, it is a natural step to hypothesize that the attenuation experienced on links to two diversity sites is approximately jointly log-normal. This means that the logarithm of the attenuations at the two sites have a joint CDF that is bivariate Gaussian. The attenuation values are **probabilistically** related by a correlation coefficient, r , that varies with the site spacing. When the sites are distant from each other, we can say that their respective rain attenuations are **uncorrelated**, which corresponds to $r = 0$. The correlation coefficient increases to a maximum of one as the sites become closer together. One would intuitively expect the diversity gain achieved with two sites to be an inverse function of this correlation coefficient.

The effective amount of rain attenuation experienced by a diversity pair of earth stations is just the minimum of the values of attenuation seen at each site, since ideally one would always be using the site that has the least. Applying this fact, the CDF of the diversity pair rain attenuation can be determined from the joint CDF of the attenuation of the individual sites. This was done by Morita and Higuti (1978) using the joint log-normal hypothesis. The resulting CDF is also approximately **log-normal**, but with parameters m and σ both less than the corresponding parameters for either site. By comparing the single-site attenuation CDF with the diversity pair attenuation CDF, the diversity gain can be found. This has been done for a range of parameter values, and the results are shown in Figure 7.4-12. The axes in this figure are normalized by dividing the variables by the median single-site attenuation value, 10^m . A significant observation made from the figure is the insensitivity of diversity gain on the value of σ , except for very low values of r .

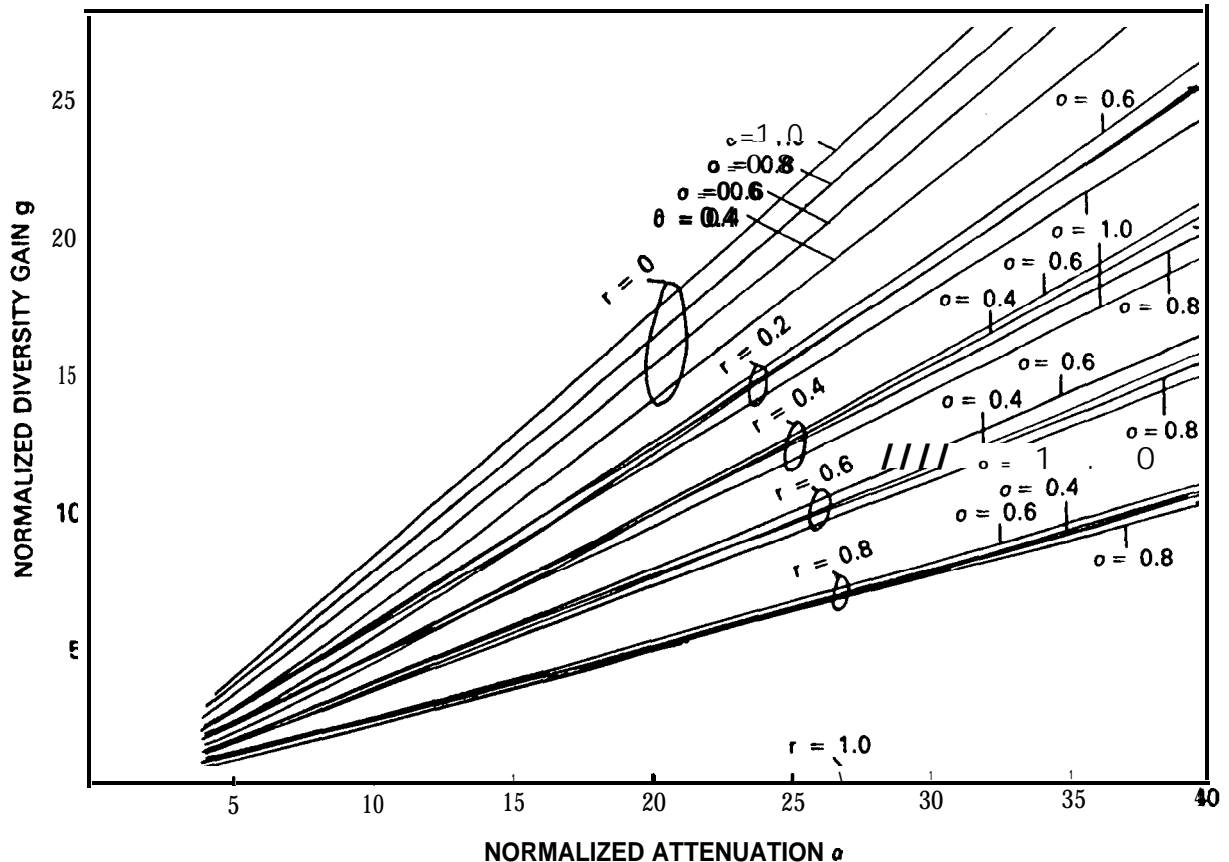


Figure 7.4-12. Diversity Gain Versus Attenuation for Varying "Distribution Parameters (Normalization is with Respect to Median Attenuation)

A drawback of this analytical model is that it requires values of parameters that are not normally computed in current experiment data analysis. Specifically, the median value of attenuation, conditioned on the presence of **rain**, is usually **unknown**, as is the correlation coefficient. Morita and Higuti (1978) computed a theoretical correlation coefficient as a function of site separation that is consistent with Japanese experimental results. **However**, there is some evidence suggesting that the Japanese correlation model does not apply as well to U.S. data (Wallace-1981). It is likely that the correlation coefficient is highly dependent on other factors besides site separation, such as local "microclimate" variations and orographic effects (Allnutt-1978).

7.4.2.1.5 Relative Diversity Gain

Based on radar-derived diversity gain data, **Goldhirsh** (1975) observed that the frequency dependence of site diversity gain can be eliminated by introducing a new parameter: relative diversity gain. Relative diversity gain $G_r(d)$ for any particular site spacing d is equal to the measured diversity gain at spacing d and frequency f divided by the maximum diversity gain achievable at that frequency:

$$G_r(d) = G_d(d, f) / \text{Max}[G_d(d, f)] \quad (7.4-22)$$

The maximum achievable diversity gain, assumed to be that corresponding to statistically independent rain attenuation at the two diversity sites, is not precisely defined. For any particular single-site attenuation value, the diversity gain approaches an asymptotic value as separation distance is **increased**, but it is often difficult to say what that value is. **Goldhirsh** assumed that 35 or 40 km was the distance giving the maximum diversity gain for purposes of defining G_r .

An analytical best-fit to the relative diversity gain versus site separation curve was found by **Goldhirsh** (1982) to be as follows:

$$G_r(d) = 1 - 1.206 \exp(-0.53 \sqrt{d}) \quad (7.4-23)$$

The difference between radar-derived G_r values and this function was less than 5% over the $d = 1$ to 30 km range.

7.4.2.2 Orbit Diversity

As already discussed, orbit diversity refers to the use of two satellites at separate orbital **positions**, which provide two paths to a single ground terminal (**Ippolito-1986**). Orbit diversity is generally less effective than site diversity for rain fade mitigation because the diversity paths are more highly correlated. Nevertheless, orbit diversity has the advantage that the two satellites can be shared (as part of a resource-sharing scheme) with many ground sites. This is in contrast to the case of site

diversity, where the redundant ground site can generally be dedicated to only one primary ground site (**Matricciani-1987**). Therefore, site diversity is somewhat inefficient in the sense that the redundant ground site is not used most of the time. On the other hand, if an orbit diversity scheme does not take advantage of its capability for resource-sharing with several ground sites it, too, is inefficient and is likely to prove too expensive for the amount of diversity gain that it does provide.

Of course, operational considerations other than rain fades can also make the use of orbit diversity more attractive. Examples of such operational considerations include satellite equipment failures, and sun transit by the primary satellite, both of which require handover to a redundant satellite to maintain communication. So the use of a redundant satellite for other reasons in addition to rain fades can help to make orbit diversity economically practical.

If a ground terminal is to take full advantage of orbit diversity, it really should have two antenna systems, so that the switching time between propagation paths can be minimized. If the terminal has only one antenna system with a relatively narrow beamwidth, switching time can be excessive because of the finite time required to slew the ground antenna from one satellite to another, and because of the finite time needed for the receivers to re-acquire **the** uplink and downlink signals. Of course, the use of two spatially separated ground antennas provides an opportunity for site diversity in addition to orbit diversity.

Satellites in geostationary orbit are desirable for orbit diversity because they appear to the ground station to be fixed in space. Such orbits simplify satellite acquisition and tracking, and alleviate satellite handover problems. However, satellite coverage of high northern and southern latitudes is limited - requiring ground antennas at these latitudes to operate at low elevation angles. In addition, rain attenuation is greater at low elevation angles because of the longer path lengths through rain cells. To overcome this difficulty with high-latitude stations, elliptical

orbits whose apogees occur at high latitudes can be used, allowing satellite coverage for a relatively large fraction of the orbit period. However, not only are the advantages of geostationary orbits then lost, but in addition several satellites must be used in order to provide coverage at all times.

Although data concerning the improvement achievable with orbit diversity are currently rather sparse, recent predictions of the achievable improvement have been made (**Matricciani-1987**). One configuration that has been analyzed consists of:

1. A ground station at Spino d'Adda in Northern Italy
- 2. Satellite 1 (Italsat) at 13 deg. E longitude**
3. Satellite 2 (Olympus) at 19 deg. W longitude.

For a 20 GHz downlink, the predicted single-path and double-path statistics are shown in Figure 7.4-13. The diversity (**double path**) predictions shown in this figure **assume that Satellite 1 is normally** used, and that Satellite 2 is switched in only when the rain attenuation for Satellite 1 exceeds some selected value. Because Satellite 2 would therefore be used only a small fraction of the time, it can be time shared with several ground stations for **large-scale** orbit diversity. The predictions are based on single-path measurements of the rain-rate probability distribution, and the joint distribution for the double-path attenuation is assumed to be log-normal.

Measurements of orbit diversity improvement have been made (**Lin, et al-1980**) for a configuration consisting of:

1. A ground station at Palmetto, GA
- 2. Path 1 - 18 GHz radiometer pointed in direction of COMSTAR D1 at 128 deg. W longitude**
3. Path 2 - 19 GHz beacon of **COMSTAR D2** at 95 deg. W longitude.

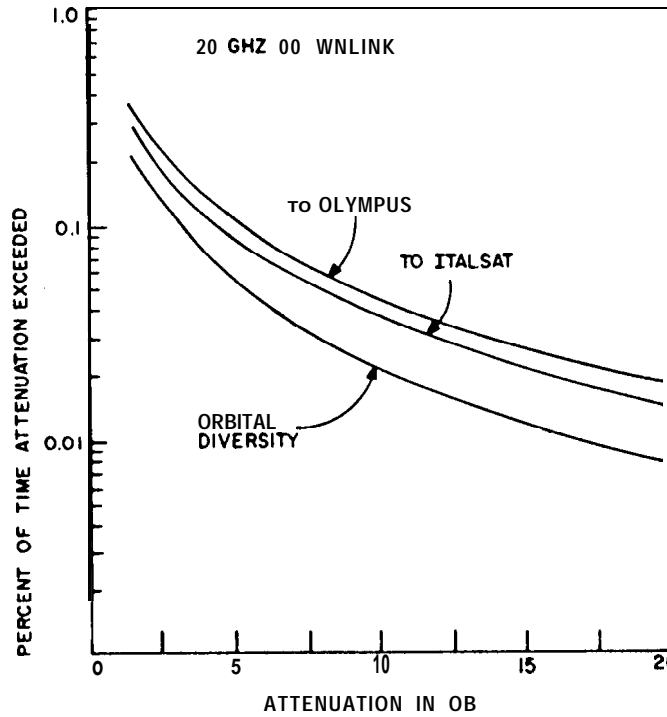


Figure 7.4-13. Predicted Orbit Diversity Performance at Spino d'Adda, Italy

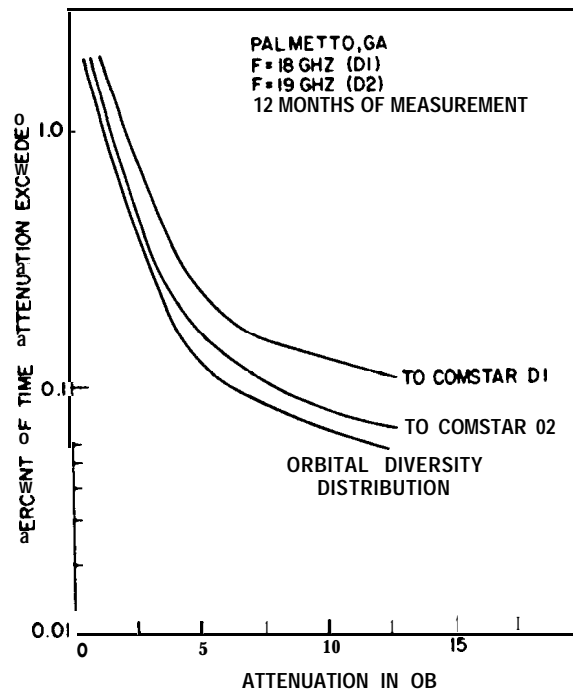


Figure 7.4-14. Orbital diversity measurements at Palmetto, GA

Figure 7.4-14 shows measurement results at 18 and 19 GHz. One might expect the diversity gain to improve markedly as the angle subtended increases. However, it turns out (Ippolito-1986) that except when the single-path attenuation is large to begin with, the diversity gain actually increases rather slowly with the subtended angle. This is because most of the rain attenuation is at low altitudes, so that even widely diverging propagation paths often pass through the same rain cell.

Of course, the measurements in Figure 7.4-14 cannot be directly compared with the predictions in Figure 7.4-13 because the rain statistics and geometrical configurations differ. Nevertheless, the limited measurements and calculations that have been made both indicate that a modest diversity gain is achievable from orbit diversity. In any case, orbit diversity gain is less than that achievable with site diversity. Figure 7.4-6, for example, shows that one can expect roughly five dB site diversity gain when the average single-site rain attenuation is 10 dB. Figures 7.4-13 and 7.4-14, on the other hand, show that one can expect only two or three dB gain from orbit diversity.

7.4.3 Signal Diversity

Rain attenuation is not only spatially sensitive, as discussed earlier, but also time and frequency sensitive. This property provides an opportunity to combat rain fades by adjusting certain signal parameters in accordance with existing propagation conditions.

Suppose, for example, that the ground terminal continually adjusts its uplink power to maintain a constant signal level at the satellite, regardless of propagation conditions. Then rain fade mitigation is achieved without a need for redundant signal paths. In a similar way, the satellite can use transmitter power control to mitigate downlink rain fades.

Alternatives to transmitter power control for combatting the time dependence of rain fades in digital communication systems are to use either forward error correction (**FEC**) or data rate control. Rather than raising the transmitter power when propagation conditions worsen, one can temporarily apply FEC to improve the power margin at the expense of a wider signaling bandwidth or longer transmission time. However in some situations, both power and bandwidth in the digital communication system may be limited. If this is the case, one can always temporarily lower the data rate to improve the power margin - the price being a slower communication rate.

The natural way to exploit the frequency dependence of rain attenuation is to use frequency diversity. When rain attenuation rises to some specified value, high priority traffic can be diverted to a lower frequency that is less susceptible to rain fades. The price paid in this case is a reduction in channel capacity during rain fades, and the requirement for additional frequency assignments

All of these techniques for incorporating signal diversity in satellite communication are discussed in the following paragraphs.

7.4.3.1 Power Control

The objective of power control is to vary the transmitted power in direct proportion to the attenuation on the **link**, so that the received power stays constant through rain fades. This can be employed, in **principle**, on either the **uplink** or downlink. There are two reasons for using power control rather than a very high transmitted power level to mitigate rain fades. When used on the **uplink**, the reason is usually to prevent the transponder on the satellite from being **overdriven**, or to keep from upsetting the power balance among several **uplink** carriers using the same transponder. (When multiple carriers share a non-linear transponder near saturation, variations 'in the input level of one of them are enhanced at the output.) When used on the downlink, the reason is

that a temporary power boost can be provided to combat fades on selected links while requiring only a modest increase in satellite solar array power. The array power not needed during clear-sky operation is used to charge batteries, which supply the energy needed to transmit the added power during fades.

Through power control, the maximum amount of rain attenuation that can be compensated is equal to the difference between the maximum output of the Earth station or satellite power amplifier and the output required under clear-sky conditions. The effect of power control on availability, assuming that control is perfect, is the same as having this power margin at all times. A perfect power control system varies the power exactly in proportion to the rain attenuation. Errors in the power control result in added outages, effectively decreasing this margin. **Maseng** and Baaken (1981) have studied this effective margin reduction due to power control delay.

A drawback of power control is a potential increase in intersystem interference. A power boost intended to overcome rain attenuation along the direct Earth-space path will produce an increase in power on interfering paths as well. If the same rain fade does not exist on these paths, the interference power received by interferers, such as other terrestrial stations, will increase. Due to the inhomogeneity of heavy rain, attenuation on interfering paths at large angles from the direct earth-space path will often be much less than the attenuation on that path. Terrestrial system interference caused by the earth station, although tolerable under clear-sky conditions, may therefore become intolerable in the presence of rain when uplink power control is used. Downlink power control will likewise increase the potential for interference with earth stations using adjacent satellites. A downlink power boost for the benefit of a receiving station experiencing a rain fade will be seen as an increase in interference by vulnerable stations that are not experiencing fades.

7.4.3.1.1 Uplink Power Control

A frequency-division multiple-access (**FDMA**) satellite communication system trying to operate with large spatial and time variations in rain fades will experience significant nonlinear distortion when fades are mitigated by the use of large power margins alone. Nonlinear distortion, which occurs when the satellite transmitter is operated near saturation, includes AM-to-PM conversion and generation of intermodulation products.

By continually adjusting the **uplink** power from each ground station in accordance with uplink fade conditions, variations in the operating point of the satellite TWTA can be minimized, thereby minimizing nonlinear distortion. However, this does not completely solve the problem because downlink rain fades must also be considered. Lyons (1976) showed that if the uplink power control algorithm accounts not only for uplink fades but **also** for downlink fades, good performance can be achieved in the presence of fading on both links by using uplink **power** control alone. Although individual signal levels at the satellite receiver will vary widely in this situation, the TWTA operating point will still remain relatively fixed so long as there is a sufficiently large number of users, **all** having controlled access to the satellite. So if deep fades occur on only a few of the uplink and downlink paths, variations in the received downlink signal levels will be relatively small, thus requiring smaller fade margins.

However, uplink power control of such systems requires that each station accessing the satellite possess knowledge not only of its uplink fade characteristics, but also of the downlink fade characteristics for all stations to which it is transmitting. Power control of all transmitting stations can be achieved from a single location at the cost of control delays, which result in relatively slow fade mitigation. If instead, we have distributed control in the sense that each station controls its own transmitted power, - delays are minimized. However, performance may suffer because the total received uplink power at the satellite can no longer **be**

maintained approximately constant under widely fluctuating propagation conditions. Furthermore, with distributed **control**, fade information must be exchanged continually among all participating stations to make the system work.

These arguments indicate that if the **uplink** power control algorithm does not take into account the downlink fade characteristics, then power control can likely be applied only to single-service, single-user links. For such links, there are two types of uplink power control that can be used (**Ippolito-1986**). The first is a closed-loop system that adjusts **uplink** power in accordance with the satellite received signal level returned to the transmitting station via telemetry. The second is an open-loop system that adjusts uplink power in accordance with either the downlink signal (or beacon) level, or the attenuation calculated from ground-based radiometer or radar measurements. Figures 7.4-15 and 7.4-16 illustrate closed-loop and open-loop uplink power control for single-carrier links.

7.4.3.1.2 Downlink Power Control

More and more satellite communication systems are going to **on-board** signal processing, not only to improve bit error rate performance (in the case of digital modulation), but also to improve terminal interconnectivity and to make downlink performance independent of the **uplink**. On-board processing simplifies power control for rain fade mitigation (especially in FDMA systems) because the uplink power control algorithm no longer needs to take into account downlink fade conditions. Therefore, uplink and downlink power control can be done independently, which alleviates many problems associated with the use of **FDMA** during rain fades. This assumes that on-board processing includes demodulation to baseband, followed by demodulation onto a downlink carrier. The following discussion assumes that downlink power control can be accomplished essentially independent of the uplink regardless of whether or not on-board processing is being used.

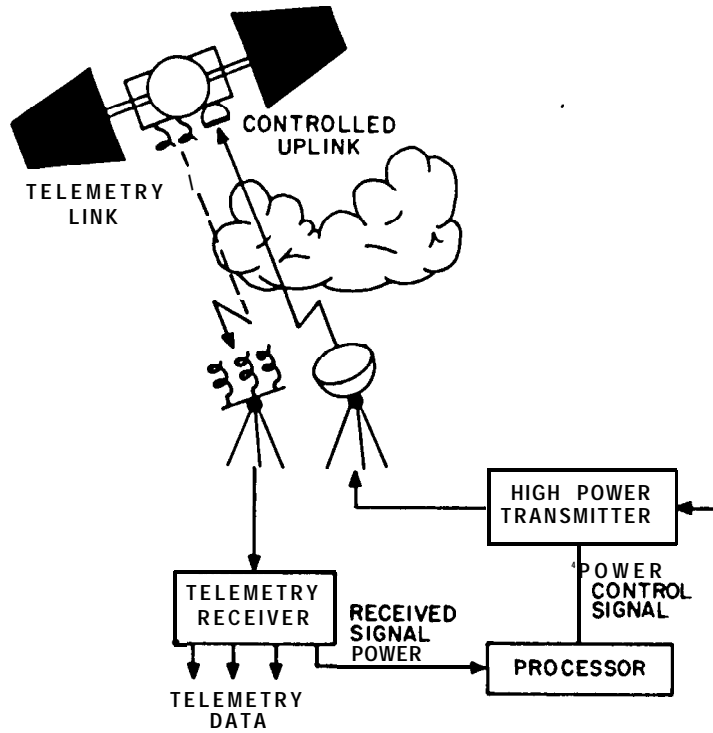


Figure 7.4-15. Closed loop **uplink** power control

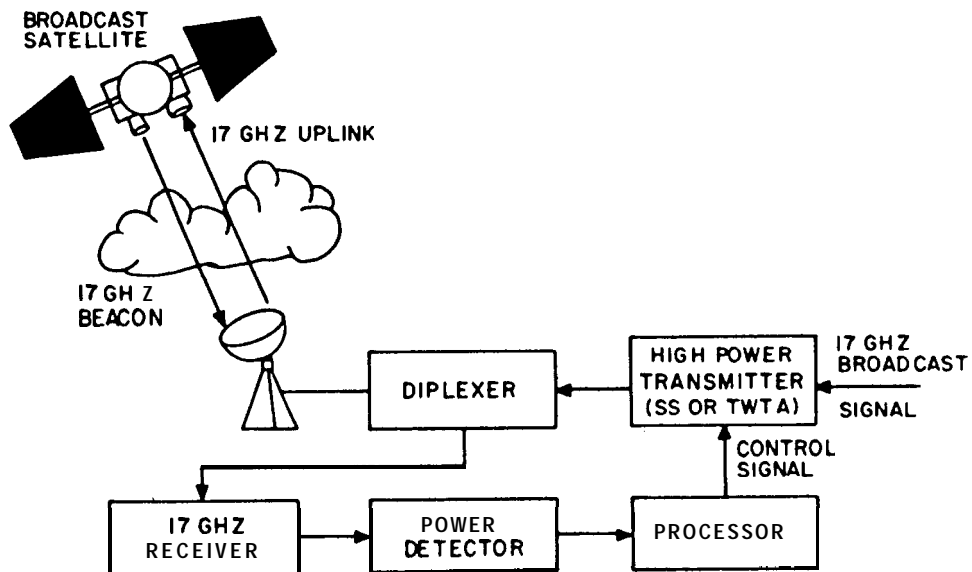


Figure 7.4-16. Open loop uplink power control

The satellite transmitter usually has only one or two switchable output power levels, so downlink power control for rain fade mitigation is less flexible than uplink power control. One example is ACTS (Holmes and Beck-1984), which operates at 30/20 MHz and has a transmitter output power of either 8 or 40 watts. The high-power mode therefore provides 7 dB additional margin against rain fades. Because the entire antenna footprint receives the added power in the high-power mode, those stations not experiencing rain attenuation will receive more power than they require. Downlink power control is therefore not efficient in directing the added power to the stations needing it.

This problem with downlink power control is somewhat alleviated by the use of **switchable** spot beams on the satellite. The reason for this is that the antenna footprints are relatively small, thereby allowing added downlink power to be directed only to those terminals that require it. In fact, switching to spot beams is, in itself, an effective technique for mitigating rain fades, even when satellite transmitter power is not controlled. The use of downlink power control together with switchable antenna beams might better be called EIRP control rather than power control.

7.4.3.2 Adaptive Forward Error Correction. In Time Division Multiple Access (**TDMA**) systems, each earth station is periodically assigned a time interval during which it alone may access the entire satellite bandwidth. The time between accesses by a given station is called the TDMA frame period, and each station is assigned a fixed fraction of the frame. This fraction is proportional to the traffic the station is carrying, or to its average bit rate. By leaving a portion of the frame period unassigned, those stations experiencing rain fades can be temporarily assigned a larger fraction of the frame for fade mitigation. One way to exploit this additional time resource is to apply forward error correction (**FEC**). The same number of information bits is transmitted each frame period as before. However FEC reduces the required received signal level, thereby at least partially offsetting the loss in received power

experienced during rain fades. Alternatively, the additional allotted time allows a reduction in data rate during rain fades. Data rate control will be discussed further in paragraph 7.4.3.4.

This scheme is adaptive in the sense that FEC is applied only when the rain attenuation has exceeded a selected threshold. When FEC is used, the symbol timing hardware still operates at the same fixed rate. In principle, FEC can be implemented in software, which may be advantageous in some systems.

There is a limit to the mitigation that coding can provide (**Bronstein-1982**) . This is because a minimum symbol energy must be maintained to ensure proper recovery of symbol timing in the receiver. Therefore, because the symbol rate is fixed, a minimum received signal power level must be maintained. The fade margin achieved with FEC must be traded off against the reduction in total system capacity that occurs. As propagation conditions worsen, the fraction of the frame duration needed for fade mitigation must increase, thereby reducing the fraction available for use during clear weather.

FEC can be used to mitigate either **uplink** or **downlink** fades. A station affected by **uplink** fades would encode its entire burst - lengthening its burst period by its allotted reserve time. Each station receiving that station's burst must decode the data in that burst. In contrast, a receiving station affected by downlink fading will *receive* all its data in coded form. Transmitting stations must encode that portion of the data that is transmitted to the affected station. It is apparent that a central control station must dynamically assign the extra time to the stations that require it. Furthermore, all stations in the network must know which stations require coding.

A satellite using on-board signal processing essentially decouples the downlink from the **uplink**, which allows the reserve time to be used more efficiently. Only those transmitting stations experiencing uplink fades then need to encode their data. The

satellite would not only demodulate the **uplink** signal, but would also decode those uplinks affected by fading. The satellite would then encode for downlink transmission only those signals affected by downlink fades. The reserve time used by faded uplinks is, in **effect**, freed up to be used by faded downlinks.

Acampora (1979, 1981) has studied the performance of a system using FEC coding to mitigate downlink fades. The hypothetical TDMA system studied operated in the 12/14 GHz bands, using a bent-pipe transponder. The traffic model used assigned traffic between the 100 most populous U.S. cities in proportion to their population ranking. The Earth stations were given a built-in fade margin, and the reduction in this margin made possible by time resource sharing was found, using a convolutional FEC code that gave a 10 **dB** power saving. A typical result of this analysis showed that reserving six percent of the frame period as a shared resource provided an outage of 30 minutes per year (.0057% of the time) with 9 **dB** less rain margin than would otherwise be needed.

Gains of up to 8 **dB** have been reported (**Mazur, et. al.-1983**) for 14/11 GHz TDMA networks with 32 ground terminals. Five of the 8 **dB** comes from the coding gain provided by a rate 1/2 code. The other 3 **dB** comes from a **QPSK/PBSK** switch capability.

7.4.3.3 Frequency Diversity. A straightforward method of improving the reliability of a millimeter-wave satellite system is to provide the capability for Earth stations to switch to a lower frequency band (say C-band) when rain fades occur at the normal operating band. This would require a satellite with a dual-band payload and a dual-frequency Earth station capability, but the improvement in overall system reliability may be worth the added cost. The bandwidth required in the lower, high-reliability, frequency band need be only a fraction of the total bandwidth **used**, since it needs to accommodate only the traffic of those stations undergoing rain fades. The probability of rain outage on a particular link with such a frequency diversity system is equal to the sum of the probabilities of two mutually exclusive events: (1) that the

reserve band is fully occupied by other links when a rain fade occurs, and (2) that a link is assigned to the reserve band, but the rain rate is so great that the reserve band suffers an outage while the link **is** using it. If 4/6 GHz is used for the reserve band, the probability of the second event can be considered nil. If the reserve band is wide enough for N links, the probability of the first event is the probability of **N+1** simultaneous fades. The bandwidth required in the reserve band is therefore established **by** the simultaneous fade probability over all the Earth stations in the system. The dependence of system performance on simultaneous fade probability is common to all resource-sharing schemes. Because of this, it will be discussed separately later (paragraph 7.4.4).

7.4.3.4 Data Rate Control. If the satellite receiver monitors the uplink received signal level and feeds this information **back to the transmitter, then various** properties of the transmitted signal can be varied to mitigate uplink rain fades. Transmitter power control (paragraph 7.4.3.1) provides an example. However, we can vary the data rate rather than the transmitted power to accomplish the same results. This is because in digital data transmission the measure of system performance is the bit error **rate**, which **ideally** depends only on the received bit energy-to-noise density ratio. The bit energy in turn is equal to the received signal power divided by the data rate. So in principle, lowering the data rate by a factor of two, for example, has the same effect on error rate performance as raising the transmitted power 3dB.

It has been shown (**Cavers-1972**) that data rate control can completely eliminate the effect of fading if the feedback from the receiver is assumed to be ideal (no control delay). Even when control delay is included, however, data rate control can often be more effective than diversity reception? at a cost of bandwidth expansion to accommodate transmission of control information.

As we have seen in. paragraph 7.4.3.2, a possible fade mitigation technique for **TDMA** communication is to leave a portion of the **frame** period unassigned - making it temporarily available to those

stations experiencing rain fades. Data rate control of such systems involves transmitting or receiving the same number of information bits each frame during the fade, but reducing the data rate in order to fully occupy the additional allotted time. As discussed above, this increases the transmitted energy per bit, which offsets the loss in received power during the fade.

For data rate control to work, the ground stations must at least have the synchronization hardware required to switch from the normal symbol rate to a lower rate. However, to achieve performance approaching that obtained when there are no **fades**, the use of several selectable data rates is required, with little delay in the control loop.

As with adaptive FEC coding, data rate reduction can be used to mitigate both uplink and downlink fades. Again, on-board signal processing essentially makes **uplink** data rate control independent of downlink control, thereby making efficient use of the reserve time and simplifying the control procedure. However, the satellite receiver must be capable of synchronizing to several data **rates**, which complicates the on-board processing hardware.

7.4.4 Simultaneous Fade Probabilities

When a resource-sharing scheme is used to provide additional fade margin, the amount of the resource (time or frequency) that must be set aside to provide the required margin is highly dependent on the probability of simultaneous fades on two or more links. If sufficient resources are reserved to back up two **links**, for **example**, then the outage probability is the probability that the fade depth exceeds the added margin provided, or that three or more links are suffering fades at the same time.

The probability of simultaneous fades is also of interest in connection with site diversity systems (paragraph 7.4.2.1). In that case, the sites are generally assumed to be close enough to each other to be affected by the same storm system. In the case of

resource-sharing systems, we are concerned with fades simultaneously occurring on links to Earth stations separated by much larger distances as well. A naive approach would be to assume that the rain attenuation at a given Earth station is statistically independent of that at another station substantially removed from the first. Closer examination reveals, however, that this is not the case.

Acampora (1981), in the analysis cited earlier, observed that the deep rain fades that are of concern are normally caused by thunderstorm activity, and that there is a definite correlation in thunderstorm activity at widely separated locations. In particular, thunderstorm activity is typically restricted to the four-month period from June through September, and to the quarter of the day lasting from **1:00 PM** to **7:00 PM** local time. Because of this, the occurrence of a deep fade at one site makes the probability of a deep fade at the same time at a second site much higher than the yearly average. The observation of the fade at the first site makes it highly probable that we are in the June-September, **1:00 PM - 7:00 PM** thunderstorm period, therefore the chances of a thunderstorm at the second site are higher than average by a factor of at least $(12/4)(24/6)$, or 12, using the broad ranges of time given. In addition to this yearly-to-thunderstorm-period factor, α , a second factor β , accounts for the additional correlation of deep fades between sites that are spaced closely enough that they are affected by the same storm systems. This factor was considered by Acampora to range from 1, which implies independence of fades during the thunderstorm period, to a maximum value of 6. The factors α and β are applied as follows: The yearly average joint probability of the attenuation (A_1 and A_2) two sites exceeding their respective thresholds (T_1 and T_2) is given by

$$P(A_1 > T_1, A_2 > T_2) = \alpha \beta P(A_1 > T_1) P(A_2 > T_2)$$

where the last two quantities are the individual yearly exceedance probabilities for the two sites. For $T_1 = T_2$, the factor $\alpha\beta$ is seen to be the diversity improvement defined in Section 7.4.1.

7.5 -REFERENCES

- Acampora, **A.S. (1979)**, "A Shared Resource TDMA Approach to Increase the Rain Margin of 12/14-GHz Satellite Systems," BSTJ, Vol. 58, No. 9 (Nov.) pp. 2097-2111.
- Acampora, **A.S. (1981)**, "Rain Margin Improvement Using Resource Sharing in 12-GHz Satellite Downlinks," BSTJ, Vol. 60, No. 2 (Feb), pp 167-192.
- Allnutt, **J.E. (1978)**, "Nature of Space Diversity in Microwave Communications via Geostationary Satellites: A Review," Proc. IEE, Vol. 125, p. 369.
- Allnutt, **J.E. and D.V. Rogers (1982)**, "Novel Method for Predicting Site Diversity Gain on Satellite-to-Ground Radio Paths," Electronics Letters, Vol. 18, No. 5, pp. 233-235, 4 March.
- Allnutt, **J.E. and D.V. Rogers (1983)**, "A Site Diversity Model for Satellite Communications Systems," IEE Third International Conference on Antennas and Propagation, April 1983, Norwich, U.K.,
- Arnold, **H.W., D.C. Cox, H.H. Hoffman, and R.P. Leek (1979)**, "Characteristics of Rain and Ice Depolarization for a 19 and 28 GHz Propagation Path from a COMSTAR Beacon," Record, Int'l Conf. on Comm. (IEEE CH 1435-7/79/0000-0220), June.
- Bonhomme, **R., B.L. Herdan, and R. Steels, (1984)**, "Development and Application of New Technologies in the ESA OLYMPUS Programmed," Proceedings of the AIAA Comm. Sat. Sys. Conf., March.
- Braham, **H.S., (1982)**, "Fleetsatcom - Current and Future," Int'l. Conf. on Comm. IEEE, pp. 6H.3.1-6H.3.5, June.
- Brayer, **K., (1978)**, "Time, not Throughput, for Net Designs. Part 1: Techniques," Data Communications, October.
- Bantin, **C. and R. Lyons (1978)**, "The Evaluation of Satellite Link Availability," IEEE Trans. Comm. Vol. COM-26, No. 6 (June)' pp. 847-853.
- Brandinger, **P. (1978)**, "Propagation Requirements for 30/20 GHz System Design," 1978 Spring URSI Meeting, Washington, D.C.

- Bronstein, L. M.** (1982), "The Enhancement of Propagation Reliability for Millimeter Wave Satellite Communication System" Record, International Conference on Communication? Philadelphia, June, pp 1B.4.1-5.
- Calo, s., L. Schiff, and H. Staras** (1978), "Effects of Rain on Multiple Access Transmission of Data via Satellite," Record, Internat. Conf. on Common. , Toronto, pp. 30.1.1-6.
- Castel, R.E. and C.W. Bostian** (1979), "Combining the Effects of Rain-Induced Attenuation and Depolarization in Digital Satellite Systems," IEEE Transactions Aerosp. Elect. Syst., Vol. 15, No. 2, p. 299-301, March.
- Cavers, J.K.** (1972), "Variable-Rate Transmission for Rayleigh Fading Channels," - IEEE Trans. Comm., Vol COM-20, No. 1 (Feb.), pp. 15-22.
- CCIR (1978) "Allowable Noise Power in the Hypothetical Reference Circuit for Frequency-Division Multiplex Telephony in the Fixed Satellite Service," Recommendation 353-3, XIVth Plenary Assembly, Kyoto.
- Crane, R.K.** (1980), "Prediction of Attenuation by Rain," IEEE Trans. Comm., Vol. COM-28, No. 9, pp.1717-1733.
- CSC (Computer Sciences Corp.)** (1971), "Automated Satellite Terminal Control," RADC-TR-70-229, Volume I, for U.S. Air Force, Rome Air Development Center, March.
- Dintelmann, F.** (1981), "Analysis of 11 GHz slant-path fade duration and fade slope," Electron. Lett., Vol. 17, No. 7, pp. 267-268.
- Donovan, R., R. Kelley, and K. Swimm**, (1983), "Evolution of the DSCS Phase III Satellite through the 1990's," Record, Int'l. Conf. on Comm. IEEE, pp. C1.6.1-C1.6.9, June.
- Engelbrecht, R.S.** (1979), "The Effect of Rain on Satellite Communications Above 10 GHz," RCA Review, June.
- Evans, J.V.**, (1986), "Twenty Years of International Satellite Communication," Radio Science, Vol. 21, No. 4, July-August.
- Freeny, A.E. and J.D. Gabbe** (1969), "A Statistical Description of Intense Rainfall," Bell System Technical Journal, Vol. 48, p. 1789.
- Friedenthal, M.J., and E.K. Heist**, (1976), "Fleet Satellite Communications Spacecraft," WESCON, September.
- Ghais, A., J. Martin, D. Arnstein, and H. Lewis**, (1982), Summary of INTELSAT VI Communications Performance Specifications COMSAT Technical Review, Vol. 12, No. 2, Fall.

- Giannone, B., E. Matricciani, A. Paraboni, and E. Saggese,** (1986), "Exploitation of the 20-40-50 GHz Bands: Propagation Experiments with ITALSAT," Proceedings of the AIAA Communication Satellite Systems Conference, March.
- Goldhirsh, J. (1975),** "prediction Methods for Rain Attenuation Statistics at Variable Path Angles and Carrier Frequencies Between 13 and 100 GHz," IEEE Trans. Ant. Prop., Vol. **AP-23**, pp. 786.
- Goldhirsh, J. (1979),** "The Use of Radar at Non-Attenuating Wavelengths as a Tool for the Estimation of Rain Attenuation at Frequencies above 10 GHz," Record, **EASCON '79**, pp. 48-55.
- Goldhirsh, J. and F. Robison (1975),** "Attenuation and Space Diversity Statistics Calculated from Radar Reflectivity Data of Rain," IEEE Trans. Ant. Prop., Vol. **AP-23**, pp. 221.
- Goldhirsh, J. (1982),** "Space Diversity Performance Prediction for Earth-Satellite Paths Using Radar Modeling Techniques," Radio Science, Vol. **17**, No. **6**, pp. (Nov.-Dec.).
- Graebner, J.C., and W.F. Cashmen, (1986),** "Advanced Communication Technology Satellite: System Description," IEEE Transactions Comm., Vol. **COM-16**, September.
- Gray, D.A. (1973),** "Earth-Space Path Diversity: Dependence on Base Line Orientation," 1973 **G-AP/URSI** Meeting, Boulder, Colorado.
- Gray, L.F. and M.P. Brown (1979),** "Transmission Planning for the First U.S. Standard C (14/11 GHz) **INTELSAT** Earth Station," COMSAT Technical Review, Volume 9, Number 1, Spring.
- GTE (General Telephone & Electronics, Lenkurt, Inc.) (1972),** Engineering Considerations for Microwave Communications Systems.
- Harrold, T.W. and P.M. Austin (1974),** "The Structure of Precipitation Systems - A Review," Journal de Recherches Atmospherique, Vol. **8**, pp. 41.
- Hedge, D.B. (1974a),** "Path Diversity for Reception of Satellite Signals," Journal de Recherches Atmospherique, Vol. **9**, pp. 443.
- Hedge, D.B. (1974b),** "A 15.3 GHz Satellite-to-ground Path Diversity Experiment Utilizing the **ATS-5** Satellite," Radio Science, Vol. **9**, pp. 1.
- Hedge D B (1976a),** "An Empirical Relationship for Path Diversity Gain," IEEE Trans. Ant. Prop. Vol. **AP-24**, pp. 250.

- Hedge, **D.B.** (1978), "Path Diversity for Earth-Space Communication Links," Radio Science, Vol. 13, pp. 481.
- Hedge, **D.B.** (1982), "An Improved Model for Diversity Gain on Earth-Science Propagation Paths", Radio Science, Vol. 17, No. 6, pp " 1393-1399.
- Hogg, **D.C.** (1968), "Millimeter Wave Communications through the Atmosphere," Science, Vol. 159, p. 39.
- Hogg, **D.C.** and **T.S.** Chu (1975), "The Role of Rain in Satellite Communications ," Proc. IEEE, September.
- Holmes, **W.M.** Jr., and **G.A.** Beck, (1984), "The ACTS Flight System: Cost-Effective Advanced Communications Technology," AIAA 10th Communications Satellite Systems Conference, AIAA CP842, Orlando, Fla., pp. 196-201, March 19-22.
- Ippolito, **L.J.**, Jr., (1986), "Radiowave Propagation in Satellite Communications ," Van Nostrand Reinhold, New York.
- Kaul, **R.** (1980), "Extension of an Empirical Site Diversity Relation to Varying Rain Regions and Frequencies," URSI Commission F Symposium, **Lennoxville**, Quebec.
- Kehchiro K., T. Muratani and A. Ogawa (1977), "On-Board Regenerative Repeaters Applied to Digital Satellite Communications," Proc. IEEE, March.
- Kirk, **K.W.** and **J.L. Osterholz** (1976), "DCS Digital Transmission System Performance," Defense Communications Engineering Center (**DCEC**) Technical Report No. 12-76, November.
- Kittiver, **C.**, and **D. Westwood** (1976), "The Composite Margin Plane - A Tool To Compute Overall Satellite Communications Link Availability," Record, Nat. **Telecommun. Conf.**, Dallas, pp. 49.4.1-7.
- Lin, **S.H.** (1973), "Statistical Behavior of Rain Attenuation," BSTJ, Vol. 52, No. 4, pp. 557-581.
- Lin, **S.H.**, **H.J. Bergmann**, and **M.V. Pursley**, (1980), "Rain Attenuation on Earth-Satellite Paths-Summary of 10-Year Experiments and Studies," Bell System Technical Journal, Vol. 59, No. 2 (Feb.), pp. 183-228.
- Lovell, **R.R.**, (1984), "Giant Step for Communication Satellite Technology," Aerospace America, March.
- Lyon, **D.L.** (1985), "Personal Computer Communications via Ku-Band Small-Earth Stations," IEEE Journal on Selected Areas in Communications, Vol. SAC-3, No. 3, May 1985.

- Lyons, R.G., (1974) "Combined Effects of Up- and Down-Link Fading Through a Power-Limiting Satellite Repeater," IEEE Trans. Comm., vol. **COM-22**, No. 4 (March), pp. 350-352.
- Lyons, R.G. (1976), "A Statistical Analysis of Transmit Power Control to Compensate Up- and Down-Link Fading in an FDMA Satellite Communications Systems," IEEE Trans. Comm., Vol. **COM-24**, No. 6 (June), pp. 622-636.
- Maseng, T. and P.M. Bakken (1981), "A Stochastic Dynamic Model of Rain Attenuation," IEEE Trans. on Comm., Vol. **COM-29**, No. 5 (May) .
- Mass, J. (1979), "Diversity and Baseline Orientation," IEEE Trans. Ant. Prop. Vol. **AP-27**, No. 1, pp. 27.
- Matricciani, E., (1987), "Orbital Diversity in Resource-Shared Satellite Communication Systems Above 10 GHz," IEEE J. on Selected Areas In Communications, Vol. SAC-5, No. 4, pp. 714-723.
- Mazur, B., Crozier, S., Lyons, R., and Matyas, R. (1983), "Adaptive Forward Error Correction Techniques in TDMA," Sixth Int. Conf. on Digital Satellite Comm. (Sept.), pp. 12-8 through 12-15 .
- McGregor, D.N. (1981), "Communication Satellite System Availability Models," ORI Technical Report 1890, prepared under contract NASW-3436 for NASA Headquarters.
- Moat, R.L., (1986), "ACTS Baseband Processing," IEEE Transactions Comm., Vol. **COM-16**, No. 4 (September), pp. 578-583.
- Morelli, T., and T. Matitti (1988), "The **ITALSAT** Satellite Program," proceedings of the AIAA 12th International Communications Satellite Systems Conference, Arlington VA, Mar. 13-17, 1988, pp. 112-121.
- Morgan, W.L., (1985), "The Olympus Familyr" Satellite Communications Magazine, pp. 35-36, June.
- Morita, K. and I. Higuti (1978), "Statistical Studies on Rain Attenuation and Site Diversity Effect on Earth-to-Satellite Links in Microwave and Millimeter Wavebands," Trans. of the IECE of Japan, Vol. E61, No. 6, pp. 425-432.
- Moy, L.L., Carroll, D.R., and Kirberg, R.J., (1986), "On the effectiveness of Onboard Processing," Proceedings of the AIAA Communication Satellite Systems Conference, March.

- Naderi, **F.M.**, and **Campanella, S.J.**, (1988), "NASA'S Advanced Communications Technology Satellite (ACTS): An Overview of the Satellite, the Network, and the Underlying Technologies," Proceedings of 12th International AIAA Communications Satellite Systems Conference, Crystal City, VA, March 1988.
- Nakony, **O.G.** (1979), "CTS 11.7 GHz Propagation Measurements - Third Year's Data and Final Report," Tech. Rep. TR 79-471.3, GTE Laboratories, Inc., Waltham, MA.
- NASA (1987), Advanced Communications Tectinology Satellite (ACTS) Notice of Intent for Experiments, NASA Headquarters, Mar. 3 [Revision 4, Dec. 1987].
- Northrop, **G.M.** (1966), "Aids for the Gross Design of Satellite Communication Systems," IEEE Transactions Comm., Vol. COM-14, February.
- Parker, **D.E.** (1977), "Design Objectives for DCS LOS Digital Radio Links," Defense Communications Engineering Center (**DCEC**) Engineering Publication No. 27-77, December (DDC AD Number **A065354**).
- Poley, W.A., G.H. Stevens, S.M. Stevenson, J. Lekan, C.H. Arth, J.E. Hollansworth, and E.F. Miller, (1986)**, "An Assessment of the Status and Trends in Satellite Communications 1986-2000," NSAS Technical Memorandum #88867, November.
- Rice, **P.L. and N.R. Holmberg (1973)**, "**Culumative** Time Statistics of SurfacePoint Rainfall Rates," IEEE Trans. Comm., Vol. COM-21, No. 10, pp. 1131-1136.
- Richens, **D.M.**, (1987), "Very Small Aperture Terminals: An Overview," Satellite Directory, pp. 131-135.
- Rosenbaum, **A.S.** (1970), "Binary PSK Error Probabilities with Multiple **Cochannel** Interferences," IEEE Transactions on Communications, June.
- Rosenbaum, **A.S. and F.E. Glave** (1974), "An Error-Probability Upper Bound for Coherent Phase-Shift Keying with Peak-Limited Interference," IEEE Transactions on Communications, January.
- Scarcella, T. and R.V. Abbott, (1983)**, "Orbital Efficiency Through Satellite Digital Switching?" IEEE Communications Magazine, May 1983, pp. 38-46.
- Schwartz, J.J., and L. Schuchman (1982), "Satellite Relayed Tracking and Data Acquisition for the 1990's," **ICC'82** Conference Record.

- Schwartz, M., W.R. Bennett, and S. Stein (1966), Communication Systems and Techniques, McGraw-Hill.
- Spilker, J.J., Jr. (1977), Digital Communications by Satellite, Prentice-Hall.
- Strickland, J.I. (1977), "Radiometric Measurements of Site Diversity Improvement at Two Canadian Locations," Proceedings, URSI Commission F Symposium, 28 April - 6 May, LaBaule, France.
- Towner, G.C., R.E. Marshall, W.L. Stutzmann, C.W. Bostian, T. Pratt, E.A. Manus, P.H. Wiley (1982), "Initial Results from the VPI and SU SIRIO Diversity Experiment," Radio Science, Vol. 17, No. 6, pp. 1489-1494.
- Wallace, R.G. (1981), "Site Diversity Effects on Communications Satellite System Availability," ORI Technical Report 1891, prepared under contract NASW-3436 for NASA Headquarters.
- Wilson, R.W. (1970), "A Three-Radiometer Path Diversity Experiment," Bell System Technical Journal, Vol. 49, p. 1239.
- Wilson, R.W. and W.L. Mammel (1973), "Results from a Three Radiometer Path Diversity Experiment," Proceedings of Conference on Propagation of Radio Waves at Frequencies above 10GHz, London, p. 23.
- Wolejsza, C.J., D. Taylor, M. Grossman, and W.P. Osborne, (1987), "Multiple Access Protocols for Data Communications via VSAT Networks," IEEE Communications Magazine, Vol. 25, No. 7, July.